

A Doctoral Dissertation

**Cytoprotective Effect of Triphlorethol-
A from *Ecklonia cava* against Oxidative
Stress-Induced Cell Damage**

Kyoung-Ah Kang

**Department of Medicine
Graduate School
Cheju National University**

February, 2009

산화적인 스트레스에 의해 유도된 세포손상에
대한 감태류에서 분리한 Triphlorethol-A의
세포보호 효과

지도교수 현진원

강경아

이 논문을 의학 박사학위 논문으로 제출함

2009년 2월

강경아의 의학 박사학위 논문을 인준함

심사위원장

이덕배

印

위

원

趙文淸

印

위

원

은수용

印

위

원

강희경

印

위

원

현진원

印

제주대학교 대학원

2009년 2월

**Cytoprotective Effect of Triphlorethol-A from
Ecklonia cava against Oxidative Stress-Induced
Cell Damage**

Kyoung-Ah Kang

(Supervised by Professor **Jin-Won Hyun**)

A thesis submitted in partial fulfillment of the requirement for the
degree of doctor of philosophy in medicine

Date Approved :

Dec, 2008

DeokBAE PARK

Moonjae Cho

Su Yong Eun

Heekyoung Kang

Wjyjh

**Department of Medicine
Graduate School
Cheju National University**

February, 2009

CONTENTS

CONTENTS i

LIST of FIGURES vi

OVERALL BACKGROUNDS. 1

PART ONE ii

PART TWO iii

PART THREE vi

PART FOUR v

PART ONE

1. ABSTRACT	4
2. INTRODUCTION	5
3. MATERIALS AND METHODS	7
3-1. Preparation of Triphlorethol-A	
3-2. Reagents	
3-3. Cell culture	
3-4. Intracellular Reactive Oxygen Species (ROS) Measurement and Image Analysis	
3-5. Lipid Peroxidation Inhibitory Activity	
3-6. Cell Viability	
3-7. Flow cytometry analysis	
3-8. Nuclear Staining with Hoechst 33342	
3-9. Superoxide Dismutase (SOD) Activity	
3-10. Catalase (CAT) Activity	
3-11. Glutathione Peroxidase (GPx) Activity	
3-12. Statistical Analysis	
4. Results	15
4-1. Radical Scavenging Activity of Triphlorethol-A	
4-2. Effect of Triphlorethol-A on Lipid Peroxidation	
4-3. Effect of Triphlorethol-A on Cell Damage Induced by H ₂ O ₂	
4-4. Effect of Triphlorethol-A on ERK activation	
5. Discussion	24

PART TWO

1. ABSTRACT	28
2. INTRODUCTION	29
3. MATERIALS AND METHODS	31
3-1. Cell culture	
3-2. Irradiation	
3-3. Intracellular reactive oxygen species measurement	
3-4. Cell viability	
3-5. Lipid Peroxidation Inhibitory Activity	
3-6. Flow cytometry analysis	
3-7. Nuclear Staining with Hoechst 33342	
3-8. Single cell gel electrophoresis (Comet assay)	
3-9. Statistical analysis	
4. Results	36
4-1. Radical Scavenging Activity of Triphlorethol-A on the ROS Generated by g-ray Radiation	
4-2. Effect of Triphlorethol-A on Lipid Peroxidation Generated by g-ray Radiation	
4-3. Effect of Triphlorethol-A on Cell Damage Induced by g-ray Radiation	
4-4. Cytoprotective Effect of Triphlorethol-A on Radiation-Induced Apoptosis	
5. Discussion	45

PART THREE

1. ABSTRACT 47

2. INTRODUCTION 48

3. MATERIALS AND METHODS 50

 3-1. Reagents

 3-2. Cell culture

 3-3. Cell Viability

 3-4. HO-1 assay

 3-5. Western blot

 3-6. Reverse transcriptase polymerase chain reaction

 3-7. Nuclear extract preparation and electrophoretic mobility shift assay

 3-8. Transient transfection and luciferase assay

 3-9. Immunocytochemistry

 3-10. Statistical analysis

4. Results 56

 4-1. Effect of triphlorethol-A on HO-1 expression and activity

 4-2. Triphlorethol-A increased the nuclear translocation, ARE-binding, and transcriptional activity of Nrf2

 4-3. Triphlorethol-A activates Nrf2 via phosphorylation of ERK

 4-4. Effect of triphlorethol-A on cell damage induced by oxidative stress

5. Discussion 67

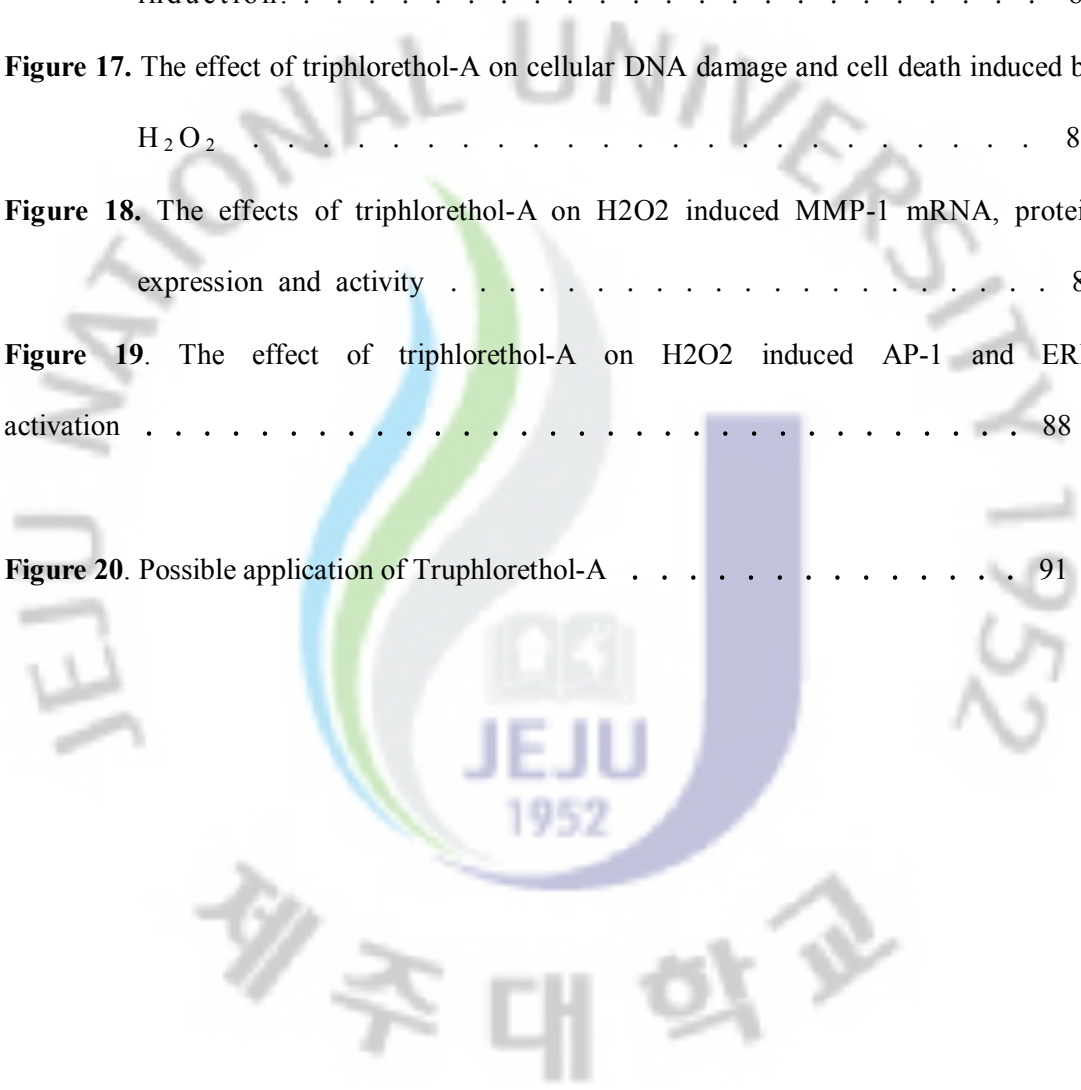
PART FOUR

1. ABSTRACT	71
2. INTRODUCTION	72
3. MATERIALS AND METHODS	74
3-1. Reagents	
3-2. Cell culture	
3-3. Intracellular reactive oxygen species (ROS) measurement	
3-4. Western blot	
3-5. Immunocytochemistry	
3-6. Comet assay	
3-7. Cell viability	
3-8. Reverse transcriptase polymerase chain reaction	
3-9. Determination of MMP-1 activity	
3-10. Preparation of nuclear extract and electrophoretic mobility shift assay	
3-11. Statistical analysis	
4. Results	81
4-1. Effect of triphlorethol-A on radical scavenging activity and catalase expression	
4-2. Effect of triphlorethol-A on cellular DNA damage and cell death induced by H ₂ O ₂	
4-3. Effects of triphlorethol-A on H ₂ O ₂ induced MMP-1 expression and activity	
4-4. Effects of triphlorethol-A on H ₂ O ₂ induced ERK-AP-1 pathway	
5. Discussion	89
6. Part conclusion	91
7. Reference	92
8. Abstract in Korean	117

LIST OF FIGURES

Figure 1. The Structures of triphlorethol-A	7
Figure 2. Effect of triphlorethol-A on scavenging intracellular ROS.	16
Figure 3. Effect of triphlorethol-A on inhibition of lipid peroxidation.	17
Figure 4. Protective effect of triphlorethol-A on H ₂ O ₂ induced oxidative damage of V79-4 cells	19
Figure 5. Effect of triphlorethol-A on ERK activation.. . . .	21
Figure 6. Effect of triphlorethol-A on the activities of antioxidative enzymes.. . . .	23
Figure 7 Effect of triphlorethol-A on scavenging intracellular ROS generated by g-ray radiation.	36
Figure 8. Protective effect of triphlorethol-A upon g-ray radiation-induced lipid membrane damage of V79-4 cells	37
Figure 9. Protective effect of triphlorethol-A upon g-ray radiation-induced cellular DNA damage of V79-4 cells	39
Figure 10. Protective effect of triphlorethol-A upon g-ray radiation-induced cell damage of V79-4 cells	43
Figure 11. Effect of triphlorethol-A on heme oxygenase-1 mRNA, protein expression and activity in V79-4 cells	58
Figure 12. Effect of triphlorethol-A on Nrf2 expression, translocation into nucleus, and its transcriptional activity in V79-4 cells	60
Figure 13. Induction of HO-1 and activation of Nrf2 by triphlorethol-A via phosphorylation of ERK	62
Figure 14. Protective effect of triphlorethol-A against oxidative stress induced cell damage	66

Figure 15. A proposed pathway for triphlorethol-A induced HO-1 via upregulation of ERK and Nrf2, which explains cytoprotection against oxidative stress in cells . . .	69
Figure 16. Effect of triphlorethol-A on radical scavenging activity and catalase induction.	82
Figure 17. The effect of triphlorethol-A on cellular DNA damage and cell death induced by H ₂ O ₂	84
Figure 18. The effects of triphlorethol-A on H ₂ O ₂ induced MMP-1 mRNA, protein expression and activity	85
Figure 19. The effect of triphlorethol-A on H ₂ O ₂ induced AP-1 and ERK activation	88
Figure 20. Possible application of Truphlorethol-A	91



OVERALL BACKGROUNDS

Reactive Oxygen species(ROS) are associated with tissue damage and are the contributing factors for inflammation, aging, cancer, arteriosclerosis, hypertension and diabetes[1-7]. Antioxidants have been shown to have some preventive or therapeutic effects against the symptoms of these diseases. Hydrogen peroxide (H₂O₂), which is one of the main ROS, may be involved in the formation of hydroxyl radicals[8-10]. Hydroxyl radicals are highly reactive and destructive substances which cause DNA damage in cells, and in turn result in cell death[11-12]. Some antioxidants have been shown to protect cells against DNA damage by ROS[13-15]. Therefore, substantial efforts have been made to identify both natural and synthetic antioxidants.

Ecklonia cava is a brown alga (Laminariaceae) that is abundant in the subtidal regions of Jeju Island in Korea. Recently, it has been reported that *Ecklonia* species exhibits radical scavenging activity,[16,17] anti-plasmin inhibiting activity,[18-20] antimutagenic activity,[21-22] bactericidal activity, HIV-1 reverse transcriptase and protease inhibiting activity,[23] and tyrosine inhibitory activity.[24,25] Phlorotannins such as eckol (a phloroglucinol trimer, a closed-chain trimer), 6,6'-bieckol (a hexamer), dieckol (a hexamer), phlorofucofuroeckol (a pentamer) were identified to be responsible for the biological activities in *Ecklonia*. During the investigation of antioxidative components in *E. cava*, we

observed that triphloethol-A has very strong activities. Triphloethol-A, an open-chain trimer of phloroglucinol, is one of phlorotannin components isolated from *E. cava* in this study, and has been previously isolated from *E. Kurome*. [18]

In the present study, Triphloethol-A, phlorotannin found in *Ecklonia cava*, exerted cytoprotective effects against various oxidative stress and the underlying molecular mechanism was investigated. We studied the cytoprotective effect of triphloethol-A against hydrogen peroxide (H₂O₂) and γ -ray radiation-induced oxidative stress. We also were investigated the capability of triphloethol-A to induce the antioxidant enzyme HO-1. Finally, oxidative stress has been demonstrated to cause the production of reactive oxygen species (ROS) in cells, which in turn induces the synthesis of matrix metalloproteinases (MMPs) and aging. So, we investigated the protective effects of triphloethol-A, derived from *Ecklonia cava*, against hydrogen peroxide (H₂O₂) using human skin keratinocytes.

Triphloethol-A was observed to protect the Chinese hamster lung fibroblast (V79-4) cells against various oxidative damage through scavenging ROS and augments cellular antioxidant defense capacity through activation of antioxidant enzyme and induction of HO-1 via ERK-Nrf2-ARE signaling pathway. Also The results suggest that the antioxidative properties of triphloethol-A involves the inhibition of MMP-1 via ERK and AP-1 inhibition, thereby protecting human keratinocyte, HaCaT cells from oxidative stress.

PART I

**Triphlorethol-A from *Ecklonia cava* Protects V79-4 Lung
Fibroblast against Hydrogen Peroxide and Radiation
Induced Cell Damage**



1. Abstract

In the present study, triphlorethol-A, a phlorotannin, was isolated from *Ecklonia cava* and its antioxidant properties were investigated. Triphlorethol-A was found to scavenge intracellular reactive oxygen species (ROS), and thus prevented lipid peroxidation. The radical scavenging activity of triphlorethol-A protected the Chinese hamster lung fibroblast (V79-4) cells exposed to hydrogen peroxide (H₂O₂) against cell death, via the activation of ERK protein. Furthermore, triphlorethol-A reduced the apoptotic cells formation induced by H₂O₂. Triphlorethol-A increased the activities of cellular antioxidant enzymes like, superoxide dismutase (SOD), catalase (CAT), and glutathione peroxidase (GPx). Hence, from the present study, it is suggestive that triphlorethol-A protects V79-4 cells against H₂O₂ damage by enhancing the cellular antioxidative activity.

Key words: Triphlorethol-A; Oxidative stress; Apoptosis; Antioxidant enzymes

2. INTRODUCTION

Reactive oxygen species (ROS) are known to cause oxidative modification of DNA, proteins, lipids and small cellular molecules. ROS are associated with tissue damage and are the contributing factors for inflammation, aging, cancer, arteriosclerosis, hypertension and diabetes.[1-7] For cytoprotection against ROS, cells have developed a variety of antioxidant defense mechanisms. Enzymatic defense mechanisms involve superoxide dismutase (SOD), which catalyzes dismutation of superoxide anion to hydrogen peroxide, catalase (CAT), which converts hydrogen peroxide into molecular oxygen and water, and glutathione peroxidase (GPx), which destroys toxic peroxides.

Ecklonia cava is a brown alga (Laminariaceae) that is abundant in the subtidal regions of Jeju Island in Korea. Recently, it has been reported that *Ecklonia* species exhibits radical scavenging activity,[16,17] anti-plasmin inhibiting activity,[18-20] antimutagenic activity,[21-23] bactericidal activity,[24] HIV-1 reverse transcriptase and protease inhibiting activity,²⁵⁾ and tyrosine inhibitory activity[26,27] Phlorotannins such as eckol (a phloroglucinol trimer, a closed-chain trimer), 6,6'-bieckol (a hexamer), dieckol (a hexamer), phlorofucofuroeckol (a pentamer) were identified to be responsible for the biological activities in *Ecklonia*. During the investigation of antioxidative components in *E. cava*, we observed that triphloethol-A has very strong activities. Triphloethol-A, an open-chain trimer

of phloroglucinol, is one of phlorotannin components isolated from *E. cava* in this study, and has been previously isolated from *E. Kurome*. [18]

In the present study, we have investigated the protective effect of triphlorethol-A on cell damage induced by hydrogen peroxide and the possible mechanism of cytoprotection.



3. Material and Methods

3-1. Preparation of Triphlorethol-A

The dried *Ecklonia cava* (4 kg), collected from Jeju Island in Korea, was immersed in 80 % methanol at room temperature for 2 days. The aqueous methanol was removed *in vacuo* to give a brown extract (1 kg), which was partitioned between ethyl acetate and water. The ethyl acetate fraction (230 g) was mixed with celite. The mixed celite was dried and packed into a glass column, and eluted in the order of hexane, methylene chloride, diethyl ether and methanol. The obtained diethyl ether fraction (14 g) was subjected to Sephadex LH-20 chromatography using CHCl_3 -MeOH gradient solvent (2/1 \rightarrow 0/1). The triphlorethol-A (220 mg) was obtained from these fractions and was identified according to the previously reported method (Fig. 1).[24] The purity of triphlorethol-A assessed by HPLC was > 90 %. Triphlorethol-A was freshly dissolved in DMSO; the final concentration of which did not exceed 0.1 %.

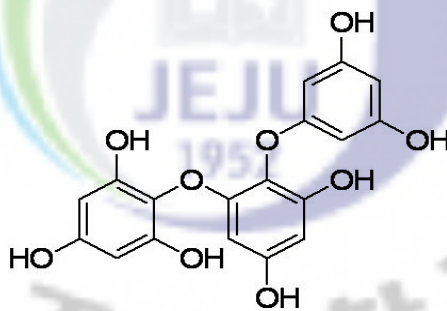


Figure 1. The structure of triphlorethol-A

3-2. Reagents

The 1,1-diphenyl-2-picrylhydrazyl (DPPH) radical, 2',7'-dichlorodihydrofluorescein diacetate (DCF-DA), and Hoechst 33342 were purchased from Sigma Chemical Company,

St. Louis, MO, USA. The other chemicals and reagents were of analytical grade. Primary rabbit polyclonal anti-ERK 2 (42kDa ERK) and -phospho-ERK1/2 (phosphorylated 44kDa/42kDa ERK) (Thr 202/Tyr 204) antibodies were purchased from Santa Cruz Biotechnology, Santa Cruz, CA, USA.

3-3. Cell Culture

It is reported that lung is an organ sensitive to oxidative stress.[25,26] To study the effect of triphlorethol-A on oxidative stress induced by hydrogen peroxide, we used Chinese hamster lung fibroblasts (V79-4 cells). The V79-4 cells from the American Type Culture Collection, were maintained at 37 °C in an incubator with a humidified atmosphere of 5 % CO₂ and cultured in Dulbecco's modified Eagle's medium containing 10 % heat-inactivated fetal calf serum, streptomycin (100 µg/ml) and penicillin (100 units/ml).

3-4. Intracellular Reactive Oxygen Species (ROS) Measurement and Image Analysis

The DCF-DA method was used to detect the intracellular ROS level.[27] DCF-DA diffuses into cells, where it is hydrolyzed by intracellular esterase to polar 2',7'-dichlorodihydrofluorescein. This non-fluorescent fluorescein analog gets trapped inside the cells and is oxidized by intracellular oxidants to a highly fluorescent, 2',7'-dichlorofluorescein. The V79-4 cells were seeded in a 96 well plate at 1×10^5 cells/ml. Sixteen hours after plating, the cells were treated with various concentrations of

triphlorethol-A and 30 minutes later, 1 mM H₂O₂ was added to the plate. The cells were incubated for an additional 30 minutes at 37 °C. After addition of 25 μM of DCF-DA solution, the fluorescence of 2',7'-dichlorofluorescein was detected at 485 nm excitation and at 535 nm emission using a PerkinElmer LS-5B spectrofluorometer.

For image analysis for production of intracellular ROS, the V79-4 cells were seeded in coverslip loaded 6 well plate at 1 × 10⁵ cells/ml. Sixteen hours after plating, the cells were treated with triphlorethol-A and 30 minutes later, 1 mM H₂O₂ was added to the plate. After changing media, 100 μM of DCF-DA was added in the well and was incubated for an additional 30 minutes at 37 °C. After washing with PBS, stained cells were mounted onto microscope slide in the mounting medium (DAKO, Carpinteria, CA, USA). Images were collected using the LSM 510 program on a Zeiss confocal microscope.

3-5. Lipid Peroxidation Inhibitory Activity

Lipid peroxidation was assayed by thiobarbituric acid reaction.[29] The V79-4 cells were seeded in a culture dish at 1 × 10⁵ cells/ml. Sixteen hours after plating, the cells were treated with various concentrations of triphlorethol-A. One hour later, 1 mM H₂O₂ was added to the plate, and was incubated for further 1 hour. The cells were then washed with cold PBS, scraped and homogenized in ice-cold 1.15 % KCl. One hundred μl of the cell lysates was mixed with 0.2 ml of 8.1 % SDS, 1.5 ml of 20 % acetic acid (adjusted to pH 3.5) and 1.5 ml

of 0.8 % thiobarbituric acid (TBA). The mixture was made up to a final volume of 4 ml with distilled water and heated to 95 °C for 2 hours. After cooling to room temperature, 5 ml of *n*-butanol and pyridine mixture (15:1, v/v) was added to each sample, and the mixture was shaken well. After centrifugation at 1000 × g for 10 minutes, the supernatant fraction was isolated, and the absorbance was measured spectrophotometrically at 532 nm.

3-6. Cell Viability

The effect of triphlorethol-A on the viability of the V79-4 cells was determined using the [3-(4,5-dimethylthiazol-2-yl)-2,5-diphenyltetrazolium bromide (MTT) assay, which is based on the reduction of a tetrazolium salt by mitochondrial dehydrogenase in the viable cells.^[30] The V79-4 cells were seeded in a 96 well plate at 1×10^5 cells/ml. Sixteen hours after plating, the cells were treated with various concentrations of triphlorethol-A. One hour later, 1 mM H₂O₂ was added to the plate and incubated at 37 °C for an additional 24 hours. Fifty µl of the MTT stock solution (2 mg/ml) was then added to each well to attain a total reaction volume of 200 µl. After incubating for 4 hours, the plate was centrifuged at 800 × g for 5 minutes and the supernatants were aspirated. The formazan crystals in each well were dissolved in 150 µl dimethylsulfoxide and the A₅₄₀ was read on a scanning multi-well spectrophotometer.

3-7. Flow cytometry analysis

Flow cytometry was performed to determine the apoptotic sub G₁ hypo-diploid cells.[31]

The V79-4 cells were placed in a 6 well plate at 1×10^5 cells/ml. Sixteen hours after plating, the cells were treated with 30 μ M of triphlorethol-A. After a further incubation of 1 hour, 1 mM H_2O_2 was added to the culture. After 24 hours, the cells were harvested, and fixed in 1 ml of 70 % ethanol for 30 minutes at 4 °C. The cells were washed twice with PBS, and then incubated for 30 minutes in the dark at 37 °C in 1 ml of PBS containing 100 μ g propidium iodide and 100 μ g RNase A. Flow cytometric analysis was performed using a FACSCalibur flow cytometer (Becton Dickinson, Mountain View, CA, USA). The proportion of sub G_1 hypo-diploid cells was assessed by the histograms generated using the computer program, Cell Quest and Mod-Fit.

3-8. Nuclear Staining with Hoechst 33342

The V79-4 cells were placed in a 24 well plate at 1×10^5 cells/ml. Sixteen hours after plating, the cells were treated with 30 μ M of triphlorethol-A and after further incubation for 1 hour, 1 mM H_2O_2 was added to the culture. After 24 hours, 1.5 μ l of Hoechst 33342 (stock 10 mg/ml), a DNA specific fluorescent dye, was added to each well (1.5 ml) and incubated for 10 minutes at 37 °C. The stained cells were then observed under a fluorescent microscope, which was equipped with a CoolSNAP-Pro color digital camera to examine the degree of nuclear condensation.

3-9. Superoxide Dismutase (SOD) Activity

The V79-4 cells were seeded at 1×10^5 cells/ml, and sixteen hours after plating, the cells were treated with various concentrations of triphlorethol-A for 1 hour. The harvested cells were suspended in 10 mM phosphate buffer (pH 7.5) and then lysed on ice by sonication twice for 15 seconds. Triton X-100 (1 %) was then added to the lysates and was incubated for 10 minutes on ice. The lysates were centrifugated at $5000 \times g$ for 30 minutes at 4 °C to remove the cellular debris. The protein content of the supernatant was determined by Bradford method,[32] with bovine serum albumin as the standard. The SOD activity was used to detect the inhibited level of auto-oxidation of epinephrine.[33] Fifty μg of the protein was added to 50 mM phosphate buffer (pH 10.2) containing 0.1 mM EDTA and 0.4 mM epinephrine. Epinephrine rapidly undergoes auto-oxidation at pH 10 to produce adrenochrome, a pink colored product, which can be measured at 480 nm using a UV/VIS spectrophotometer in kinetic mode. SOD inhibits the auto-oxidation of epinephrine. The rate of inhibition was monitored at 480 nm. The SOD activity was expressed as units/mg protein and one unit of enzyme activity was defined as the amount of enzyme required for 50 % inhibition of auto-oxidation of epinephrine.

3-10. Catalase (CAT) Activity

Fifty μg of protein was added to 50 mM phosphate buffer (pH 7) containing 100 mM (v/v) H_2O_2 . The reaction mixture was incubated for 2 minutes at 37 °C and the absorbance was

monitored at 240 nm for 5 minutes. The change in absorbance with time was proportional to the breakdown of H₂O₂. [34] The CAT activity was expressed as units/mg protein and one unit of enzyme activity was defined as the amount of enzyme required to breakdown of 1 μ M H₂O₂.

3-11. Glutathione Peroxidase (GPx) Activity

Fifty μ g of the protein was added to 25 mM phosphate buffer (pH 7.5) containing 1 mM EDTA, 1 mM NaN₃, 1 mM glutathione (GSH), 0.25 unit of glutathione reductase, and 0.1 mM NADPH. After incubation for 10 minutes at 37 °C, H₂O₂ was added to the reaction mixture at a final concentration of 1 mM. The absorbance was monitored at 340 nm for 5 minutes. The GPx activity was measured as the rate of NADPH oxidation by change in absorbance at 340 nm. [35] The GPx activity was expressed as units/mg protein and one unit of enzyme activity was defined as the amount of enzyme required to oxidize 1 mM NADPH.

3-12. Western Blot

The V79-4 cells were placed in a plate at 1×10^5 cells/ml. Sixteen hours after plating, the cells were treated with 30 μ M of triphlorethol-A. The cells were harvested at the indicated times, and washed twice with PBS. The harvested cells were then lysed on ice for 30 minutes in 100 μ l of lysis buffer [120 mM NaCl, 40 mM Tris (pH 8), 0.1 % NP 40] and centrifuged at $13,000 \times g$ for 15 minutes. Supernatants were collected from the lysates and protein

concentrations were determined. Aliquots of the lysates (40 µg of protein) were boiled for 5 minutes and electrophoresed in 10 % SDS-polyacrylamide gel. Blots in the gels were transferred onto nitrocellulose membranes (Bio-Rad, Hercules, CA, USA), which were then incubated with primary rabbit monoclonal -ERK1/2 and -phospho ERK1/2. The membranes were further incubated with goat anti-rabbit immunoglobulin G-horseradish peroxidase conjugates (Pierce, Rockland, IL, USA), and then exposed to X-ray film. Protein bands were detected using an enhanced chemiluminescence Western blotting detection kit (Amersham, Little Chalfont, Buckinghamshire, UK).

3-13. Statistical Analysis

All the measurements were made in triplicate. The results were subjected to an analysis of the variance (ANOVA) using the Tukey test to analyze the difference. $p < 0.05$ were considered significantly.

4. Results

4.1 Radical Scavenging Activity of Triphlorethol-A

The radical scavenging effect of triphlorethol-A on the intracellular ROS and DPPH free radical scavenging activities was measured. The intracellular ROS scavenging activity of triphlorethol-A was 43, 69 and 76 % at concentrations of 0.3, 3 and 30 μ M, respectively (Fig. 2A). In the presence of 2 mM of N-acetylcysteine (positive control), there was 85 % of ROS inhibition (data not shown). As shown in Fig. 2B, the fluorescent intensity of DCF-DA staining was enhanced in H₂O₂ treated V79-4 cells. However, triphlorethol-A reduced the red fluorescence intensity by H₂O₂ treatment, reflecting a reduction of ROS generation.

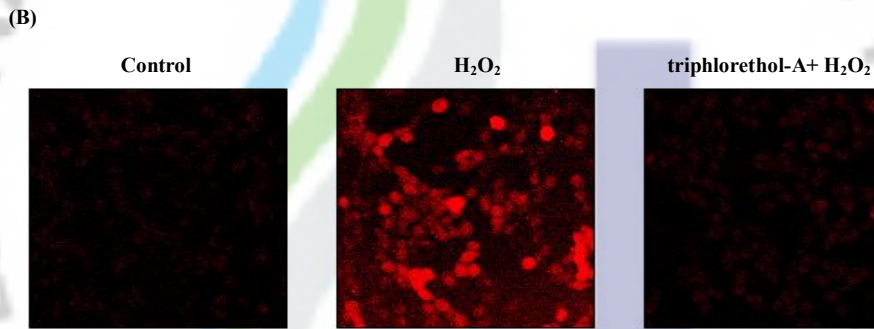
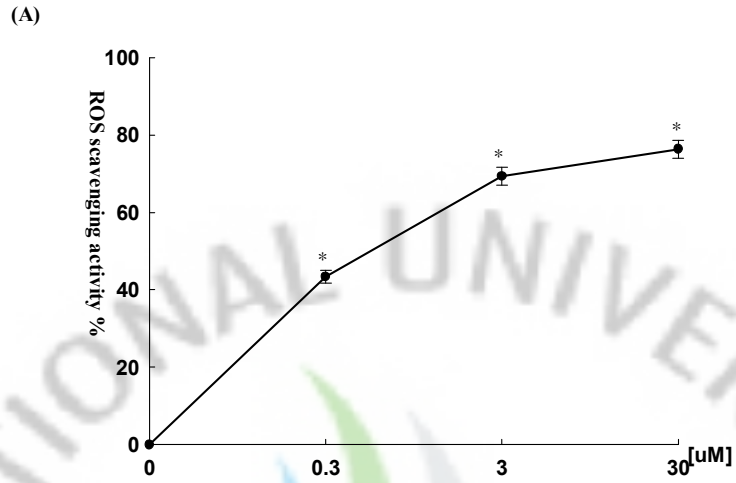


Fig. 2. Effect of triphlorethol-A on scavenging intracellular ROS. The intracellular ROS generated was detected by DCF-DA method (A) and by confocal microscopy (B). Representative confocal images illustrate the increase in red fluorescence intensity of DCF produced by ROS in H₂O₂ treated V79-4 cells as compared to control and the lowered fluorescence intensity in H₂O₂ treated V79-4 cells in the presence of triphlorethol-A (original magnification × 400). *significantly different from control (p<0.05).

4.2 Effect of Triphlorethol-A on Lipid Peroxidation

The ability of triphlorethol-A to inhibit lipid peroxidation in H₂O₂ treated V79-4 cells was also investigated. The generation of thiobarbituric acid reactive substance (TBARS) was inhibited in the presence of triphlorethol-A. The inhibitory effect of triphlorethol-A was 15, 21 and 32 % at concentration of 0.3, 3, and 30 μ M, respectively, when compared to 11 % inhibition in 0.1 % DMSO treated group (Fig. 3).

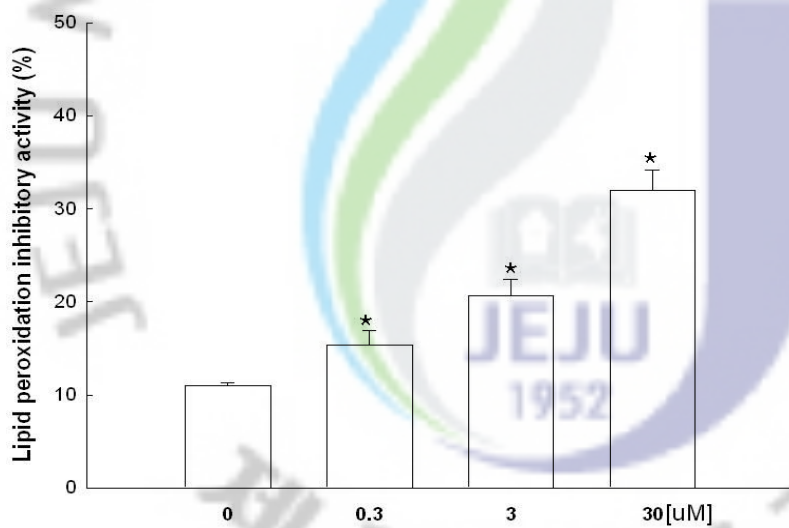


Fig. 3. Effect of triphlorethol-A on inhibition of lipid peroxidation. Lipid peroxidation was assayed by measuring the amount of TBARS. *significantly different from control ($p < 0.05$).

4.3 Effect of Triphlorethol-A on Cell Damage Induced by H₂O₂

The protective effect of triphlorethol-A on cell survival in H₂O₂ treated V79-4 cells was also measured. Cells were treated with triphlorethol-A at various concentrations for 1 hour, prior to the addition to H₂O₂. The cell viability was determined 24 hours later by MTT assay. As shown in Fig. 4A, treatment with triphlorethol-A induced a dose dependent increase in the cell survival rate; 7 % at 0.3 μM, 22 % at 3 μM, and 42 % at 30 μM. In order to study the cytoprotective effect of triphlorethol-A on apoptosis induced by H₂O₂, nuclei of V79-4 cells were stained with Hoechst 33342 for microscopy and with propidium iodide for flow cytometric analysis. The microscopic pictures in Fig. 4B showed that the control cells had intact nuclei, and the H₂O₂ treated cells showed significant nuclear fragmentation, characteristic of apoptosis. However, when the cells were treated with triphlorethol-A for 1 hour prior to H₂O₂ treatment, a dramatic decrease in nuclear fragmentation was observed. In addition to the morphological evaluation, the protective effect of triphlorethol-A against apoptosis was confirmed by flow cytometry. As shown in Fig. 4C, an analysis of the DNA content in the H₂O₂ treated cells revealed an increase of 65 % of apoptotic sub-G₁ DNA content, as compared to 2 % of apoptotic sub-G₁ DNA content in untreated cells. Treatment with 30 μM of triphlorethol-A decreased the apoptotic sub-G₁ DNA content to 52 %. These results suggest that triphlorethol-A protects cell viability by inhibiting H₂O₂ induced

apoptosis.

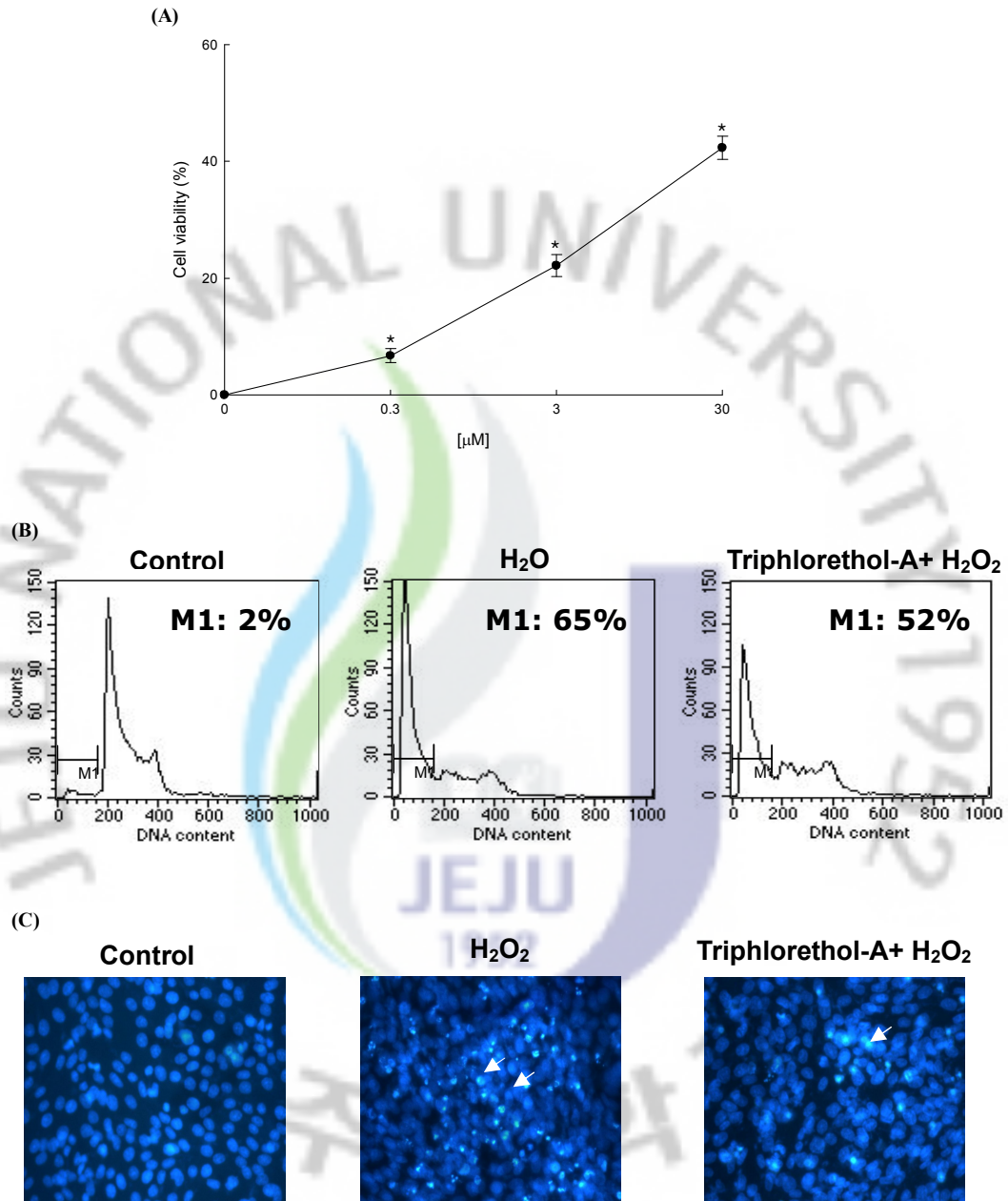
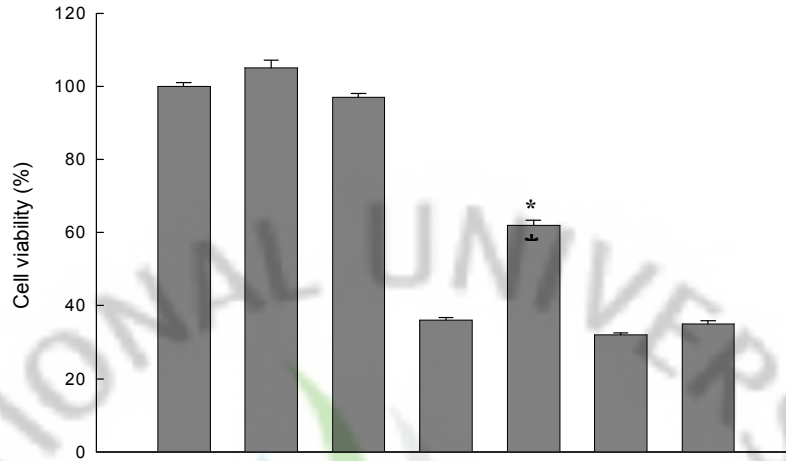


Fig. 4. Protective effect of triphlorethol-A on H_2O_2 induced oxidative damage of V79-4 cells. (A) The viability of V79-4 cells was determined by MTT assay. (B) Apoptotic body formation was observed under a fluorescent microscope after Hoechst 33342 staining and apoptotic bodies are indicated by arrows. (C) Apoptotic sub- G_1 DNA content was detected by flow cytometry after propidium iodide staining.

4.4 Effect of Triphlorethol-A on ERK activation

The activation of extracellular signal regulated kinase (ERK) is known to induce cell proliferation.^[28] To better understand the protective mechanism of triphlorethol-A on V79-4 cells, we examined the activation of the ERK protein by western blot analysis with the phospho-ERK specific antibody. As shown in Fig. 5A, within 6 hours triphlorethol-A activated phosphorylated ERK dramatically. However, there was no change in the total ERK protein level. To determine the effect of ERK inhibitor on protection of triphlorethol-A from H₂O₂ induced damage, V79-4 cells were pre-treated for 30 minutes with U0126 (10 nM), specific inhibitor of ERK kinase, followed for 30 minutes with triphlorethol-A and exposed to 1 mM H₂O₂ for 24 hours. As shown in Fig. 5B, U0126 treatment abolished the protection activity of triphlorethol-A in H₂O₂ damaged cells.

(A)



Triphlorethol-A	-	+	-	-	+	-	+
H ₂ O ₂	-	-	-	+	+	+	+
U0126	-	-	+	-	-	+	+

(B)

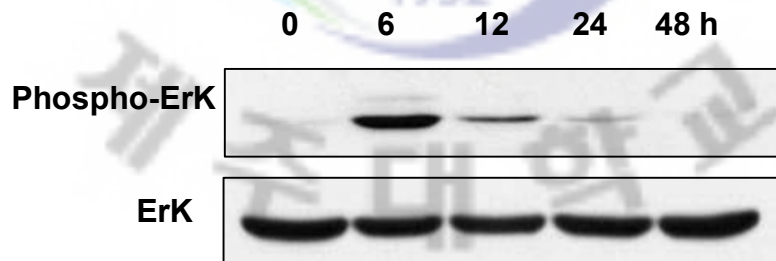


Fig. 5. Effect of triphlorethol-A on ERK activation. (A) Cell lysates were electrophoresed and proteins of ERK1/2 and phospho-ERK1/2 were detected by their respective antibodies. (B) After treatment of U0126, triphlorethol-A or/and H₂O₂, the viability of V79-4 cells was determined by MTT assay. *significantly different from H₂O₂ treated cells (p<0.05).

4.5 Effect of Triphlorethol-A on the Intracellular Antioxidant Systems

In order to investigate whether the radical scavenging activity of triphlorethol-A was mediated by the activities of antioxidant enzymes, the SOD, CAT and GPx activities in triphlorethol-A treated V79-4 cells were measured. Triphlorethol-A increased the activities of these three enzymes (Fig. 6A); in the case of SOD activity, at concentration of 0.3, 3, and 30 μM of triphlorethol-A, the activity was 16, 18, and 21, as compared to 11 U/mg protein of the control; in the case of CAT activity, it was 15, 23, and 31 U/mg protein at concentration of 0.3, 3, and 30 μM , as compared to 15 U/mg protein of the control; in the case of GPx activity, it was 12, 14, and 17 U/mg protein at concentration of 0.3, 3, and 30 μM , as compared to 7 U/mg protein of the control. The 3-amino-1,2,4 triazol (ATZ) is known as a specific inhibitor of catalase.^[36] To determine the effect of catalase inhibitor on protection of triphlorethol-A from H_2O_2 induced damage, V79-4 cells were pre-treated with 20 mM of ATZ for 1 hour, followed for 30 minutes with triphlorethol-A and exposed to 1 mM H_2O_2 for 24 hours. As shown in Fig. 6B, ATZ treatment abolished the protection activity of triphlorethol-A in H_2O_2 damaged cells. It is reported that most polyphenolic compounds interact with commonly used cell culture media to generate H_2O_2 .^[37] This generated low level of H_2O_2 can trigger the rise in antioxidant enzymes.

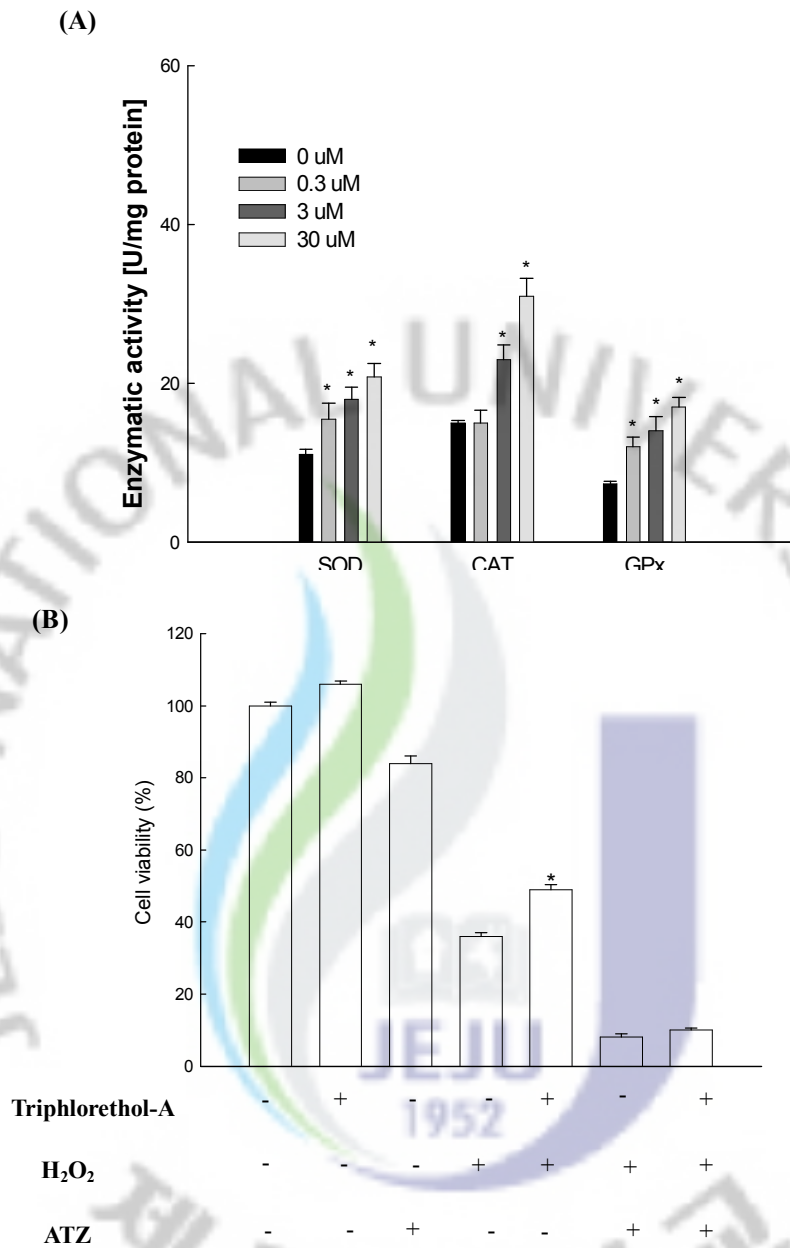


Fig. 6. Effect of triphlorethol-A on the activities of antioxidative enzymes. (A) The data represents three experiments and are expressed as average enzyme unit per mg protein \pm S.E. *significantly different from control ($p < 0.05$). (B) After treatment of ATZ, triphlorethol-A or/and H₂O₂, the viability of V79-4 cells was determined by MTT assay. *significantly different from H₂O₂ treated cells ($p < 0.05$).

4. Discussion

Phlorotannins, which are marine algal polyphenols and are also known as brown algae, are polymers of phloroglucinol.^[38] Although some reports suggest that phlorotannins from algae exhibit the antioxidant effect on free radicals,^[13,39,40] there are no reports on the antioxidant activity of triphlorethol-A, isolated from *Ecklonia cava*. In our present study, it was observed that upon exposure to H₂O₂, triphlorethol-A decreased intracellular ROS generation and DPPH radical level. Triphloroethol-A has a polyphenol structure. Polyphenols are electron-rich compounds and prone to enter into efficient electron-donation reactions with oxidizing agents to produce phenoxyl radical (PhO·) species as intermediates. Phenoxyl radicals are stabilized by resonance delocalization of the unpaired electron to the *ortho* and *para* positions of the ring. In addition to the resonance stability, phenoxyl radicals can also be stabilized by hydrogen bonding with an adjacent hydroxyl group. Phenoxyl radicals also undergo dimerization (“phenol coupling”) to produce new C-C or C-O linkage.^[41] These intrinsic stability of phenolic structures might be related to antioxidant activity of triphloroethol A. The cells exposed to H₂O₂ exhibited distinct morphological features of apoptosis, such as nuclear fragmentation and an increase in sub G₁ DNA content. However, cells that were pretreated with

triphlorethol-A had significantly reduced percentage of apoptotic cells, as shown by morphological changes and reduction in sub G₁ DNA content. Our results are also consistent with the antioxidant activity of N-acetylcysteine, which also prevents H₂O₂ induced apoptosis, indicating that the inhibition of ROS formation may be important for cytoprotection against oxidative damage. In many cell types, extracellular signal regulated kinase (ERK) pathway is induced by a variety of extracellular stimuli.^[42] The phosphorylation of ERK can phosphorylate cytoplasmic and nuclear targets and participates in a wide range of cellular programs including proliferation, differentiation, and movement.^[43-46] The level of phosphorylated ERK in triphlorethol-A treated V79-4 cells was induced, and treatment of U0126, specific inhibitor of ERK kinase, suppressed the protection activity of triphlorethol-A in H₂O₂ damaged cells, suggesting that the protective effect of triphlorethol-A on cells may also be involved in activating ERK pathway. Antioxidant enzymes, like SOD, CAT, and GPx, play significant roles in effective augmentation of antioxidant defense mechanisms in cells. SOD converts superoxide radicals to hydrogen peroxide and subsequently to water by the activity of CAT and GPx. Triphlorethol-A increased SOD, CAT, and GPx activities, suggesting that the scavenging of ROS may be related to the increased antioxidant activity. Therefore, the effects of triphlorethol-A

on cell viability might involve dual actions: direct action on oxygen radical scavenging, as shown by intracellular ROS scavenging, and indirect action through induction of anti-oxidative enzymes.

In conclusion, triphlorethol-A, a phlorotannin, exerted intracellular ROS scavenging activity, promoted cell viability via activation of ERK protein, inhibited H₂O₂ induced apoptosis, and enhanced the effects of antioxidant enzymes.



PART II

**Protective Effect of Triphlorethol-A from *Ecklonia cava*
against Ionizing Radiation *in vitro***



3. Abstract

We studied the cytoprotective effect of triphlorethol-A against γ -ray radiation-induced oxidative stress. Triphlorethol-A was observed to scavenge intracellular reactive oxygen species (ROS) that were generated by γ -ray radiation. This compound protected membrane lipid peroxidation and cellular DNA damage which are the main targets of radiation-induced damage. In addition, triphlorethol-A reduced the apoptotic cells formation induced by radiation. Taken together, the results suggest that triphlorethol-A protects cells against oxidative damage induced by radiation through scavenging ROS.

Keywords: radiation protection, oxidative stress, reactive oxygen species

2. INTRODUCTION

Most of Ionizing radiation's toxic effects are attributed to the free radicals (HO[•], H[•], H₂O₂ etc) generated by the radiolysis of water. Interaction of free radicals with DNA can induce DNA damage lead to mutagenesis and carcinogenesis. [47] The damaging effects of free radicals lead to cell death are associated with an increased risk for numerous genetically determined diseases by ionizing radiation. [48] The potential application of radioprotective chemicals in the event of planned exposure or radiation accidents has been investigated from the beginning of the nuclear era [49]. Historically, sulfhydryl compounds have been among the first radioprotective agents. Amifostine as a thiol compound is a powerful radioprotective agent, but its application is clinically limited due to side effects and toxicity.[50,51] In recent years, The screening of the compounds having the ability to scavenge these ROS could lead to promising radioprotectors. Most of the antioxidants identified till date are derived from the natural sources and exploration of the phytochemicals, as radioprotectors is one among the competent strategies in lead identification. [51] Most of these plant products have many compounds with medicinal value that protect biological systems from ionizing radiation with minimum side effects. Recently, we reported that triphlorethol-A, derived from *Ecklonia cava*, decreased H₂O₂-induced cell damage

through activation of an antioxidant system.[52]

In this study, we investigated the protective effects of triphlorethol-A on cell damage that is induced by γ -ray radiation and the possible mechanism of the cytoprotection.



3. Material and Methods

3-1. Cell culture

Chinese hamster lung fibroblasts (V79-4) cells from the American Type Culture Collection were maintained at 37 °C in an incubator with a humidified atmosphere of 5 % CO₂ and cultured in Dulbecco's modified Eagle's medium containing 10 % heat-inactivated fetal calf serum, streptomycin (100 µg/ml) and penicillin (100 units/ml).

3-2. Irradiation

Cells were exposed to γ -ray from a ⁶⁰Co γ -ray source (MDS Nordion C-188 standard source, located in Cheju National University, Jeju, Korea).

3-3. Intracellular reactive oxygen species measurement

The DCF-DA method was used to detect the intracellular ROS level.[8] The V79-4 cells were treated with triphlorethol-A at 30 µM and 1 h later, γ -ray radiation at 10 Gy was applied to the cells. The cells were incubated for an additional 24 h at 37 °C. After the addition of 25 µM of DCF-DA solution, the fluorescence of 2',7'-dichlorofluorescein was detected at 485 nm excitation and at 535 nm emission using a PerkinElmer LS-5B spectrofluorometer.

3-4. Cell viability

The effect of triphlorethol-A on the viability of the V79-4 cells was determined using the [3-(4,5-dimethylthiazol-2-yl)-2,5-diphenyltetrazolium] bromide (MTT) assay, which is based on the reduction of a tetrazolium salt by mitochondrial dehydrogenase in viable cells.[30]

The V79-4 cells were treated with triphlorethol-A at 30 μM and 1 h later, γ -ray radiation at 10 Gy was applied to the cells. The cells were incubated for an additional 48 h at 37 °C. Fifty μl of the MTT stock solution (2 mg/ml) was then added to each well to attain a total reaction volume of 200 μl . After incubating for 4 h, the plate was centrifuged at $800 \times g$ for 5 min and the supernatants were aspirated. The formazan crystals in each well were dissolved in 150 μl of DMSO and the A_{540} was read on a scanning multi-well spectrophotometer.

3-5. Lipid Peroxidation Inhibitory Activity

Lipid peroxidation was assayed by a thiobarbituric acid reaction.[29] The V79-4 cells were treated with triphlorethol-A at 30 μM and 1 h later, γ -ray radiation at 10 Gy was applied to the cells. The cells were incubated for 24 h at 37 °C. The cells were then washed with cold PBS, scraped and homogenized in ice-cold 1.15 % KCl. One hundred μl of the cell lysates was mixed with 0.2 ml of 8.1 % SDS, 1.5 ml of 20 % acetic acid (adjusted to pH 3.5) and 1.5 ml of 0.8 % thiobarbituric acid (TBA). Distilled water was added to the mixture to a final volume of 4 ml and heated to 95 °C for 2 h. After cooling to room temperature, 5 ml of an n-

butanol and pyridine mixture (15:1, v/v) was added to each sample, and the mixture was shaken. After centrifugation at $1000 \times g$ for 10 min, the supernatant fraction was isolated, and the absorbance was measured spectrophotometrically at 532 nm.

3-6. Flow cytometry analysis

Flow cytometry was performed in order to determine the apoptotic sub-G₁ hypodiploid cells.[31] The V79-4 cells were treated with triphlorethol-A at 30 μ M and 1 h later, γ -ray radiation at 10 Gy was applied to the cells. The cells were then incubated for an additional 48 h at 37 °C, subsequently harvested, and fixed in 1 ml of 70 % ethanol for 30 min at 4 °C. The cells were washed twice with PBS, and then incubated for 30 min in the dark at 37 °C in 1 ml of PBS containing 100 μ g propidium iodide and 100 μ g RNase A. Flow cytometric analysis was performed using a FACS Calibur flow cytometer (Becton Dickinson, Mountain View, CA, USA). The proportion of sub-G₁ hypodiploid cells was assessed based on the histograms generated using the computer programs, Cell Quest and Mod-Fit.

3-7. Nuclear Staining with Hoechst 33342

The V79-4 cells were treated with triphlorethol-A at 30 μ M and 1 h later, γ -ray radiation at 10 Gy was applied to the cells. The cells were then incubated for 48 h at 37 °C. After 24 h, 1.5 μ l of Hoechst 33342 (stock 10 mg/ml), a DNA-specific fluorescent dye, was added to

each well (1.5 ml) and incubated for 10 min at 37 °C. The stained cells were observed under a fluorescent microscope, which was equipped with a CoolSNAP-Pro color digital camera to order to examine the degree of nuclear condensation.

3-8. Single cell gel electrophoresis (Comet assay)

Comet assay was performed to determine the oxidative DNA damage.[54,55] The cell suspension was mixed with 75 µl of 0.5 % low melting agarose (LMA) at 39 °C and spread on a fully frosted microscopic slide that was pre-coated with 200 µl of 1 % normal melting agarose (NMA). After solidification of the agarose, the slide was covered with another 75 µl of 0.5 % LMA and then immersed in a lysis solution (2.5 M NaCl, 100 mM Na-EDTA, 10 mM Tris, 1 % Trion X-100, and 10 % DMSO, pH 10) for 1 h at 4 °C. The slides were then placed in a gel-electrophoresis apparatus containing 300 mM NaOH and 10 mM Na-EDTA (pH 13) for 40 min to allow DNA unwinding and the expression of the alkali labile damage. An electrical field was then applied (300 mA, 25 V) for 20 min at 4 °C to draw negatively charged DNA toward an anode. After electrophoresis, the slides were washed three times for 5 min at 4 °C in a neutralizing buffer (0.4 M Tris, pH 7.5) and then stained with 75 µl of propidium iodide (20 µg/ml). The slides were observed with a fluorescence microscope and image analysis (Kinetic Imaging, Komet 5.5, UK). The percentage of total fluorescence in

the tail and the tail length of the 50 cells per slide were recorded.

3-9. Statistical analysis

All measurements were made in triplicate and all values were represented as means \pm S.E.

The results were subjected to an analysis of the variance (ANOVA) using the Tukey test to analyze the difference. $p < 0.05$ were considered significantly.



4. Results

4.1 Radical Scavenging Activity of Triphlorethol-A on the ROS Generated by γ -ray

Radiation

The radical scavenging effect of triphlorethol-A on the ROS generated by γ -ray radiation was measured. Triphlorethol-A at 30 μ M decreased the level of intracellular ROS induced by radiation (Figs. 7A and B).

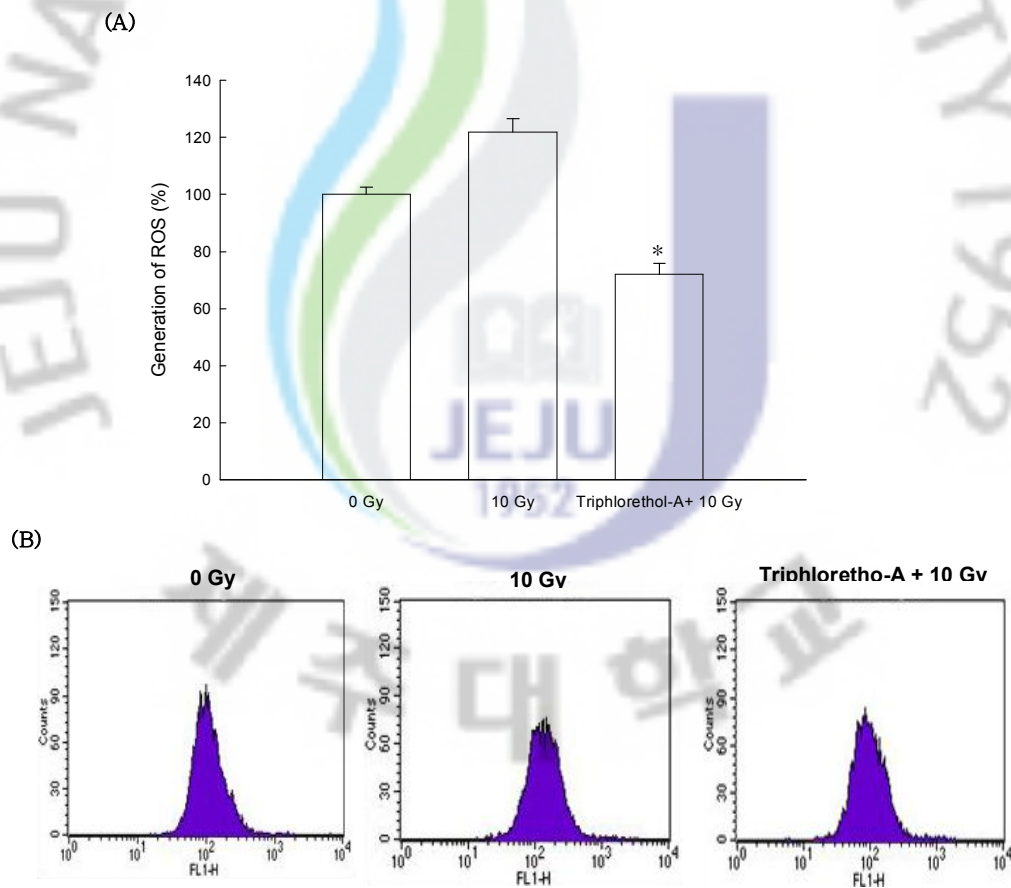


Fig. 7. Effect of triphlorethol-A on scavenging intracellular ROS generated by γ -ray radiation. The intracellular ROS was detected using fluorescence spectrophotometer (A) and flow cytometry (B) after DCF-DA staining. The measurements were made in triplicate and values are expressed as means \pm S.E. FI means fluorescence intensity. *Significantly different from radiation ($p < 0.05$).

4.2 Effect of Triphlorethol-A on Lipid Peroxidation

The ability of triphlorethol-A to inhibit membrane lipid peroxidation and cellular DNA damage in radiated cells was also investigated. Ionizing radiation induced damage to cell membrane and this one of the most important lesions was responsible for loss of viability. The peroxidation of membrane lipids is the major lesion in the membranes. As shown in Fig. 8, V79-4 cells exposed to γ -rays *in vitro* showed an increase in the lipid peroxidation, which was monitored by the generation of thiobarbituric acid reactive substance (TBARS). However, triphlorethol-A prevented the radiation-induced peroxidation of lipids.

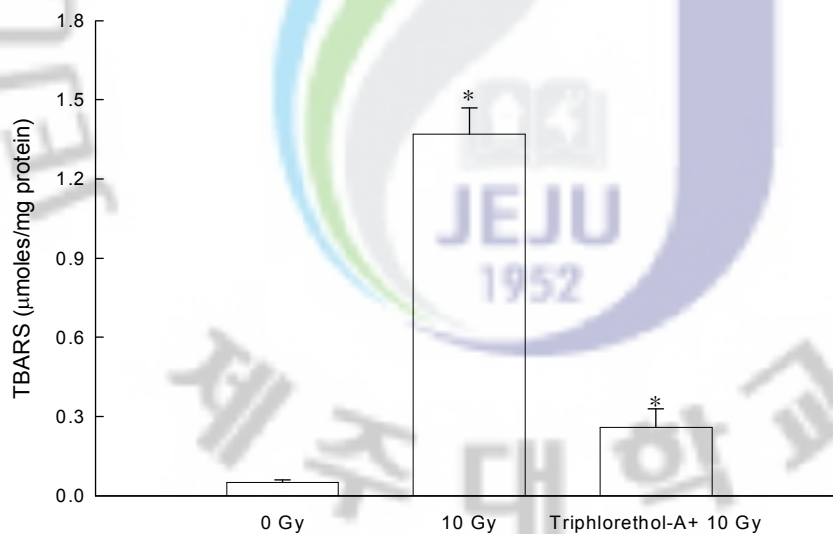


Fig. 8. Protective effect of triphlorethol-A upon γ -ray radiation-induced lipid membrane damage of V79-4 cells. Lipid peroxidation was assayed by measuring the amount of TBARS. The measurement was made in triplicate and values are expressed as means \pm S.E. *Significantly different from control ($p < 0.05$).

4.3 Effect of Triphlorethol-A on Cell Damage Induced by Radiation

Damage to cellular DNA induced by γ -radiation exposure was detected using an alkaline comet assay. The exposure of cells to radiation increased comet parameters like tail length and percentage of DNA in the tails of cells, which suggested radiation-induced damage from γ -radiation. Treatment with triphlorethol-A before irradiation resulted in a decrease of tail length (Fig. 9A). When the cells were exposed to γ -radiation at 10 Gy, the percent of DNA in the tail was increased 50.1 ± 3.4 as shown in Fig. 9B. Treatment with triphlorethol-A resulted in a decrease to 29.5 ± 2.3 , which indicated a protective effect of triphloroethol-A on radiation-induced DNA damage *in vitro*.

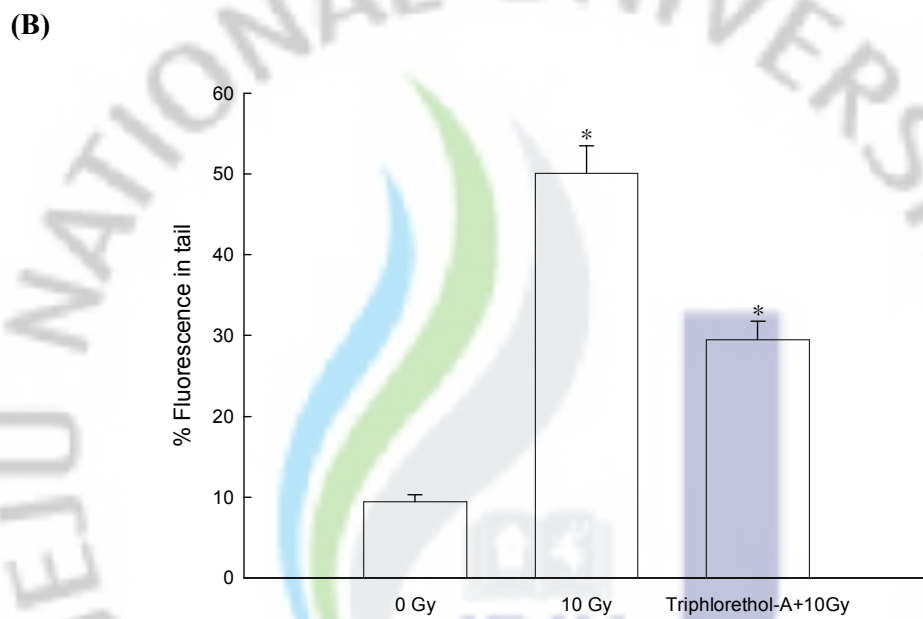
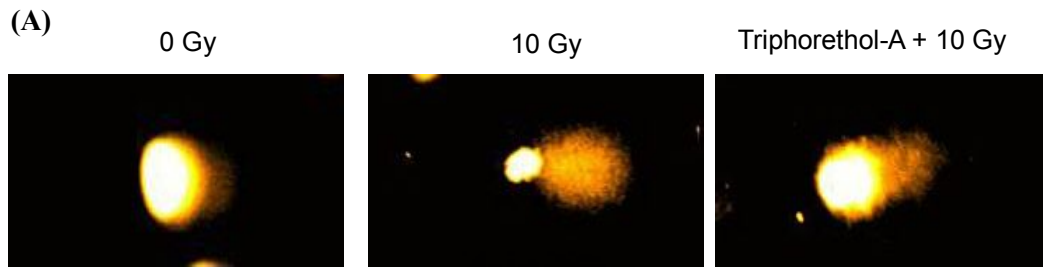


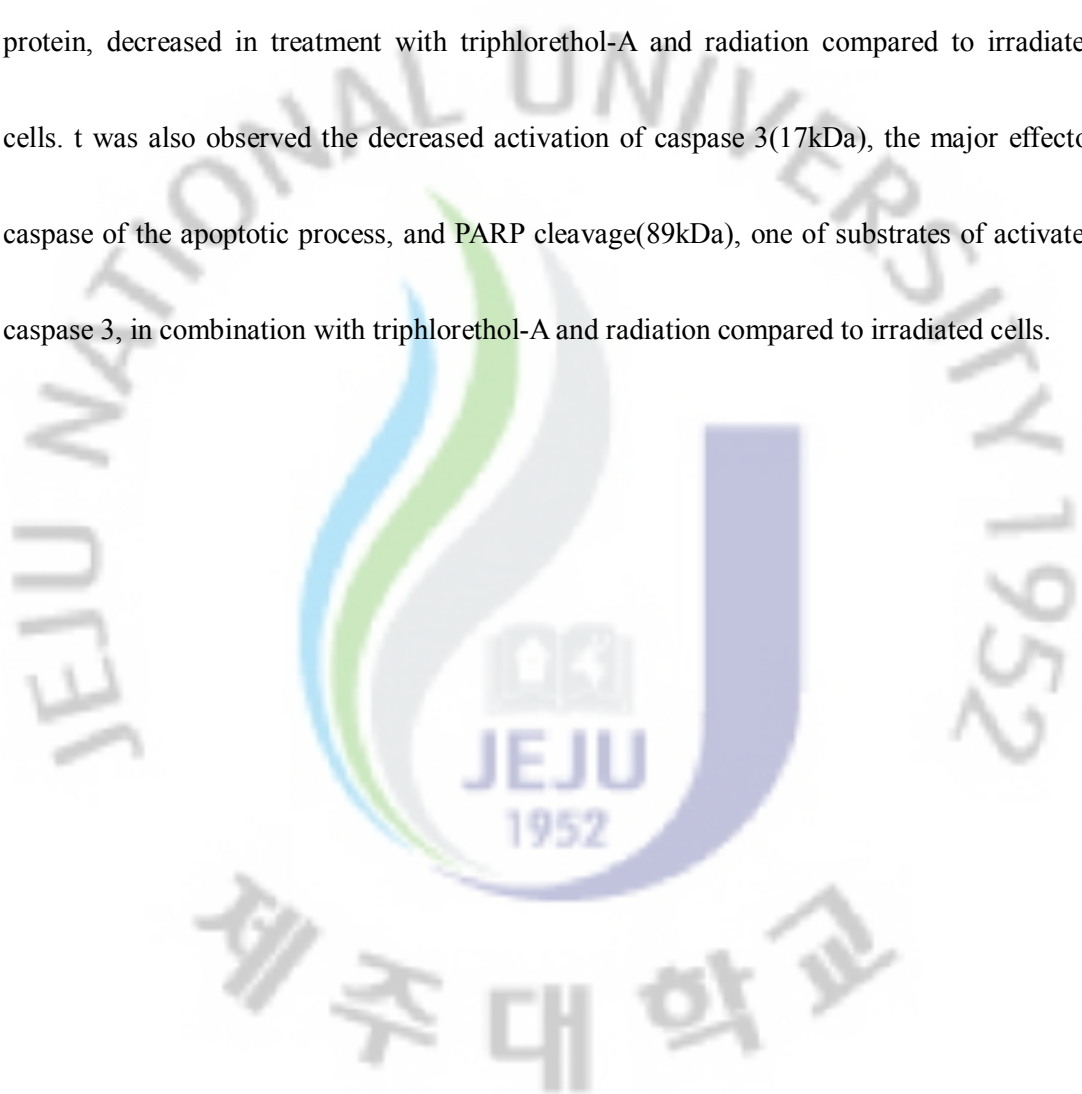
Fig. 9. Protective effect of triphlorethol-A upon γ -ray radiation-induced cellular DNA damage of V79-4 cells. The cellular DNA damage was detected by an alkaline comet assay. The measurement was made in triplicate and values are expressed as means \pm S.E. *Significantly different from control ($p < 0.05$).

4.4 Cytoprotective Effect of Triphlorethol-A on Radiation-Induced Apoptosis

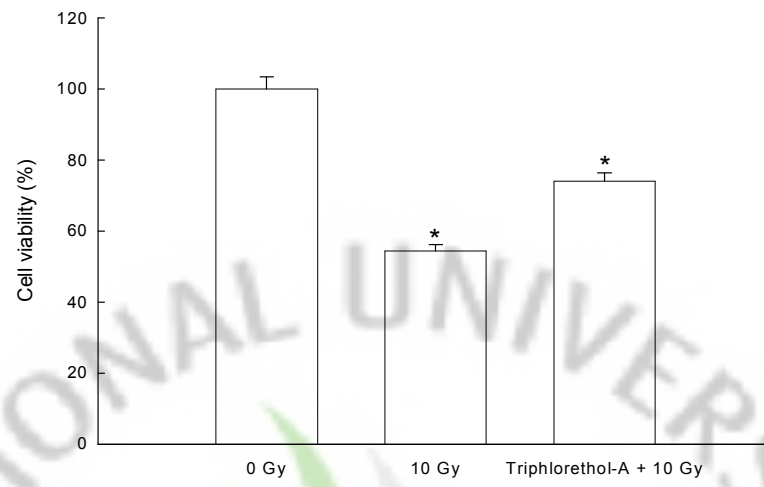
The protective effect of triphlorethol-A on cell survival in V79-4 cells exposed to radiation was also measured. As demonstrated in Fig. 10A, treatment with triphlorethol-A at 30 μ M increased 74 % of the cell survival compared with 54 % of the cell survival in irradiated cells. In order to study the cytoprotective effect of triphlorethol-A on radiation-induced apoptosis, nuclei of V79-4 cells were stained with Hoechst 33342 for microscopy and with propidium iodide for flow cytometric analysis. The microscopic pictures in Fig. 10B demonstrated that the control cells had intact nuclei, and the radiation-exposed cells demonstrated significant nuclear fragmentation, which is characteristic of apoptosis. However, when the cells were treated with triphlorethol-A for 1 h prior to radiation, dramatic decrease in nuclear fragmentation was observed. In addition to the morphological evaluation, the protective effect of triphlorethol-A against apoptosis was confirmed by flow cytometry. As demonstrated in Fig. 10C, an analysis of the DNA content in the radiation-exposed cells revealed an increase of 35 % in apoptotic sub-G₁ DNA content, compared with 2 % of apoptotic sub-G₁ DNA content in untreated cells. Treatment with 30 μ M of triphlorethol-A decreased the apoptotic sub-G₁ DNA content to 18 %. These results suggested that triphlorethol-A protects cell viability by inhibiting radiation-induced apoptosis. To understand how triphlorethol-A protects radiation-induced apoptosis, we examined changes

of Bcl-2 families and caspase activities by western blot.

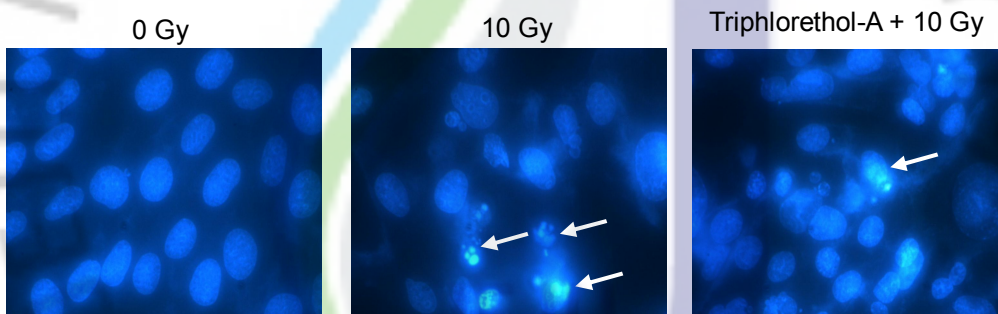
As shown in Fig. 10. D the Bcl-2, an anti-apoptotic protein, recovered in treatment with triphlorethol-A and radiation compared to irradiated cells and the Bax, a pro-apoptotic protein, decreased in treatment with triphlorethol-A and radiation compared to irradiated cells. It was also observed the decreased activation of caspase 3(17kDa), the major effector caspase of the apoptotic process, and PARP cleavage(89kDa), one of substrates of activated caspase 3, in combination with triphlorethol-A and radiation compared to irradiated cells.



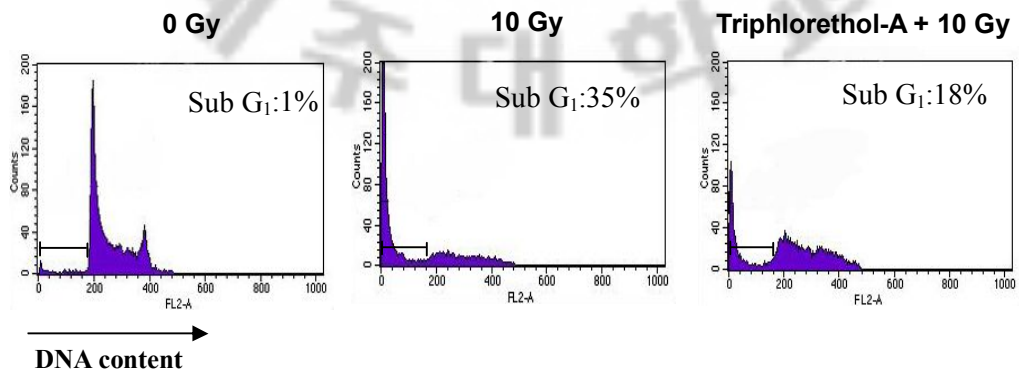
(A)



(B)



(C)



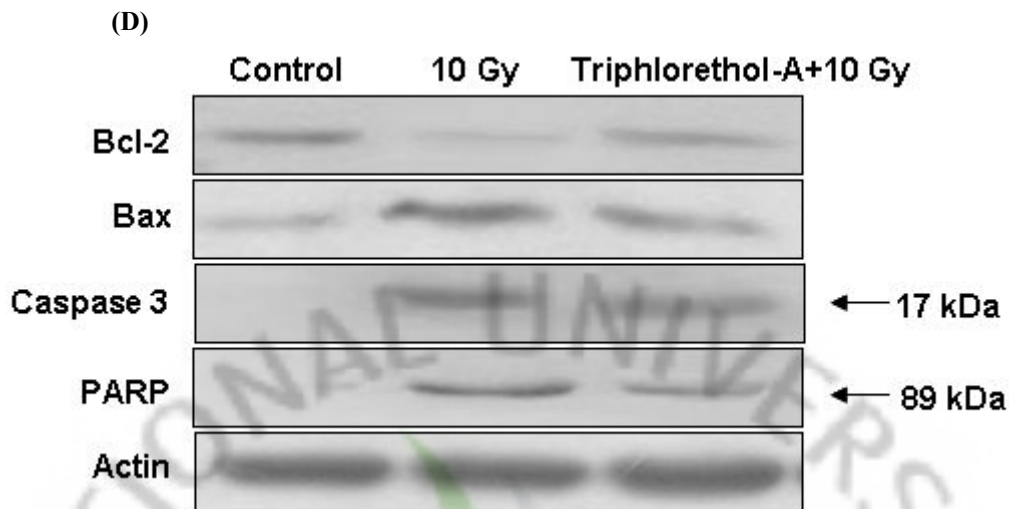


Fig. 10. Protective effect of triphlorethol-A upon γ -ray radiation-induced cell damage of V79-4 cells. (A) The viability of V79-4 cells upon radiation was determined by MTT assay. The measurements were made in triplicate and values are expressed as means \pm S.E. *Significantly different from control ($p < 0.05$). (B) Apoptotic body formation was observed under a fluorescence microscope after Hoechst 33342 staining and apoptotic bodies are indicated by arrows. (C) Apoptotic sub- G_1 DNA content was detected by flow cytometry after propidium iodide staining. (D) Western blot analysis was performed using anti-bcl-2, -bax, -caspase 3 and -PARP antibodies.

4. Discussion

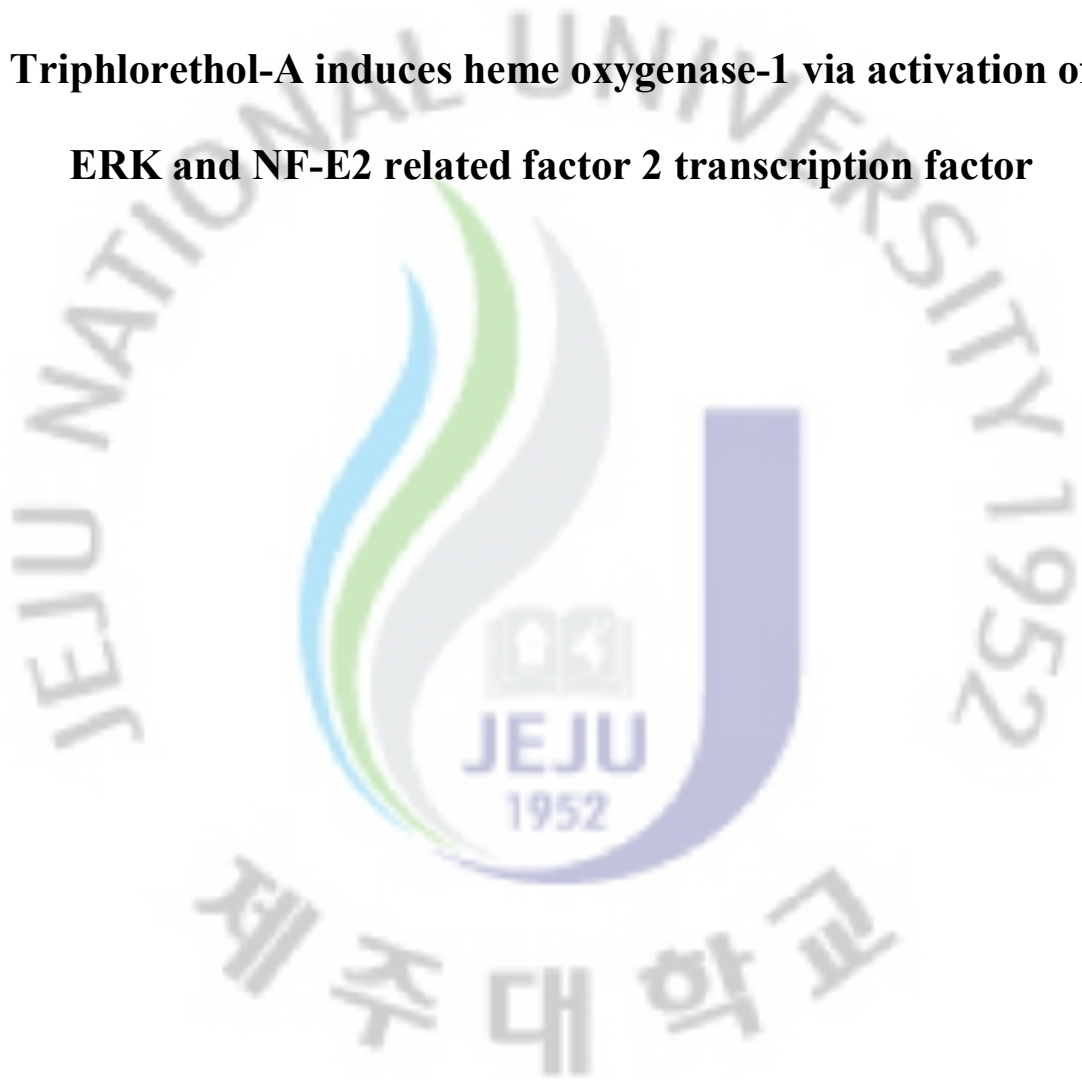
Exposure to ionizing radiation causes cell damage through the production of ROS which induces oxidative stress.[55] The role of ROS in radiation injury and the potential of antioxidants to reduce these deleterious effects have been studied for more than 50 years.[56] Radioprotective agents minimize this damage by reducing the generation of free radicals.[57] Increased understandings of the interrelationship between the effects of oxygen and radiation exposure lead to a rational application of naturally occurring antioxidants.[58] Our study demonstrated that in addition to an antioxidant effect,[59] triphlorethol-A has protective activity against γ -radiation *in vitro*. Triphlorethol-A scavenged the ROS generated by radiation. Radiation-induced cellular lethality occurs through the formation of aqueous free radicals, which attack vital cellular sites, such as DNA and cell membranes. The cellular membrane and DNA are the two main targets of radiation-induced lethality. The formation of lipid peroxides in cells exposed to γ -radiation is one of the markers of the membrane damage. Triphloroethol-A protected the cell membrane lipids from the peroxidation damage induced by radiation. In addition, triphlorethol-A inhibited the increase of radiation-induced comet parameters, which indicated the protection of cellular DNA.

These inhibition effects of triphlorethol-A against lipid and DNA damage resulted in protective effects against radiation- induced cell death. Triphlorethol-A is polymer of phloroglucinol and has a polyphenol structure. The presence of a phenolic group with aromatic conjugation, which exists in the structure of triphlorethol-A, contributes to the scavenging ROS generated by irradiation. Our study demonstrated that triphlorethol-A has a radioprotective effect through scavenging ROS generated by radiation.



PART III

**Triphloretol-A induces heme oxygenase-1 via activation of
ERK and NF-E2 related factor 2 transcription factor**



1. Abstract

Triphlorethol-A, phlorotannin found in *Ecklonia cava*, exerted cytoprotective effects against oxidative stress and the underlying molecular mechanism was investigated. Triphlorethol-A induced heme oxygenase-1 (HO-1) expression at mRNA and protein levels, leading to increased HO-1 activity. NF-E2 related factor 2 (Nrf2), transcription factor involved in the cellular protection against oxidative stress, regulates antioxidant response element (ARE)-directed induction of several phase 2 detoxifying and antioxidant enzymes. Triphlorethol-A increased nuclear translocation, ARE binding, and transcriptional activity of Nrf2. Moreover, triphlorethol-A exhibited activation of extracellular signal regulated protein kinase (ERK). U0126, inhibitor of ERK kinase, suppressed triphlorethol-A induced activation of Nrf2 and finally decreased HO-1 protein level. Pharmacological inhibitors of HO-1 and ERK attenuated the cytoprotective effect of triphlorethol-A on H₂O₂ or radiation induced oxidative stress. Taken together, these data suggest that triphlorethol-A augments cellular antioxidant defense capacity through induction of HO-1 via ERK-Nrf2-ARE signaling pathway, thereby protecting cells from oxidative stress.

Keywords: triphlorethol-A; heme oxygenase-1; NF-E2 related factor 2; antioxidant response element

2. INTRODUCTION

Heme oxygenase-1 (HO-1) catalyzes the rate-limiting step in heme catabolism, leading to the formation of biliverdin, free iron and carbon monoxide. In the presence of biliverdin reductase, biliverdin is further converted to bilirubin, which is a potent antioxidant [60-62]. HO-1 expression is induced in response to various chemically or physiologically produced oxidative stresses in cells and tissues [63-66]. The HO-1 pathway represents a primer cellular defense system against oxidative stress [63, 67-71]. Recently, a new class of AP-1 related sequences has been shown to mediate the oxidative stress responsiveness of the HO-1 gene. These regions, termed stress responses elements (StRE) or antioxidant responses elements (ARE), are tightly regulated by the redox-sensitive transcription factor, NF-E2 regulated factor 2 (Nrf2) [72]. ARE is a *cis*-acting enhancer sequence that mediates transcriptional activation of Nrf2 in response to oxidative stress [73]. ARE is found in the promoters of genes that encode HO-1 [74] and other cellular antioxidant enzymes, such as γ -glutamylcysteine synthetase [75]. Therefore, genes regulated by the ARE encode proteins that help control of the cellular redox status and protect the cells from oxidative damage [76]. Mitogen activated protein kinase (MAPK) family are important signaling intermediates involved transducing a variety of signals from

the cell surface to the nucleus. MAPKs pathway associates with the modulation of ARE driven gene expression via Nrf2 activation. ERK and p38 MAPK pathways involved the nucleus binding of Nrf2 to the ARE [77]. Inhibition of ERK and p38 abrogated binding of Nrf2 and induction of ARE-driven γ -glutamylcysteine synthetase [78].

In view of the increasing evidence explaining the importance of carbon monoxide and bilirubin in counteracting cellular dysfunction [79-82], attention has recently been focused on up-regulation of HO-1 by natural compounds [83-87]. Recently, we reported that triphlorethol-A protected cells from H₂O₂ induced oxidative stress via radical quenching and catalase activation⁴² and from ionizing radiation induced cellular damage [94].

In the present study, we investigated the capability of triphlorethol-A to induce the antioxidant enzyme HO-1 via activation of the Nrf2 transcription factor.

3. Material and Methods

3-1. Reagents

[3-(4,5-dimethylthiazol-2-yl)-2,5-diphenyltetrazolium] bromide (MTT) and zinc protoporphyrin (ZnPP) were purchased from Sigma Chemical Company, St. Louis, MO, USA. Primary rabbit polyclonal anti-ERK, phospho-ERK, Nrf2, and actin antibodies were purchased from Santa Cruz Biotechnology, Santa Cruz, CA, USA. U0126 was provided from Calbiochem, San Diego, CA, USA. The ARE-luciferase reporter gene was kindly provided by Dr. Young-Joon Surh (Seoul National University, Seoul, Korea). The other chemicals and reagents were of analytical grade.

3-2. Cell culture

The lung is an organ sensitive to oxidative stress [110-111]. To study the effect of triphlorethol-A on oxidative stress, we used Chinese hamster lung fibroblasts (V79-4 cells). The V79-4 cells (American type culture collection) were maintained at 37°C in an incubator with a humidified atmosphere of 5% CO₂ and cultured in Dulbecco's modified Eagle's medium containing 10% heat-inactivated fetal calf serum, streptomycin (100 µg/ml) and penicillin (100 units/ml).

3-3. Cell Viability

The effect of triphlorethol-A on the viability of the V79-4 cells was determined by the MTT assay [63]. The cells were treated with 30 µM triphlorethol-A, followed 1 h later by H₂O₂ or

γ -irradiation at 5 Gy. The cells were seeded in a 96 well plate at a density of 1×10^5 cells/ml and incubated for 48 h at 37°C. Fifty μ l of the MTT stock solution (2 mg/ml) was then added to each well to attain a total reaction volume of 200 μ l. After incubation for 4 h, the plate was centrifuged at $800 \times g$ for 5 min and the supernatants were aspirated. The formazan crystals in each well were dissolved in 150 μ l DMSO, and the A_{540} was read on a scanning multi-well spectrophotometer.

3-4. HO-1 assay

HO-1 enzyme activity was measured as described previously [114]. Cells were homogenized in 0.5 ml ice-cold 0.25 M sucrose solution containing 50 mM potassium phosphate buffer (pH 7.4). Homogenates were centrifuged at $200 \times g$ for 10 min. The supernatants were centrifuged at $9000 \times g$ for 20 min, and further centrifuged at $105,000 \times g$ for 60 min. The pellet was then resuspended in 50 mM potassium phosphate buffer (pH 7.4) and the amount of protein was determined. The reaction mixture (200 μ l) containing 0.2 mM of the substrate hemin, 500 μ g/ml of cell lysate, 0.5 mg/ml rat liver cytosol as a source of biliverdin reductase, 0.2 mM $MgCl_2$, 2 mM glucose-6-phosphate, 1U/ml glucose-6-phosphate dehydrogenase, 1 mM NADPH and 50 mM potassium phosphate buffer (pH 7.4) was incubated at 37°C for 2 h. The reaction was stopped with 0.6 ml of chloroform and after extraction, the chloroform layer was measured spectrophotometrically. Bilirubin formation

was calculated from the difference in absorption between 464 and 530 nm.

3-5. Western blot

The V79-4 cells were plated at 1×10^5 cells/ml, and sixteen hours after plating, the cells were treated with 30 μ M triphlorethol-A. The cells were harvested at the indicated times, and washed twice with PBS. The harvested cells were then lysed on ice for 30 min in 100 μ l of lysis buffer [120 mM NaCl, 40 mM Tris (pH 8), 0.1% NP 40] and centrifuged at $13,000 \times g$ for 15 min. Supernatants were collected from the lysates and protein concentrations were determined. Aliquots of the lysates (40 μ g of protein) were boiled for 5 min and electrophoresed on a 10% SDS-polyacrylamide gel. Blots in the gels were transferred onto nitrocellulose membranes (Bio-Rad, Hercules, CA, USA), which were then incubated with primary antibodies. The membranes were further incubated with secondary antibody-horseradish peroxidase conjugates (Pierce, Rockland, IL, USA), and exposed to X-ray film. Protein bands were detected using an enhanced chemiluminescence Western blotting detection kit (Amersham, Little Chalfont, Buckinghamshire, UK).

3-6. Reverse transcriptase polymerase chain reaction

Total RNA was isolated from V79-4 cells using Trizol (GibcoBRL, Grand Island, NY, USA). Reverse transcriptase polymerase chain reaction (RT-PCR) was performed as described previously.[115] PCR conditions for HO-1 and for the housekeeping gene, β -actin, were: 35

cycles of 94°C for 45 sec; 53°C for 45 sec; and 72°C for 60 sec. The primer pairs (Bionics, Seoul, Korea) were follows (forward and reverse, respectively): HO-1, 5'-GAG AAT GCT GAG TTC ATG -3' and 5'-ATG TTG AGC AGG AAG GC-3'; and β -actin, 5'-GTG GGC CGC CCT AGG CAC CAG G-3'; and 5'-GGA GGA AGA GGA TGC GGC AGT G-3'. Amplified products were resolved by 1% agarose gel electrophoresis, stained with ethidium bromide, and photographed under ultraviolet light.

3-7. Nuclear extract preparation and electrophoretic mobility shift assay

The cells were harvested at the indicated times, and were then lysed on ice with 1 ml of lysis buffer (10 mM Tris-HCl, pH 7.9, 10 mM NaCl, 3 mM MgCl₂, and 1% NP-40) for 4 min. After 10 min of centrifugation at 3,000 × g, the pellets were re-suspended in 50 μ l of extraction buffer (20 mM HEPES, pH 7.9, 20% glycerol, 1.5 mM MgCl₂, 0.2 mM EDTA, 1 mM DTT, and 1 mM PMSF), incubated on ice for 30 min, and centrifuged at 13,000 × g for 5 min. The supernatant was then harvested as nuclear protein extracts and stored at -70°C after determination of protein concentration. Synthetic double strand oligonucleotide containing the Nrf2-binding domain (ARE) was labeled with [γ -³²P] ATP using T4 polynucleotide kinase, and used as probes. The probes (50,000 cpm) were incubated with 6 μ g of the nuclear extracts at 4°C for 30 min in a final volume of 20 μ l containing 12.5% glycerol, 12.5 mM HEPES (pH 7.9), 4 mM Tris-HCl (pH 7.9), 60 mM KCl, 1 mM EDTA,

and 1 mM DTT with 1 μ g of poly (dI-dC). Binding products were resolved on a 5% polyacrylamide gel and the bands were visualized by autoradiography.

3-8. Transient transfection and luciferase assay

A day before transfection, cells were sub-cultured at a density of 1×10^6 cells in 60 mm dish to maintain approximately 60-80% confluency. The cells were transiently transfected with the plasmid harboring the ARE-promoter using the transfection reagent DOTAP according to the manufacturer's instructions (Roche, Mannheim, Germany). After overnight transfection, cell were treated with 30 μ M triphlorethol-A. Cell were then washed twice with PBS and lysed with reporter lysis buffer. After vortex-mixing and centrifugation at $12,000 \times g$ for 1 min at 4°C, the supernatant was stored at -70°C for the luciferase assay. After 20 μ l of the cell extract was mixed with 100 μ l of the luciferase assay reagent at room temperature, the mixture was placed in a luminometer to measure the light produced.

3-9. Immunocytochemistry

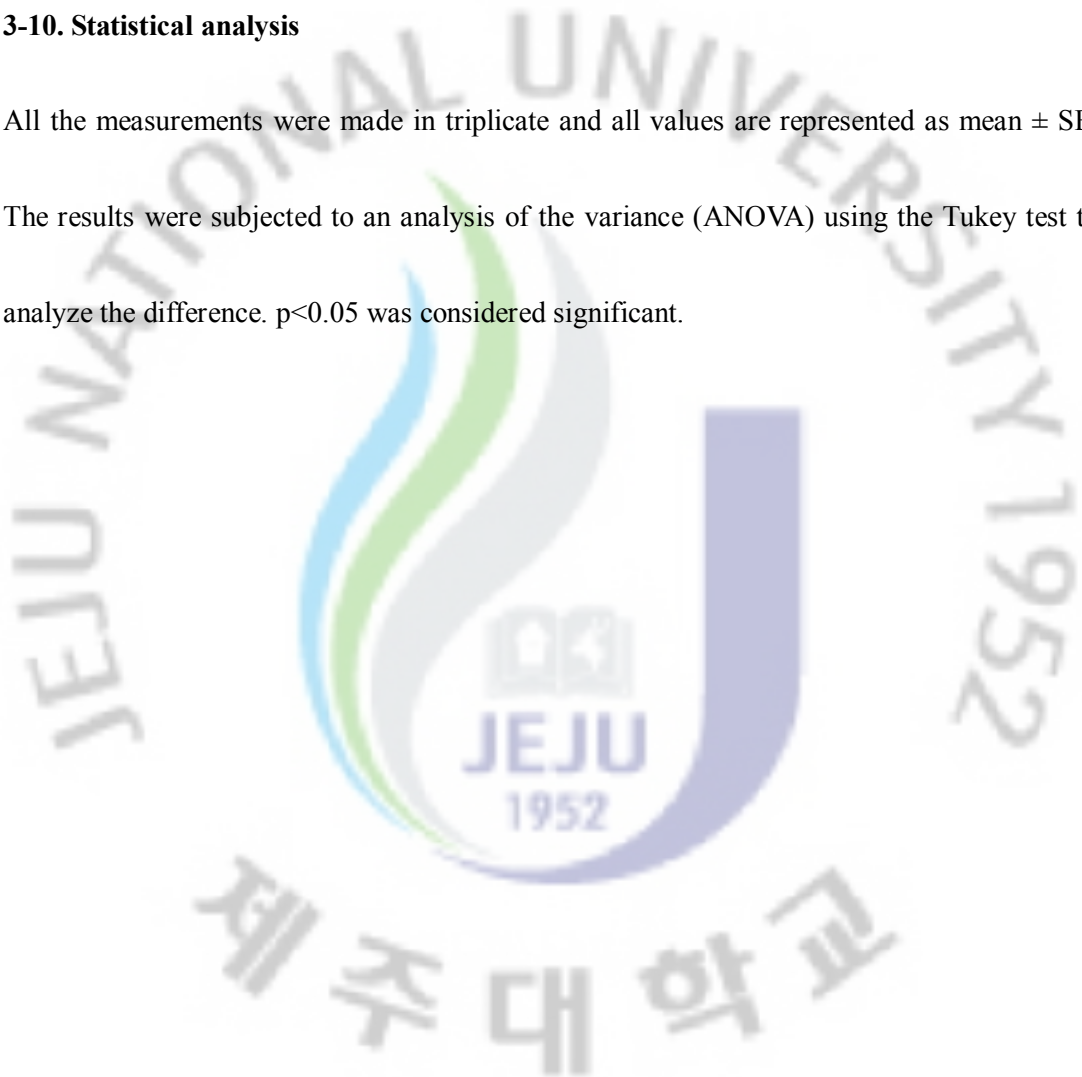
Cells plated on coverslips were fixed with 4% paraformaldehyde for 30 min and permeabilized with 0.1% Triton X-100 in PBS for 2.5 min. Cells were treated with blocking medium (3% bovine serum albumin in PBS) for 1 h and incubated with Nrf2 antibody diluted in blocking medium for 2 h. Immuno-reacted primary Nrf2 antibody was detected by a 1:500 dilution of FITC-conjugated secondary antibody (Jackson ImmunoResearch

Laboratories, West Grove, PA, USA) for 1 h. After washing with PBS, stained cells were mounted onto microscope slides in mounting medium with DAPI (Vector, Burlingame, CA, USA). Images were collected using the LSM 510 program on a Zeiss confocal microscope.

3-10. Statistical analysis

All the measurements were made in triplicate and all values are represented as mean \pm SE.

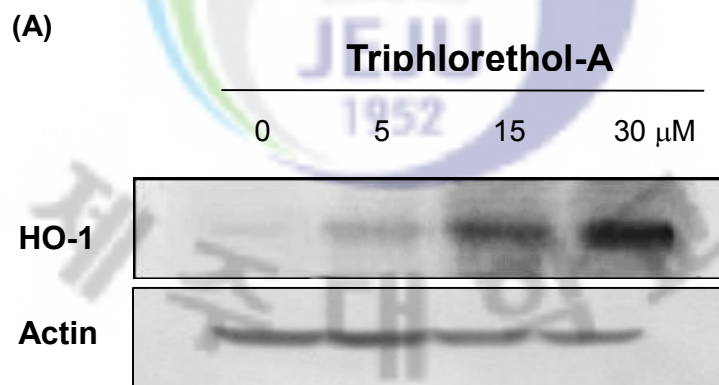
The results were subjected to an analysis of the variance (ANOVA) using the Tukey test to analyze the difference. $p < 0.05$ was considered significant.



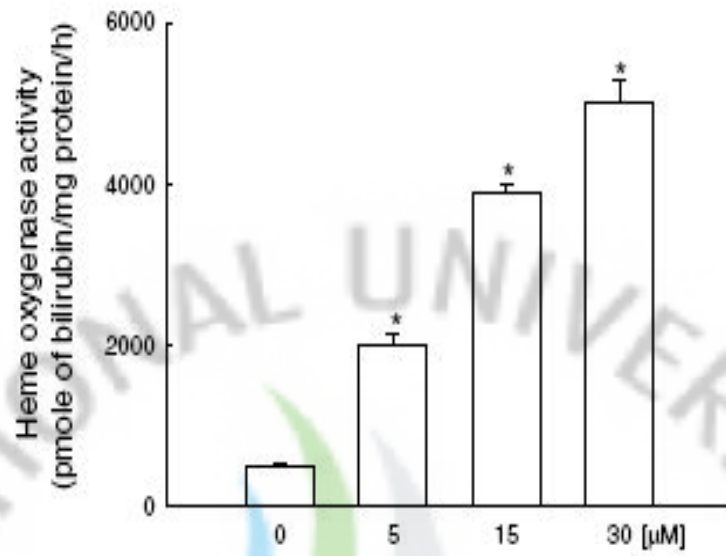
4. Results

4.1 Effect of triphlorethol-A on HO-1 expression and activity

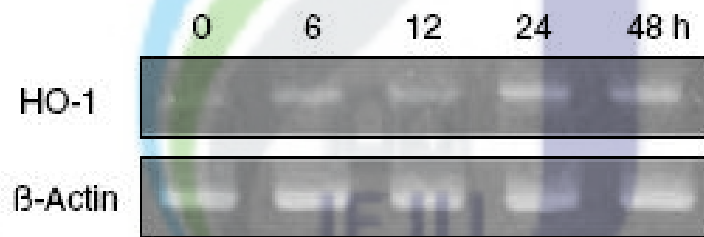
As HO-1 is an important component of the cellular defense against oxidative stress, we assessed whether triphlorethol-A could induce HO-1 expression in relation to its antioxidant activity. V79-4 cells exposed to triphlorethol-A for 48 h showed a concentration-dependent increase in HO-1 protein expression (Figure 11A). The enhanced HO-1 expression correlated with increased HO-1 activity (Figure 11B). Treatment of cells with 30 μ M triphlorethol-A resulted in a time-dependent increase in HO-1 mRNA and protein expression (Figures 11C and 11D), which was accompanied by a gradual increase in HO-1 activity (Figure 11E).



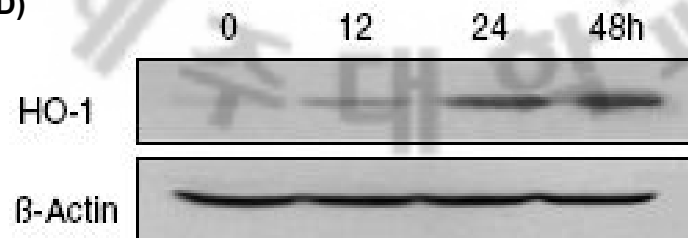
(B)



(C)



(D)



(E)

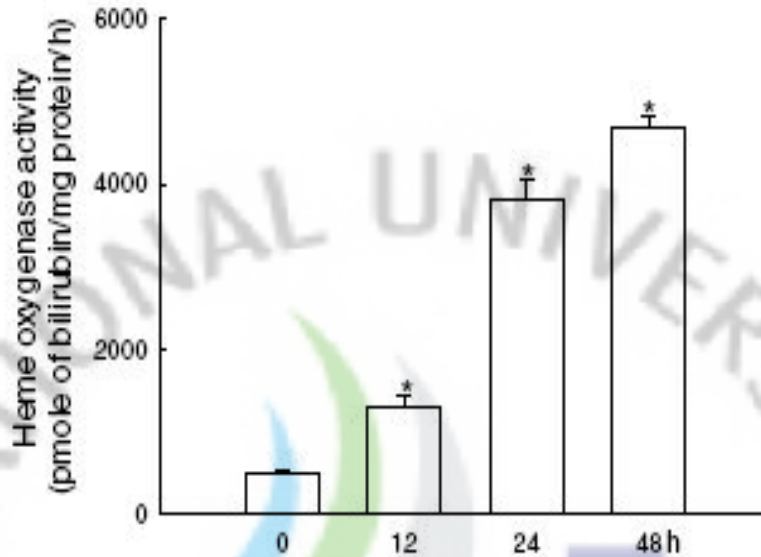


Figure 11. Effect of triphlorethol-A on heme oxygenase-1 mRNA, protein expression and activity in V79-4 cells. (A) Cell lysates treated by various concentration of triphlorethol-A at 48 h were electrophoresed and the expression of HO-1 expression was detected by a HO-1 specific antibody. Control cells were incubated in 0.1% DMSO in medium, which is the same concentration used to dissolve triphlorethol-A. (B) HO-1 activity was measured at 48 h after exposure to various concentration of triphlorethol-A. Each bar represents the mean \pm SE in triplicate experiments. *Significantly different from control ($p < 0.05$). (C) Cells were exposed to 30 μ M of triphlorethol-A and total RNA was extracted at the times indicated. HO-1 mRNA expression was analyzed at indicated times by RT-PCR. The β -actin band is shown to confirm integrity and equal loading of RNA. (D) Cell lysates were electrophoresed and the expression of HO-1 protein was detected at indicated times by a HO-1 specific antibody. (E) Cells were exposed to 30 μ M triphlorethol-A and HO-1 activity was measured at indicated times. Data are expressed as the mean \pm SE in triplicate experiments. *Significantly different from control ($p < 0.05$).

4.2 Triphlorethol-A increased the nuclear translocation, ARE-binding, and transcriptional activity of Nrf2

Most of the genes encoding phase II detoxifying and antioxidant enzymes have an ARE sequence in their promoter region. Nrf2 is an important transcription factor that regulates ARE-driven HO-1 gene expression. Subsequently, we examined whether triphlorethol-A could activate Nrf2 in association with HO-1 up-regulation in V79-4 cells. Triphlorethol-A treatment resulted in increased Nrf2 accumulation in the nucleus (Figure 12A and 12B). Nrf2 activation in triphlorethol-A treated cells was assessed by EMSA with an oligonucleotide harboring a consensus Nrf2 binding element. Triphlorethol-A treated cells exhibited a high level of Nrf2 activation (Figure 12C). The transcriptional activity of Nrf2 was also assessed using an ARE promoter construct containing the Nrf2 binding DNA consensus site linked to a luciferase reporter gene. As illustrated in Figure 12D, triphlorethol-A increased the transcriptional activity of Nrf2.

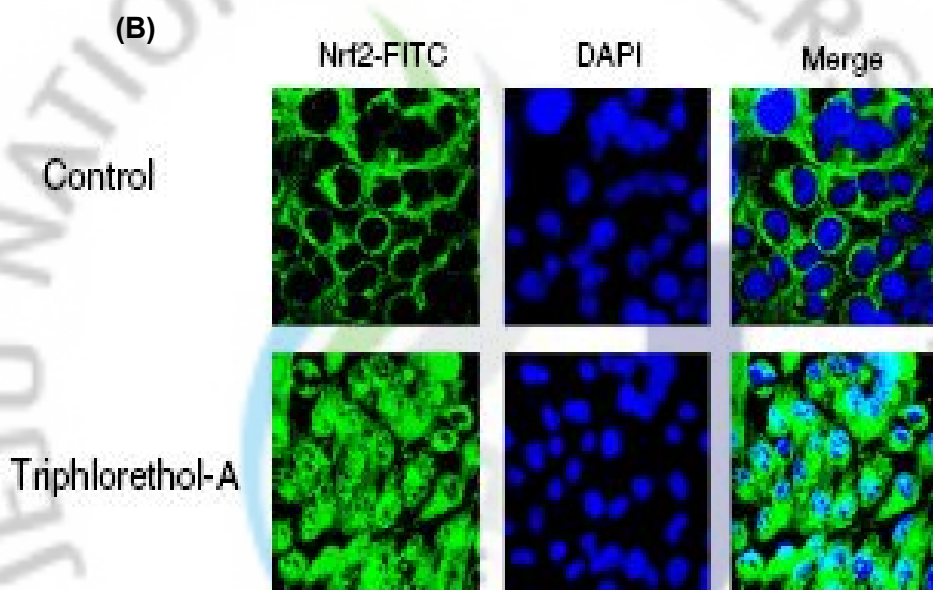
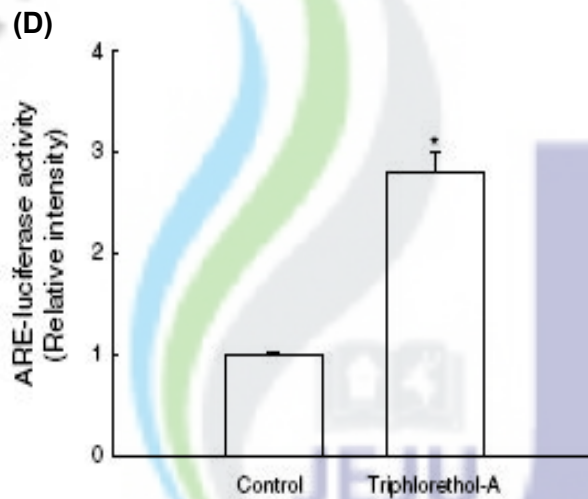
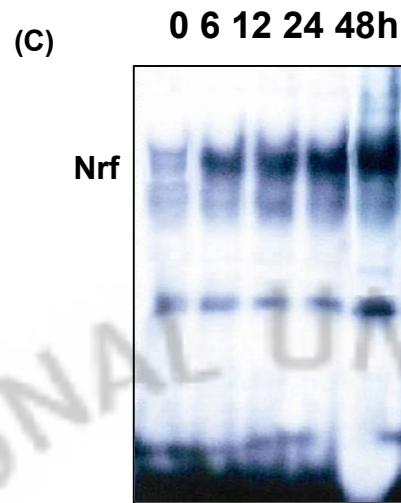


Figure 12. Effect of triphlorethol-A on Nrf2 expression, translocalization into nucleus, and its transcriptional activity in V79-4 cells. (A) Effect of triphlorethol-A on the protein levels of nuclear Nrf2. Nuclear extract from V79-4 cells was prepared from after treatment with 30 μ M triphlorethol-A for the indicated times. Immunoblots for nuclear lysates from treated V79-4 cells were detected with a Nrf2 specific antibody. (B) Effect of triphlorethol-A on nuclear localization of Nrf2. Confocal image shows that FITC-conjugated secondary antibody staining indicates the location of Nrf2 (green) by anti- Nrf2 antibody, DAPI staining indicates the location of the nucleus (blue), and merged image in triphlorethol-A treated cells indicates the nuclear location of Nrf2 protein.

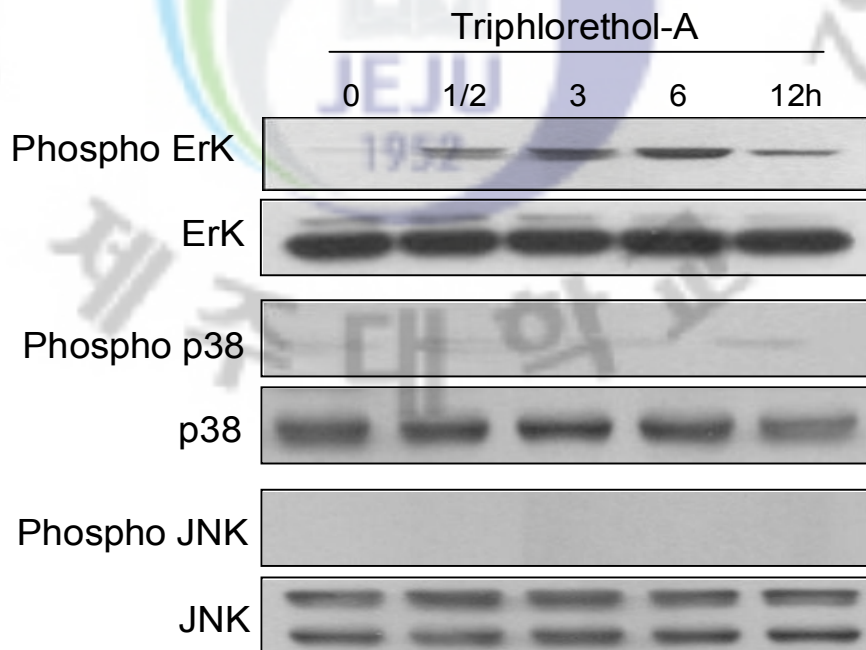


(C) Effect of triphlorethol-A on the ARE-binding activity of Nrf2 in V79-4 cells. Nuclear extracts prepared from V79-4 cells were treated with 30 μ M of triphlorethol-A for the indicated times. (D) Effect of triphlorethol-A on the transcriptional activity of Nrf2 in V79-4 cells. V79-4 cells were transfected with an ARE-luciferase construct (1 μ g per well) or control vector (1 μ g per well). After overnight, cells were treated with triphlorethol-A, cell lysates were mixed with a luciferase substrate, and the luciferase activity was measured by the luminometer. Data are expressed as the mean \pm SE in triplicate experiments. *Significantly different from control ($p < 0.05$).

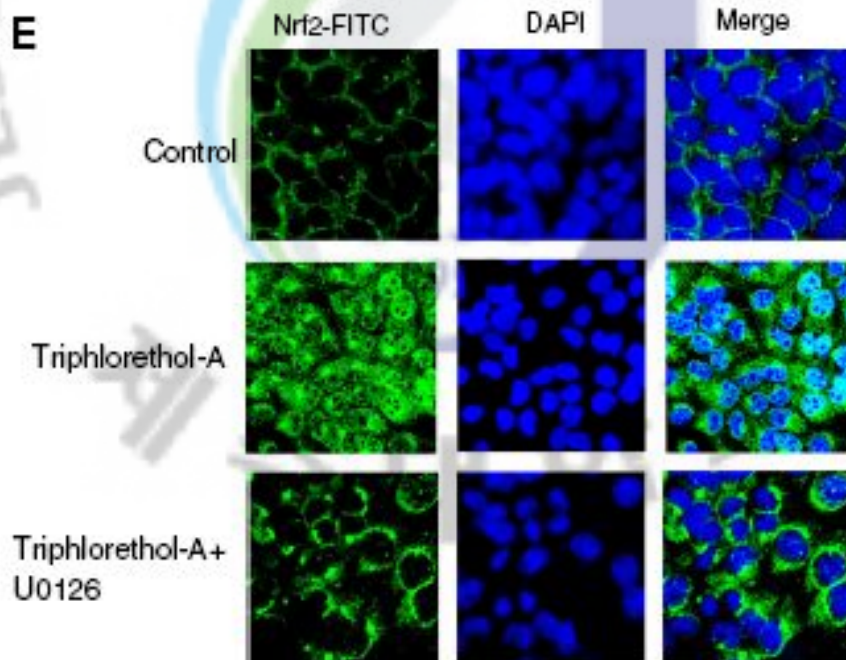
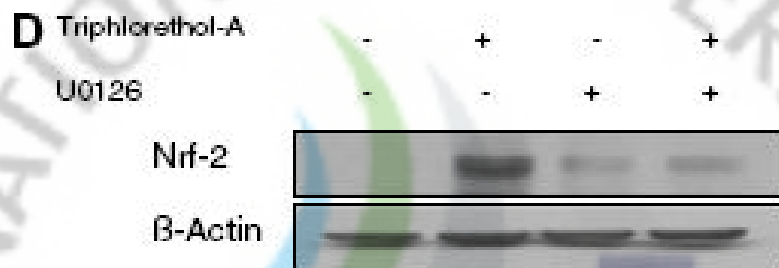
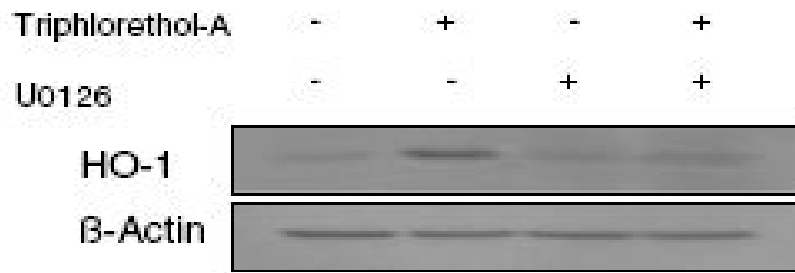
4. 3 Triphlorethol-A activates Nrf2 via phosphorylation of ERK

To further elucidate the upstream signaling pathway involved in triphlorethol-A mediated Nrf2 activation and induction of HO-1, we examined the activation of ERK, a major signaling enzyme involved in cell survival against oxidative stress. As shown in Figure 13A, Western blot analysis showed that triphlorethol increased ERK phosphorylation but unchanged in phospho p38 kinase and not detectable phospho JNK . . Pretreatment with U0126 effectively suppressed triphlorethol-A induced HO-1 induction (Figure 13B). The nuclear accumulation of Nrf2 was significantly inhibited by U0126 (Figure 13C and 13D). Likewise, transcriptional activity of Nrf2 was effectively blocked by U0126 (Figure 13E).

(A)



(B)



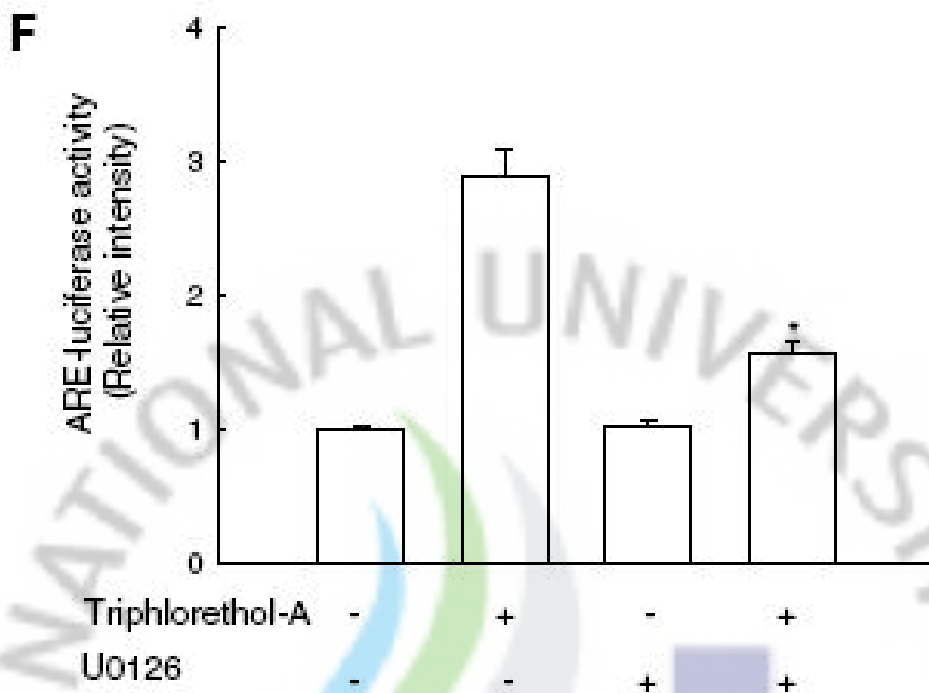
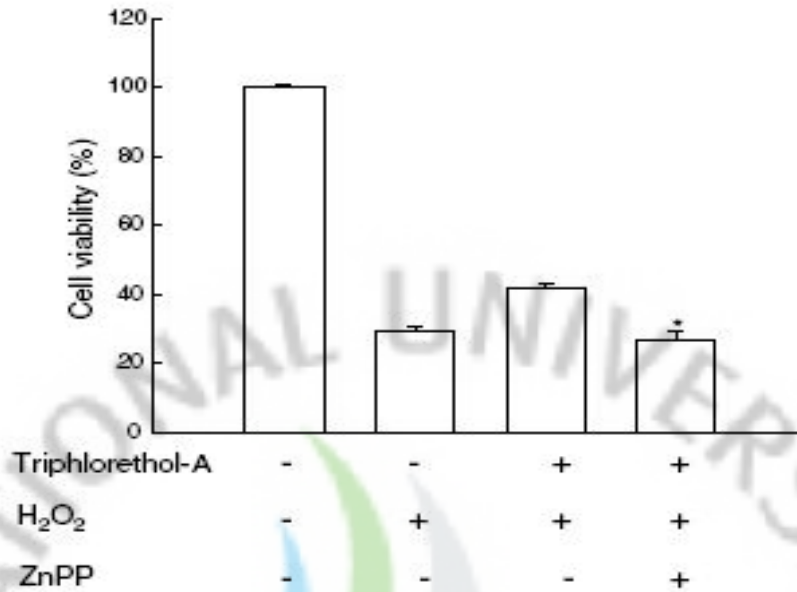


Figure 13. Induction of HO-1 and activation of Nrf2 by triphlorethol-A via phosphorylation of ERK. (A) Effect of triphlorethol-A on the phosphorylation of ERK. Cells were exposed to 30 μ M triphlorethol-A for the time indicated. Cell lysates were electrophoresed, ERK and phospho-ERK were detected by their respective specific antibodies. (B) After treatment with U0126, cell lysates were electrophoresed and ERK and phospho-ERK were detected by their respective specific antibodies. (C) Effect of U0126 on triphlorethol-A induced HO-1 expression. Cells were incubated with 30 μ M triphlorethol-A in the absence or presence of U0126 for 3 h. Cell lysates were electrophoresed and HO-1 was detected by a HO-1 specific antibody. (D) Nuclear extract were prepared from V79-4 cells treated with 30 μ M of triphlorethol-A in the absence or presence of U0126 for 3 h and subjected to western blot for the measurement of Nrf2 protein expression. (E) V79-4 cells treated with 30 μ M triphlorethol-A in the absence or presence of U0126 for 3 h, and immunostained to detect the nuclear localization of Nrf2. (F) V79-4 cells were transfected with the ARE-luciferase construct (1 μ g per well). After overnight, cells were treated with triphlorethol-A in the absence or presence of U0126, cell lysates were mixed with a luciferase substrate, and the luciferase activity was measured by the luminometer. Data are expressed as the mean \pm SE in triplicate experiments. *Significantly different from triphlorethol-A treated cells ($p < 0.05$).

4.4 Effect of triphlorethol-A on cell damage induced by oxidative stress

The protective effect of triphlorethol-A on oxidative stress induced in H₂O₂ treated V79-4 cells was assessed. Cells were treated with 30 μM triphlorethol-A for 1 h prior to the addition of 1 mM of H₂O₂. To determine whether the increased HO-1 activity induced by triphlorethol-A could confer cytoprotection against oxidative stress, V79-4 cells were pretreated with the HO-1 inhibitor ZnPP. ZnPP attenuated the protective effect of triphlorethol-A on H₂O₂-induced cytotoxicity (Figure 14A), suggesting that the cytoprotective effect of triphlorethol-A is partly mediated through HO-1 induction. Moreover, U0126 also attenuated the protective effect of triphlorethol-A on H₂O₂-induced cytotoxicity (Figure 14B), suggesting the involvement of ERK signaling in triphlorethol-A mediated HO-1 gene induction and cytoprotection.

(A)



(B)

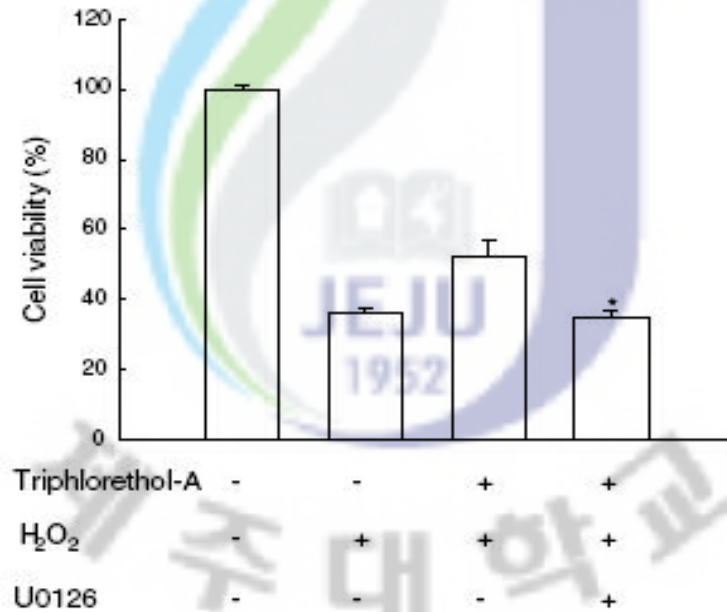


Figure 14. Protective effect of triphlorethol-A against oxidative stress induced cell damage. (A) V79-4 cells were pre-incubated with 30 μ M triphlorethol-A and HO-1 inhibitor (ZnPP) at 10 μ M for 6 h, followed by exposure to 1 mM H₂O₂. Cytotoxicity was assessed by the MTT assay after H₂O₂ treatment. *Significantly different from H₂O₂ treated cells ($p < 0.05$). (B) After treatment with U0126, triphlorethol-A or/and H₂O₂, the viability of V79-4 cells was determined by MTT assay. *Significantly different from triphlorethol-A plus H₂O₂ treated cells ($p < 0.05$).

4. Discussion

Phlorotannin components, which are present in some brown algae, are polymers of phloroglucinol [39]. They are phytoalexins that have defensive or protective functions against herbivores. Recently, we reported that phlorotannins isolated from *E. cave* showed antioxidant and cytoprotective effects against oxidative stress; triphlorethol-A protected cell damage from H₂O₂ and radiation induced oxidative stress via radical quenching effect [96,97]; eckol attenuates oxidative stress induced cell damage via ERK and nuclear factor kappa B activation [98]; phloroglucinol induced cytoprotection via catalase and ERK activation [99].

In this study, we demonstrated that triphlorethol-A up-regulated HO-1 expression through activation of Nrf2. Most studies on the regulation of HO-1 gene expression have focused on the role of the MAPK pathways. For instance, the glutathione depletor pherone and arsenite promote JNK-dependent induction of HO-1 gene expression [100,101]. Curcumin induces HO-1 expression by promoting dissociation of the Nrf2-Keap1 complex in a p38 dependent manner [85]. Resveratrol activates Nrf2-driven ARE activation and HO-1 expression via the ERK pathway [89]. Our results indicate a requirement for ERK activation in the induction of HO-1 expression by triphlorethol-A because an ERK inhibitor significantly reduced HO-1

protein expression in response to triphlorethol-A. The transcription factor Nrf2 is a member of the Cap-N-Collar family of basic leucine transcription factors, and plays an essential role in the ARE-mediated expression of HO-1 in response to oxidative stress [102-107]. Under normal physiological conditions, Nrf2 is sequestered by cytoskeleton associated cytoplasmic 'Kelch-like ECH-associated protein 1 (Keap 1)' which hampers the nuclear translocation of Nrf2. However, upon stimulation by electrophilic agents or reactive oxygen species, Nrf2 dissociates from its cytoplasmic docking protein Keap1, translocates into the nucleus and binds to ARE site [108]. This leads to the *de novo* synthesis of antioxidant enzymes that efficiently protect cells from oxidative stress. The actual mechanism of dissociation of Nrf2 from Keap1 is largely unresolved, but it is thought to involve phosphorylation of Nrf2 [109]. It is reported that ERK phosphorylates Nrf2 which may facilitate the release of Nrf2 from the Keap1-Nrf2 complex, allowing activated Nrf2 to translocate into the nucleus where it forms a heterodimer with small Maf protein [110-112]. Triphlorethol-A increases the nuclear levels of the Nrf2, its binding to the ARE and transcriptional activity. Treatment with U0126 prior to exposure to triphlorethol-A reduced Nrf2 nuclear translocation and transcriptional activity of Nrf2, suggesting that Nrf2 might be a direct downstream target of ERK.

In summary, the present results suggest that triphlorethol-A protects V79-4 cells against oxidative stress induced cell death through up-regulation of HO-1. V79-4 cells treated with triphlorethol-A exhibited elevated activation of ERK, which appears to be responsible for nuclear translocation of Nrf2 and its subsequent binding to ARE, thereby up-regulating HO-1 gene expression (Figure 15).

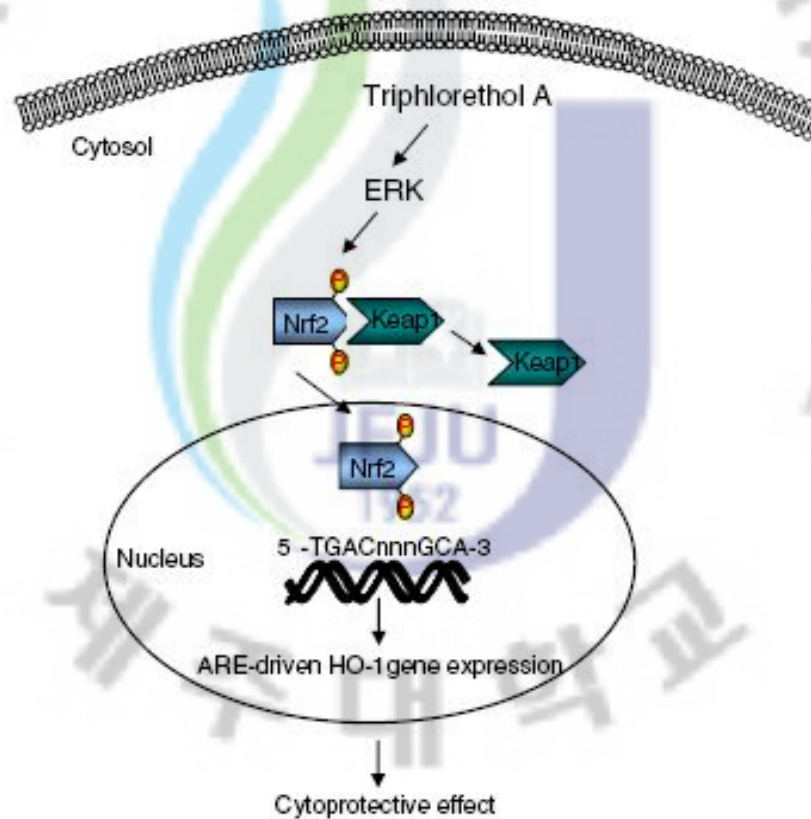


Figure 15. A proposed pathway for triphlorethol-A induced HO-1 via upregulation of ERK and Nrf2, which explains cytoprotection against oxidative stress in V79-4 cells.

PART IV

**Inhibitory Effect of Triphlorethol-A on MMP-1 Induced by
the Oxidative Stress in Human Keratinocytes via ERK and
AP-1 Inhibition**



1. Abstract

Oxidative stress has been demonstrated to cause the production of reactive oxygen species (ROS) in cells, which in turn induces the synthesis of matrix metalloproteinases (MMPs) and aging. We investigated the protective effects of triphlorethol-A, derived from *Ecklonia cava*, against hydrogen peroxide (H₂O₂) using human skin keratinocytes.

We found that triphlorethol-A inhibited ROS formation, induced catalase expression, inhibited DNA damages, and increased cell viability. Triphlorethol-A treatment significantly reduced MMP-1 expression and production, compared to H₂O₂ treated cells. In addition, triphlorethol-A abrogated the activation of extracellular signal regulated protein kinase (ERK), which originates upstream of MMP-1 expression, induced by H₂O₂ treatment. Moreover, triphlorethol-A inhibited DNA binding activity of activator protein-1 (AP-1), a downstream transcription factor of ERK. The results suggest that the antioxidative properties of triphlorethol-A involves the inhibition of MMP-1 via ERK and AP-1 inhibition.

Key words: Triphlorethol-A; Oxidative stress; Matrix metalloproteinases (MMPs); ERK and AP-1 pathway

2. INTRODUCTION

Collagen is the most common component of dermal connective tissue. In addition, collagen is biosynthesized by dermal fibroblasts and broken down by enzymatic degradation. Under normal conditions, these two processes are generally in balance[115]. Previous research has reported that a loss in collagen may arise from accelerated enzymatic degradation, due to collagenase release from oxidative stress, resulting in the rate of collagen degradation exceeds the rate of biosynthesis [116-118]. The matrix metalloproteinase (MMP) family is involved in the collagen degradation process, including MMP-1 (interstitial collagenase), MMP-2 (72 kDa type IV collagenase, gelatinase A), MMP-8 (neutrophil collagenase), and MMP-13 (collagenase 3) [115,119]. Of these, MMP-1 is the pivotal MMP in the degradation of extracellular matrix by oxidative stress [120]. A number of reports suggest that the ERK pathway plays a role in the transcriptional regulation of MMP-1. Blocking of the ERK pathway was found to abrogate the Ras and serum induced stimulation of the MMP-1 promoter, indicating the role of ERK in the transcriptional regulation of MMP-1 [121]. Furthermore, the overexpression of the dominant negative MEK blocks the insulin elicited induction of a reporter construct under the control of an AP-1 element from the MMP-1 promoter [122]. Taken together, these studies suggest that the ERK-AP-1 pathway may be the major activator of MMP-1 gene expression. Reactive oxygen species

(ROS) undergo facile reactions with thiol groups and may serve as a common mechanism of activation for several different MMPs, including MMP-1 [122]. Hydrogen peroxide has the potential to modulate the activity of critical signaling molecules, which lead to MMP-1 expression. However, in many circumstances, this signaling is successfully blocked by antioxidants [118,123]. The expression of MMP-1 is effectively blocked by antioxidants such as N-acetylcysteine, which is a precursor of glutathione [124-125]. Recently, we reported that triphlorethol-A protects cells from H₂O₂ induced oxidative stress via radical quenching and catalase activation [53]. In addition, triphlorethol-A protected cellular damage from ionizing radiation via inhibition of apoptosis[125]. Triphlorethol-A induced the antioxidant enzyme heme oxygenase-1 via activation of the NF-E2 related factor 2 transcription factor [126]. In the present study, we investigated the ability of triphlorethol-A to reduce MMP-1 via ERK and AP-1 inhibition.

3. Material and Methods

3-1. Reagents

Triphlorethol-A compound (Figure 1) was prepared from professor Nam Ho Lee of Cheju National University (Jeju, Korea). The 2', 7'-dichlorodihydrofluorescein diacetate (DCF-DA) was purchased from the Sigma Chemical Company (St. Louis, MO). Primary anti-ERK and anti-phospho ERK antibodies were purchased from Cell Signaling Technology (Beverly, MA), primary anti-catalase antibody from Biodesign International Company (Saco, Maine) and primary anti-phospho H2A.X antibody from Upstate Biotechnology (Lake Placid, NY).

3-2. Cell culture

The HaCaT (human keratinocyte) cells were maintained at 37°C in an incubator, at a humidified atmosphere of 5% CO₂, and cultured in Dulbecco's modified Eagle's medium containing 10% heat-inactivated fetal calf serum, streptomycin (100 µg/ml) and penicillin (100 units/ml).

3-3. Intracellular reactive oxygen species (ROS) measurement

The DCF-DA method was used to detect levels of intracellular ROS [30]. For image analysis for generation of intracellular ROS, the cells were seeded on cover-slip loaded six well plate at 2×10^5 cells/well. At sixteen hours after plating, the cells were treated with

triphenylethol-A with 30 μ M and 30 min later, 1 mM H₂O₂ was added to the plate. After changing the media, 100 μ M of DCF-DA was added to each well and then was incubated for an additional 30 min at 37°C. After washing with PBS, the stained cells were mounted onto microscope slide in mounting medium (DAKO, Carpinteria, CA). Images were collected using the Laser Scanning Microscope 5 PASCAL program (Carl Zeiss, Jena, Germany) on a confocal microscope.

3-4. Western blot

The cells were harvested, and washed twice with PBS. The harvested cells were then lysed on ice for 30 min in 100 μ l of lysis buffer [120 mM NaCl, 40 mM Tris (pH 8), 0.1% NP 40] and centrifuged at 13,000 \times g for 15 min. The resultant supernatants were collected from the lysates and the protein concentrations were determined. Aliquots of the lysates (40 μ g of protein) were boiled for 5 min and electrophoresed in 10% sodium dodecylsulfate-polyacrylamide gel. Blots in the gels were transferred onto nitrocellulose membranes (Bio-Rad, Hercules, CA), which were then incubated with primary antibodies. The membranes were further incubated with secondary immunoglobulin-G-horseradish peroxidase conjugates (Pierce, Rockford, IL). Protein bands were detected using an enhanced chemiluminescence Western blotting detection kit (Amersham Pharmacia Biotech, Buckinghamshire, UK), and then exposed to X-ray film.

3-5. Immunocytochemistry

Cells plated on coverslips were fixed with 4% paraformaldehyde for 30 min and permeabilized with 0.1% Triton X-100 in PBS for 2.5 min. Cells were treated with blocking medium (3% bovine serum albumin in PBS) for 1 h and incubated with anti-phospho histone H2A.X antibody diluted in blocking medium for 2 h. Immunoreactive primary phospho histone H2A.X antibody was detected by a 1:500 dilution of FITC-conjugated secondary antibody (Jackson ImmunoResearch Laboratories, West Grove, PA) for 1 h. After washing with PBS, the stained cells were mounted onto microscope slides in mounting medium with DAPI (Vector, Burlingame, CA). Images were collected using the Laser Scanning Microscope 5 PASCAL program (Carl Zeiss) on a confocal microscope.

3-6. Comet assay

A Comet assay was performed to assess oxidative DNA damage [58,59]. The cell pellet (1.5×10^5 cells) was mixed with 100 μ l of 0.5% low melting agarose (LMA) at 39°C and spread on a fully frosted microscopic slide that was pre-coated with 200 μ l of 1% normal melting agarose (NMA). After solidification of the agarose, the slide was covered with another 75 μ l of 0.5% LMA and then immersed in lysis solution (2.5 M NaCl, 100 mM Na-EDTA, 10 mM Tris, 1% Triton X-100, and 10% DMSO, pH 10) for 1 h at 4°C. The slides were then placed in a gel-electrophoresis apparatus containing 300 mM NaOH and 10 mM

Na-EDTA (pH 13) for 40 min to allow DNA unwinding and the expression of the alkali labile damage. An electrical field was applied (300 mA, 25 V) for 20 min at 4°C to draw negatively charged DNA toward an anode. After electrophoresis, the slides were washed three times for 5 min at 4°C in a neutralizing buffer (0.4 M Tris, pH 7.5) and then stained with 75 µl of ethidium bromide (20 µg/ml). The slides were observed using a fluorescence microscope and image analysis (Komet 5.5, Andor Technology, Belfast, UK). The percentage of total fluorescence in the tail and the tail length of the 50 cells per slide were recorded.

3-7. Cell viability

The effect of triphlorethol-A on the viability of the HaCaT cells was determined using the [3-(4,5-dimethylthiazol-2-yl)-2,5-diphenyltetrazolium] bromide (MTT) assay [20]. Fifty µl of the MTT stock solution (2 mg/ml) was then added into each well to attain a total reaction volume of 200 µl. After incubating for 4 h, the plate was centrifuged at 800 × g for 5 min and the supernatants were aspirated. The formazan crystals in each well were dissolved in 150 µl of dimethylsulfoxide and read at A₅₄₀ on a scanning multi-well spectrophotometer.

3-8. Reverse transcriptase polymerase chain reaction

Total RNA was isolated from cells using Trizol (GibcoBRL, Grand Island, NY). The PCR conditions for MMP-1 and for the housekeeping gene, GAPDH, were as follows: 40

cycles of 94°C for 1 min; 55°C for 1 min; and 72°C for 1 min. The primer pairs (Bionics, Seoul, Korea) were as follows (forward and reverse, respectively): human MMP-1, 5'- GGA GGA AAT CTT GCT CAT -3' and 5'- CTC AGA AAG AGC AGC ATC -3'; and human GAPDH, 5'- AAG GTC GGA GTC AAC GGA TTT -3'; and 5'- GCA GTG AGG GTC TCT CTC CT -3'. The amplified products were resolved by 1% agarose gel electrophoresis, stained with ethidium bromide, and photographed under ultraviolet light.

3-9. Determination of MMP-1 activity

The measurement of the secreted active MMP-1 was performed using the Fluorokine® E human active MMP-1 fluorescent assay (Roche Diagnostics, Mannheim, Germany) according to the manufacturer's instructions. The HaCaT cells were treated with triphlorethol-A at 30 µM and 1 h later, 1 mM H₂O₂ was added to the plate during 1 day. After centrifugation at 1,000 × g for 5 min, 150 µl of culture supernatants from HaCaT cells was mixed with 100 µl of assay diluent buffer in 96-well ELISA plates. The plates were gently shaken for 3 h at room temperature before unbound material was washed off. Subsequently, 200 µl of activation reagent (0.5 M APMA in DMSO) was added to each well for pro-MMP-1 activation. The plates were incubated for 2 h at 37°C in a humidified environment. After washing, 200 µl of fluorogenic substrate was added. After another 20 h at 37°C, fluorescence was determined using a fluorescence plate reader set (FLUOstar Optima Microplate Reader,

BMG Labtech, NC) with an excitation wavelength set to 320 nm and emission wavelength set to 405 nm [21].

3-10. Preparation of nuclear extract and electrophoretic mobility shift assay

The cells were harvested, and were then lysed on ice with 1 ml of lysis buffer (10 mM Tris-HCl, pH 7.9, 10 mM NaCl, 3 mM MgCl₂, and 1% NP-40) for 4 min. After 10 min of centrifugation at 3,000 × g, the pellets were resuspended in 50 µl of extraction buffer (20 mM HEPES, pH 7.9, 20% glycerol, 1.5 mM MgCl₂, 0.2 mM EDTA, 1 mM DTT, and 1 mM PMSF), incubated on ice for 30 min, and centrifuged at 13,000 × g for 5 min. The supernatant (nuclear protein) stored at -70°C after determination of protein concentration. Oligonucleotides containing the transcription factor AP-1 consensus sequence (5'- CGC TTG ATG ACT CAG CCG GAA - 3') were annealed, labeled with [γ -³²P] ATP using T4 polynucleotide kinase, and used as probes. The probes (50,000 cpm) were incubated with 6 µg of the nuclear extracts at 4°C for 30 min in a final volume of 20 µl containing 12.5% glycerol, 12.5 mM HEPES (pH 7.9), 4 mM Tris-HCl (pH 7.9), 60 mM KCl, 1 mM EDTA, and 1 mM DTT with 1 µg of poly (dI-dC). Binding products were resolved on 5% polyacrylamide gel and the bands were visualized by autoradiography.

3-11. Statistical analysis

All the measurements were made in triplicate and all values were represented as means ±

standard error. The results were subjected to an analysis of the variance (ANOVA) using the Tukey test to analyze the differences. $p < 0.05$ were considered to be significant.

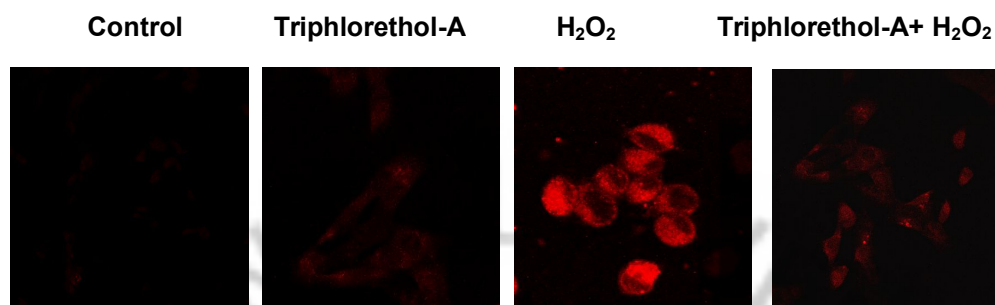


4. Results

4.1 Effect of triphlorethol-A on radical scavenging activity and catalase expression

The intracellular ROS scavenging activity of triphlorethol-A was detected using a confocal microscope after the staining of DCF-DA (a ROS specific dye). The analysis of confocal microscope showed that triphlorethol-A reduced the red fluorescence intensity of ROS generated by H₂O₂ treatment as shown in Figure 16A, thus reflecting the ROS scavenging activity of triphlorethol-A. To determine whether the radical scavenging activity of triphlorethol-A was mediated by catalase, which converts H₂O₂ into molecular oxygen and water [131], the protein expression of catalase in triphlorethol-A treated HaCaT cells were measured. As shown in Figure 16B, in the presence of triphlorethol-A at 30 μM, the protein expression of catalase was increased at the time dependent pattern. Consequently, these results suggest that triphlorethol-A has a ROS scavenging effect and catalase induction.

(A)



(B)

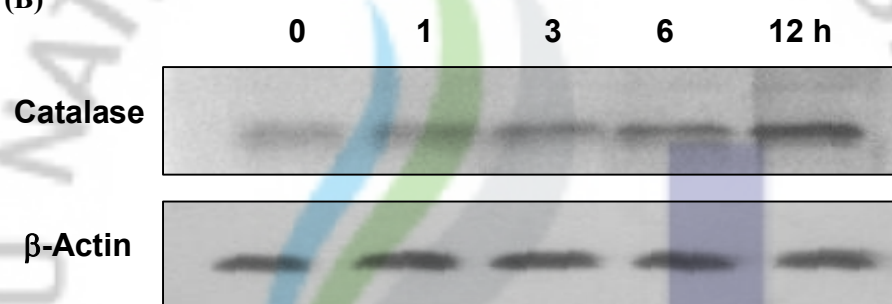


FIG. 16. Effect of triphlorethol-A on radical scavenging activity and catalase induction.

(A) The intracellular ROS was detected using confocal microscope after DCF-DA treatment. The representative confocal images illustrate the increase in red fluorescence intensity of DCF produced by ROS in H₂O₂ treated cells as compared to control and the lowered fluorescence intensity in H₂O₂ treated cells with triphlorethol-A (original magnification \times 400). (B) The cell lysates were electrophoresed and the protein expression of catalase was detected with a specific catalase antibody.

4.2 Effect of triphlorethol-A on cellular DNA damage and cell death induced by H₂O₂

The ability of triphlorethol-A to inhibit cellular DNA damage in H₂O₂ treated cells was investigated by assessing phospho histone-H2A.X expression, and comet assay. The phosphorylation of nuclear histone H2A.X, which is a sensitive marker for breaks of double stranded DNA [132], revealed an increase in the H₂O₂ treated cells as shown by western blot and immuno-fluorescence results (Figures 17A and B). However, the triphlorethol-A in H₂O₂ treated cells decreased the expression of phospho H2A.X. In addition, comet assay showed that the exposure of cells to H₂O₂ was increased the tail length of cells, whereas treatment with triphlorethol-A resulted in a decrease of tail length as shown in Figure 17C. The cytoprotective effect of triphlorethol-A on H₂O₂ treated cells was measured. Cells were treated with triphlorethol-A at 30 μM for 1 h, prior to the addition of H₂O₂. Cell viability was determined 24 h later via MTT assay and flow cytometry, respectively. As shown in Figure 17D, treatment with triphlorethol-A increased cell survival by 58%, compared to 43% of H₂O₂ treatment. Hence, these results suggest that triphlorethol-A protects cell viability by inhibiting H₂O₂ induced DNA damage.

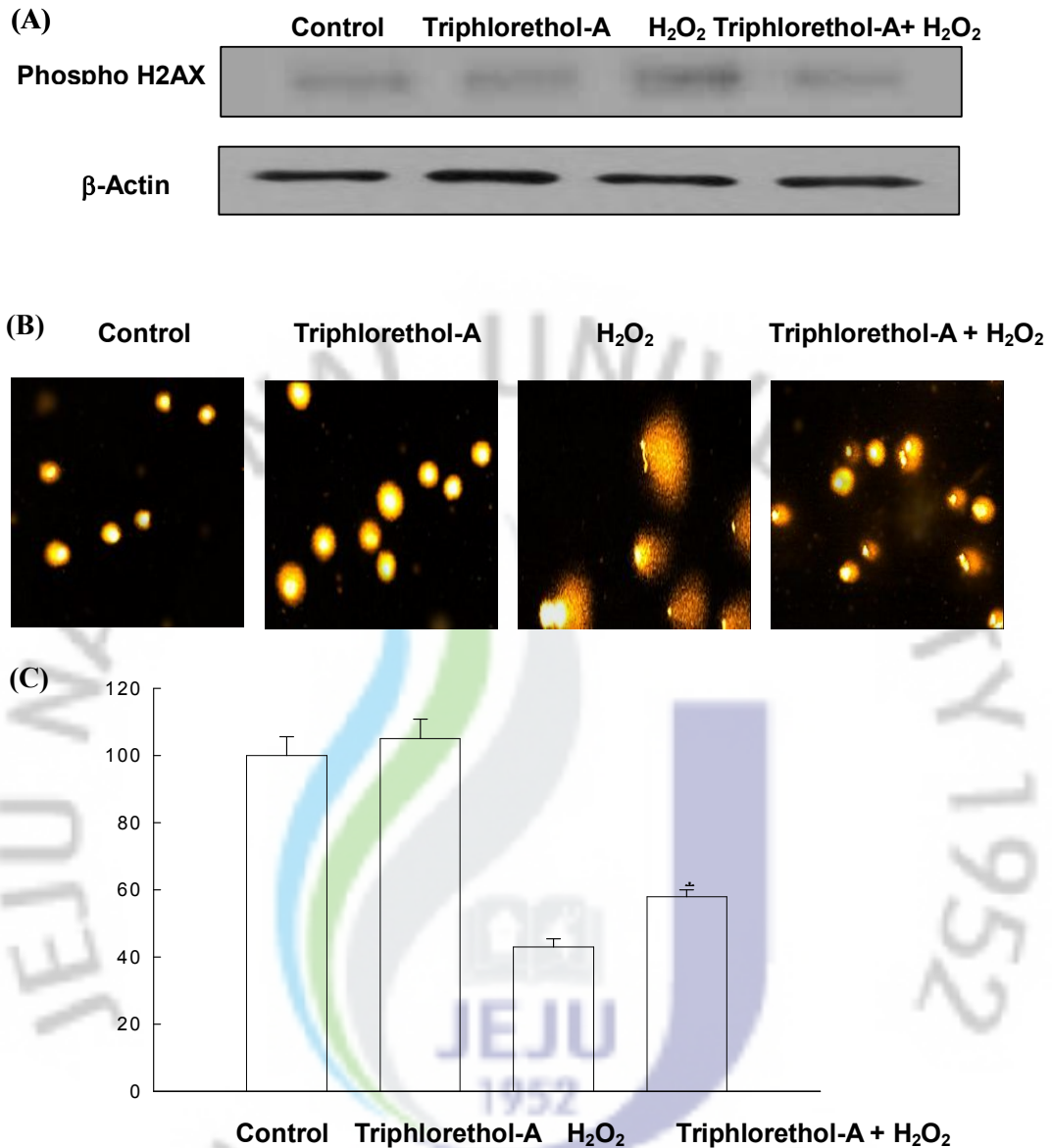
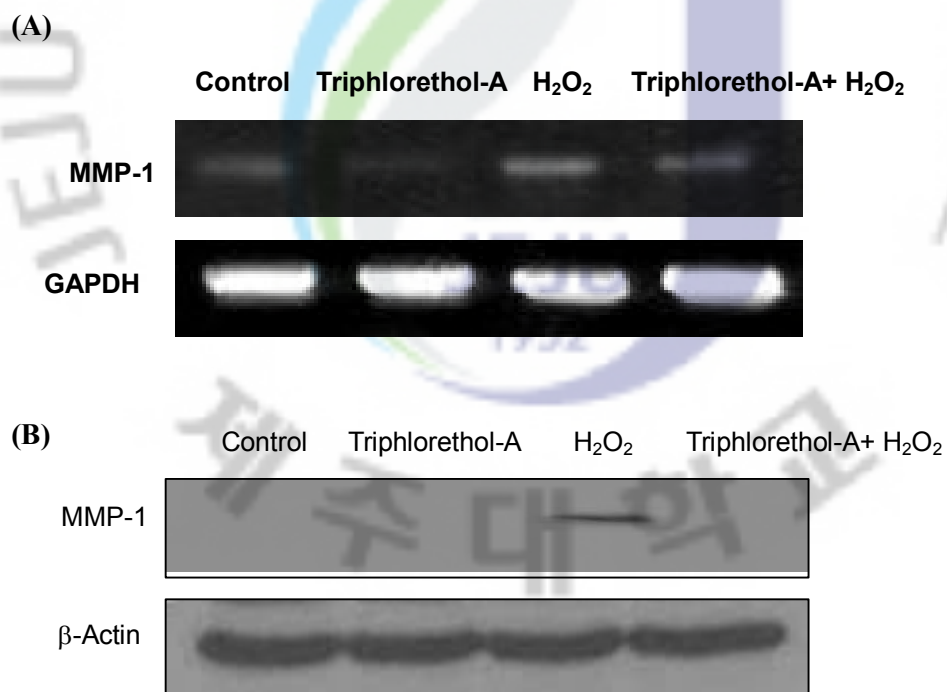


FIG. 17. The effect of triphlorethol-A on cellular DNA damage and cell death induced by H₂O₂

(A) The cell lysates were electrophoresed and phospho H2A.X protein was detected by specific antibody. (B) Confocal image shows that FITC-conjugated secondary antibody staining indicates the location of phospho H2A.X (green) by anti-phospho H2A.X antibody. DAPI staining reveals the location of the nucleus (blue), and the merged image indicates the location of the phospho H2A.X protein in nucleus. (C) Representative images of the cellular DNA damage were detected by an alkaline comet assay. (D) The viability of HaCaT cells on H₂O₂ treatment was determined by MTT assay. Each bar represents the mean \pm standard error in triplicate experiments. *Significantly different from H₂O₂ treated cells ($p < 0.05$).

4.3 Effects of triphlorethol-A on H₂O₂ induced MMP-1 expression and activity

H₂O₂ treatment was found to considerably increase MMP-1 mRNA levels, as revealed by the RT-PCR analysis, whereas, triphlorethol-A blocked the expression of MMP-1 mRNA (Figure 18A). Consistent with the RT-PCR result, a western blotting analysis revealed that triphlorethol-A inhibited the expression of MMP-1 protein induced by H₂O₂ treatment (Figure 18B). Moreover, the decreased MMP-1 expression by triphlorethol-A treatment correlated with the suppression of MMP-1 activity (Figure 18C).



(C)

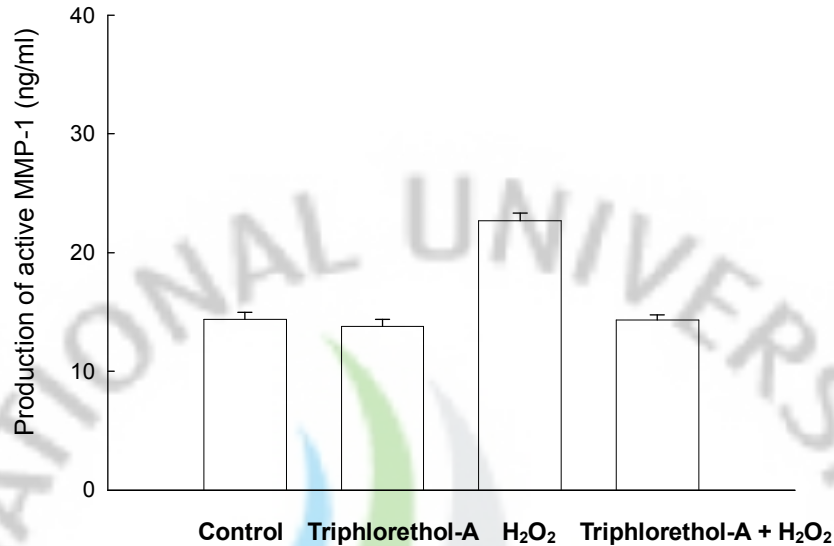


FIG. 18. The effects of triphlorethol-A on H₂O₂ induced MMP-1 mRNA, protein expression and activity

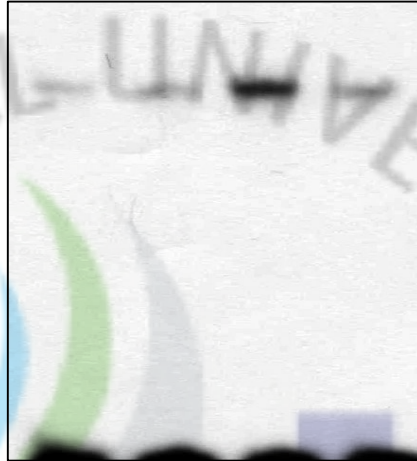
The cells were pretreated with triphlorethol-A prior to H₂O₂ treatment and harvested 24 h later. (A) Total RNA was extracted and MMP-1 mRNA expression was analyzed by RT-PCR. The GAPDH band is shown to confirm the integrity and equal loading of RNA. (B) Cell lysates were electrophoresed and the expression of MMP-1 protein was detected by a MMP-1 specific antibody. (C) The MMP-1 activity was measured by ELISA. Each bar represents the mean \pm standard error in triplicate experiments. *Significantly different from H₂O₂ treated cells ($p < 0.05$).

4.4 Effects of triphlorethol-A on H₂O₂ induced ERK-AP-1 pathway

In many circumstances, the transcriptional regulation of MMP genes involves the activation of the AP-1 transcriptional factor [24]. We examined the effect of triphlorethol-A on the DNA binding activity of AP-1. As shown in Figure 19A, the treatment of cells with H₂O₂ increased the DNA binding activity of AP-1, but triphlorethol-A was found to inhibit AP-1 activity. The activation of the transcriptional factor AP-1 can in turn be regulated by the ERK protein [25]. To assess the effects of triphlorethol-A on H₂O₂ induced ERK activation, cells were pretreated with triphlorethol-A for 1 h before the addition of H₂O₂. As shown in Figure 19B, incubation of cells with H₂O₂ induced ERK activation. Moreover, the preincubation of cells with triphlorethol-A significantly inhibited ERK activation. These results suggest that triphlorethol-A inhibits H₂O₂ induced MMP-1 via the suppression of ERK and AP-1 activation.

(A)

Triphlorethol-A	-	+	-	+
H ₂ O ₂	-	-	+	+



(B)

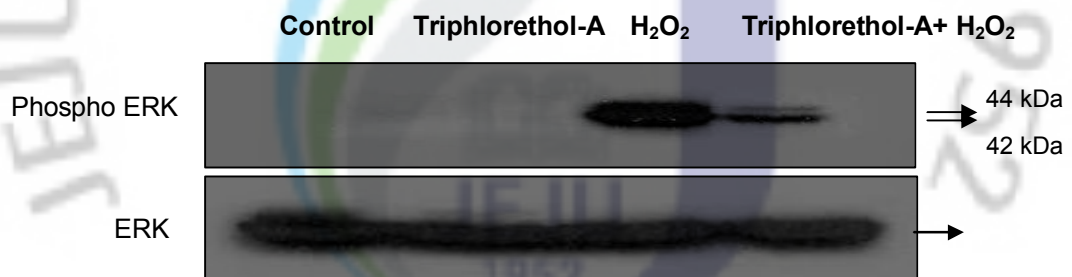


FIG. 19. The effect of triphlorethol-A on H₂O₂ induced AP-1 and ERK activation. (A) AP-1 specific oligonucleotide-protein complexes were detected by the electrophoresis mobility shift assay. (B) Cell lysates were electrophoresed and cell lysates were immunoblotted using anti-phospho ERK and anti-ERK antibodies.

4. Discussion

Connective tissue and skin cells are particularly susceptible to oxidative stress via processes such as photodamage, and inflammation [118]. Fibrillar collagens are the most abundant structural components (intercellular matrix proteins) of connective tissue and skin cells. Moreover, MMP-mediated collagen damage is a major contributor to the phenotype of aged human skin [135]. Since the inhibition of MMPs production appears to be a useful intervention in preventing collagen damages [136], we investigated the inhibitory effect of MMP-1 production by triphlorethol-A. MMP-1 is a collagenase (collagenase-1, interstitial collagenase), which breaks down collagen types I and III with high specificity. In the present study, triphlorethol-A was found to decrease the intracellular ROS and increase catalase expression. Cells pretreated with triphlorethol-A showed a significant reduce in DNA damage and cell death through its ROS scavenging effect. Recent studies have reported that UV rapidly and significantly increases H₂O₂ levels in human skin in vivo, suggesting that increase in ROS may participate in the triggering of the mitogen activated protein kinase (MAPK) cascade. Hence, the topical treatment with antioxidants may interrupt induced MMP expression in human skin [137] (Kang et al., 2003). Triphlorethol-A was found to protect cells from oxidative stress via radical

quenching and activation of antioxidant enzymes [53-55]. A significant increase in the production of MMP-1 was observed at 24 h after H₂O₂ treatment. However, pretreatment with triphlorethol-A, which has an antioxidant effect, resulted in the significantly inhibition of MMP-1 production. H₂O₂ can modulate MMP expression by indirect activation of ERK, which is important in the regulation of MMP-1 [121,122]. Subsequently, ERK phosphorylation leads to the activation of the AP-1 member, c-Fos, resulting in the induction of MMP-1 transcription. Moreover, the AP-1 transcription factor is important in the regulation of MMP family members and is sensitive to regulation by redox conditions. In the present study, H₂O₂ treatment induced a phospho form of ERK, however, triphlorethol-A was found to decrease the expression of the phospho ERK protein. In addition, a gel mobility shift analysis revealed that an increase in the DNA binding activity of AP-1 induced by H₂O₂ was inhibited by triphlorethol-A, suggesting that the ERK and AP-1 pathways may be involved in MMP-1 induction.

In conclusion, we demonstrated that triphlorethol-A attenuates MMP-1 production through the inhibition of the ROS-mediated ERK and AP-1 signaling pathway in HaCaT cells.

6. PART Conclusion

We suggested that triphlorethol-A has cytoprotective effect against H₂O₂ and γ -ray radiation via scavenging of ROS and antioxidant enzymes induction. Also, triphlorethol-A inhibited MMP-1 by oxidative stress. This will contribute to provide the basis of radioprotector and anti-aging agent for development.

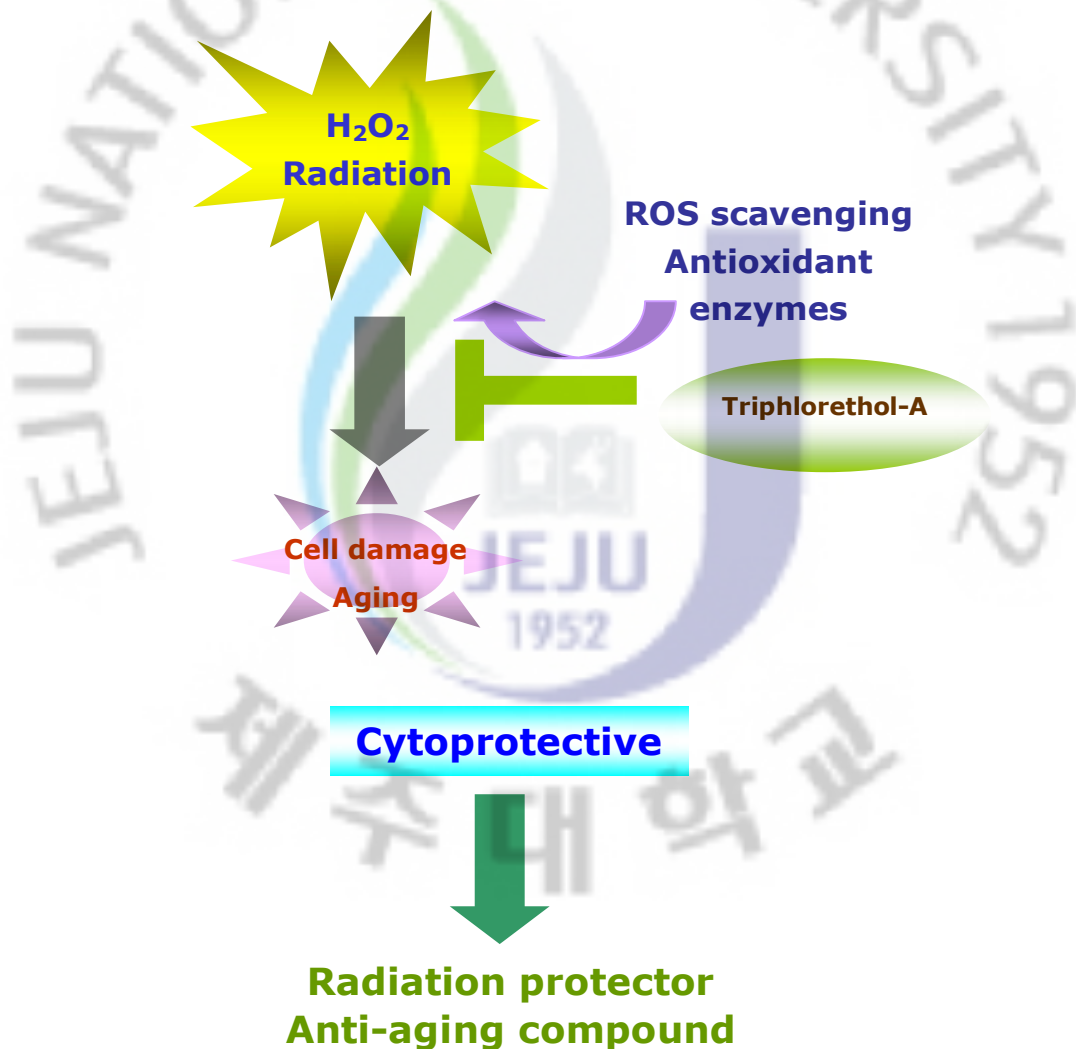


Figure 20. Possible application of Truphlorethol-A

7. Reference

7. 1. Part I

- [1] Cooke, M.S., Mistry, N., Wood, C., Herbert, K.E. and Lunec, J. (1997)
"Immunogenicity of DNA damaged by reactive oxygen species implications for anti-DNA antibodies in lupus", *Free Radic. Biol. Med.* **22**, 151-159.
- [2] Darley-Usmar, V. and Halliwell, B. (1996) "Blood radicals: reactive nitrogen species, reactive oxygen species, transition metal ions, and the vascular system", *Pharm. Res.* **13**, 649-662.
- [3] Farinati, F., Cardin, R., Degan, P., Rugge, M., Mario, F.D., Bonvicini, P. and Naccarato, R. (1998) "Oxidative DNA damage accumulation in gastric carcinogenesis", *Gut* **42**, 351-356.
- [4] Laurindo, F.R., da Luz, P.L., Uint, L., Rocha, T.F., Jaeger, R.G. and Lopes, E.A. (1991)
"Evidence for superoxide radical-dependent coronary vasospasm after angioplasty in intact dogs" *Circulation* **83**, 1705-1715.
- [5] Nakazono, K., Watanabe, N., Matsuno, K., Sasaki, J., Sato, T. and Inoue, M. (1991)
"Does superoxide underlie the pathogenesis of hypertension?" *Proc. Natl. Acad. Sci. USA.* **88**, 10045-10048.

- [6] Palinski, W., Miller, E. and Witztum, J.L. (1995) "Immunization of low density lipoprotein (LDL) receptor-deficient rabbits with homologous malondialdehyde-modified LDL reduces atherogenesis", *Proc. Natl. Acad. Sci. USA*. **92**, 821-825.
- [7] Parthasarathy, S., Steinberg, D. and Witztum, J.L. (1992) "The role of oxidized low-density lipoproteins in the pathogenesis of atherosclerosis", *Annu. Rev. Med.* **43**, 219-225.
- [8] Halliwell B., Gutteridge J. M., Cross. C. E., *J. Lab. Clin. Med.*, **119**, 598-620 (1992).
- [9] Wu Y. F., Fu S. L., Kao C. H., Yang C. W., Lin C. H., Hsu M. T., Tsai T. F., *Cancer Res.*, **68**, 2033-2042 (2008).
- [10] Pensalfini A., Cecchi C., Zampagni M., Becatti M., Favilli F., Paoli P., Catarzi S., Bagnoli S., Nacmias B., Sorbi S., Liguri G., *Free Radic. Biol. Med.*, **44**, 1624-1639 (2008).
- [11] Halliwell B., Aruoma O. I., *FEBS Lett.*, **281**, 9-19 (1991).
- [12] Spencer J. P., Jenner A., Chimel K., Aruoma O. I., Cross C. E., Wu R., Halliwell B., *FEBS Lett.*, **374**, 233-236 (1995).
- [13] Melidou M., Riganakos K., Galaris D., *Free Radic. Biol. Med.*, **39**, 1591-1600 (2005).
- [14] Arranz N., Haza A. I., García A., Delgado E., Rafter J., Morales P., *Chem. Biol. Interact.*, **169**, 63-71 (2007).

- [15] Plazar J., Zegura B., Lah T. T., Filipic M., *Mutat. Res.*, **632**, 1-8 (2007).
- [16] Kang, H.S., Chung, H.Y., Kim, J.Y., Son, B.W., Jung, H.A. and Choi, J.S. (2004) "Inhibitory phlorotannins from the edible brown alga *Ecklonia stolonifera* on total reactive oxygen species (ROS) generation", *Arch. Pharm. Res.* **27**, 194-198.
- [17] Kang, K., Park, Y., Hwang, H.J., Kim, S.H., Lee, J.G. and Shin, H.C. (2003) "Antioxidative properties of brown algae polyphenolics and their perspectives as chemopreventive agents against vascular risk factors", *Arch. Pharm. Res.* **26**, 286-293.
- [18] Fukuyama, Y., Kodama, M., Miura, I., Kinzyo, Z., Mori, H., Nakayama, Y. and Takahashi, M. (1990) "Anti-plasmin inhibitor. VI. Structure of phlorofucofuroeckol A, a novel phlorotannin with both dibenzo-1,4-dioxin and dibenzofuran elements, from *Ecklonia kurome* Okamura", *Chem. Pharm. Bull. (Tokyo)*. **38**, 133-135.
- [19] Fukuyama, Y., Kodama, M., Miura, I., Kinzyo, Z., Kido, M., Mori, H., Nakayama, Y. and Takahashi, M. (1989) "Structure of an anti-plasmin inhibitor, eckol, isolated from the brown alga *Ecklonia kurome* Okamura and inhibitory

- activities of its derivatives on plasma plasmin inhibitors", *Chem. Pharm. Bull. (Tokyo)*. **37**, 349-353.
- [20] Fukuyama, Y., Kodama, M., Miura, I., Kinzyo, Z., Mori, H., Nakayama, Y. and Takahashi, M. (1989) "Anti-plasmin inhibitor. V. Structures of novel dimeric eckols isolated from the brown alga *Ecklonia kurome* Okamura", *Chem. Pharm. Bull. (Tokyo)*. **37**, 2438-2440.
- [21] Ahn, M.J., Yoon, K.D., Min, S.Y., Lee, J.S., Kim, J.H., Kim, T.G., Kim, S.H., Kim, N.G., Huh, H. and Kim, J. (2004) "Inhibition of HIV-1 reverse transcriptase and protease by phlorotannins from the brown alga *Ecklonia cava*", *Biol. Pharm. Bull.* **27**, 544-547.
- [22] Park, D.C., Ji, C.I., Kim, S.H., Jung, K.J., Lee, T.G., Kim, I.S., Park, Y.H. and Kim, S.B. (2000) "Characteristics of tyrosinase inhibitory extract from *Ecklonia stolonifera*", *J. Fish. Sci. Tech.* **3**, 195-199.
- [23] Fukuyama, Y., Kodama, M., Miura, I., Kinzyo, Z., Kido, M., Mori, H., Nakayama, Y. and Takahashi, M. (1989) "Structure of an anti-plasmin inhibitor, eckol, isolated from the brown alga *Ecklonia kurome* Okamura and inhibitory activities of its derivatives on plasma plasmin inhibitors", *Chem. Pharm. Bull.* **37**, 349-353.

- [24] Pryor, W.A., Stone, K., Zang, L.Y. and Bermudez, E. (1998) "Fractionation of aqueous cigarette tar extracts: fractions that contain the tar radical cause DNA damage", *Chem. Res. Toxicol.* **11**, 441-448.
- [25] Murray, J.I., Whitfield, M.L., Trinklein, N.D., Myers, R.M., Brown, P.O. and Botstein, D. (2004) "Diverse and specific gene expression responses to stresses in cultured human cells", *Mol. Biol. Cell*, **15**, 2361-2374.
- [26] Rosenkranz, A.R., Schmaldienst, S., Stuhlmeier, K.M., Chen, W., Knapp, W. and Zlabinger, G.J. (1992) "A microplate assay for the detection of oxidative products using 2',7'-dichlorofluorescein-diacetate", *J. Immunol. Meth.* **156**, 39-45.
- [27] Lo, S.F., Nalawade, S.M., Mulabagal, V., Matthew, S., Chen, C.L., Kuo, C.L. and Tsay, H.S. (2004) "In vitro propagation by asymbiotic seed germination and 1,1-diphenyl-2-picrylhydrazyl (DPPH) radical scavenging activity studies of tissue culture raised plants of three medicinally important species of *Dendrobium*", *Biol. Pharm. Bull.* **27**, 731-735.
- [28] Nourooz-Zadeh, J., Sarmadi-Tajaddini, J. and Wolff, S.P. (1994) "Measurement of plasma hydrogenperoxide concentrations by the ferrous oxidation-xylene orange assay in conjunction with triphenylphosphine", *Anal. Biochem.* **220**, 403-409.

- [29] Ohkawa, H., Ohishi, N. and Yagi, K. (1979) "Assay for lipid peroxides in animal tissues by thiobarbituric acid reaction", *Anal. Biochem.* **95**, 351-358.
- [30] Carmichael, J., DeGraff, W.G., Gazdar, A.F., Minna, J.D. and Mitchell, J.B. (1987) "Evaluation of a tetrazolium-based semiautomated colorimetric assay: assessment of chemosensitivity testing", *Cancer Res.* **47**, 936-941.
- [31] Nicoletti, I., Migliorati, G., Pagliacci, M.C., Grignani, F. and Riccardi, C. (1991) "A rapid and simple method for measuring thymocyte apoptosis by propidium iodide staining and flow cytometry", *J. Immunol. Meth.* **139**, 271-279.
- [32] Bradford, M.M. (1976) "A rapid and sensitive method for the quantitation of microgram quantities of protein utilizing the principle of protein-dye binding", *Anal. Biochem.* **72**, 248-254.
- [33] Misra, H.P. and Fridovich, I. (1972) "The role of superoxide anion in the autoxidation of epinephrine and a simple assay for superoxide dismutase", *J. Biol. Chem.* **247**, 3170-3175.
- [34] Carrillo, M.C., Kanai, S., Nokubo, M. and Kitani, K. (1991) "(-) Deprenyl induces activities of both superoxide dismutase and catalase but not of glutathione peroxidase in the striatum of young male rats", *Life Sci.* **48**, 517-521.

- [35] Paglia, D.E. and Valentine, W.N. (1967) "Studies on the quantitative and qualitative characterization of erythrocyte glutathione peroxidase", *J. Lab. Clin. Med.* **70**, 158-164.
- [36] Pages, G., Lenomand, P., L'Allemania, G., Chambard, J.C., Meloche, S. and Pouyssegur, J. (1991) "Mitogen activated protein kinases p42mapk and p44mapk are required for fibroblast proliferation", *Proc. Natl. Acad. Sci. USA.* **90**, 319-323.
- [37] Margoliash, E., Novogrodsky, A., Schejter, A. and Chejter, A. (1960) "Irreversible reaction of 3-amino-1:2:4-triazole and related inhibitors with the protein of catalase", *Biochem. J.* **74**, 339-348.
- [38] Long, L.H., Clement, M.V. and Halliwell, B. (2000) "Artifacts in cell culture: rapid generation of hydrogen peroxide on addition of (-)-epigallocatechin, (-)-epigallocatechin gallate, (+)-catechin, and quercetin to commonly used cell culture media", *Biochem Biophys Res Commun.* **273(1)**, 50-53.
- [39] Shibata, T., Yamaguchi, K., Nagamura, K., Kawaguchi, S. and Nagamura, T. (2002) "Inhibitory activity of brown algae phlorotannins against glycosidases from the viscera of the turban shell *Turbo cornutus*", *Eur. J. Phycol.* **37**, 493-500.
- [40] Kim, J.A., Lee, J.M., Shin, D.B. and Lee, N.H. (2004) "The antioxidant activity and tyrosinase inhibitory activity of phlorotannins in *Ecklonia cava*", *Food Science and*

Biotechnology **13**, 476-480.

- [41] Nakamura, T., Nagayama, K., Uchida, K. and Tanaka, R. (1996) "Antioxidant activity of phlorotannins isolated from the brown alga *Eisenia bicyclis*", *Fisheries Science* **62**, 923-926.
- [42] Larson, R.A. (1997) Phenolic and enolic antioxidants., In: Larson, R.A., ed, Naturally occurring antioxidants (Lewis publishers, New York), pp 83-87.
- [43] McCubrey, J.A., May, W.S., Durno, V. and Mufson, A. (2000) "Serine/threonine phosphorylation in cytokine signal transduction", *Leukemia* **14**, 9-21.
- [44] Pages, G., Lenomand, P., L'Allemania, G., Chambard, J.C., Meloche, S. and Pouyssegur, J. (1991) "Mitogen activated protein kinases p42mapk and p44mapk are required for fibroblast proliferation", *Proc Natl Acad Sci USA* **90**, 8319-8323.
- [45] Robinson, M.J. and Cobb, M.H. (1997) "Mitogen activated protein kinase pathways", *Curr Opin Cell Biol* **9**, 180-186.
- [46] Widmann, C., Gibson, S., Jarpe, B. and Johnson, G.L. (1999) "Mitogen activated protein kinase: conservation of a three kinase module from yeast to human", *Physiol. Rev.* **79**, 143-180.

7. 2. Part II

- [47] Halliwell, B. and Aruoma, O.I.(1991) DNA damage by oxygen-derived species. Its mechanism and measurement in mammalian systems. FEBS Lett. 281: 9-19.
- [48] Sankaranarayanan, K.(1999) Ionizing radiation and genetic risks. X. the potential "disease phenotypes" of radiation-induced genetic damage in humans:perspectives from human molecular biology and radiation genetics. Mutat. Res. 429:45-83.
- [49] Weiss JF, Simic MG. Perspectives in radioprotection. Pharmacol. Ther. 1988 Mar;39(1-3):1-14.
- [50] Hosseinimehr, S. J., Shafiee, A., Mozdarani, H. and Akhlagpour, S.(2001) Radioprotective effects of 2-iminothiazolidine derivatives against lethal doses of gamma radiation in mice. J. Radiat. Res. 42:401-408.
- [51] Hosseinimehr, S. J., Shafiee, A., Mozdarani, H., Akhlagpour, S.and Froughizadeh, M.(2002) Radioprotective effects of 2-imino-3{(chromone-2-yl) carbonyl} thiazolidines against gamma radiation in mice. J. Radiat. Res. 43:293-300.
- [52] J.F. Weiss, M.R. Landauer, Protection against ionizing radiation by antioxidant nutrients, Toxicology 189 (2003) 1-20.
- [53] Kang, K. A., Lee, K. H., Chae, S., Koh, Y. S., Yoo, B. S., Kim, J. H., Ham, Y. M., Baik, J. S., Lee, N. H. and Hyun, J. W. (2005) Triphlorethol-A from *Ecklonia cava* protects

V79-4 lung fibroblast against hydrogen peroxide induced cell damage. Free Radic. Res. **39**: 883-892.

[54] Singh, N. P. (2000) Microgels for estimation of DNA strand breaks, DNA protein cross links and apoptosis. Mutat. Res. **455**: 111-127.

[55] Rajagopalan, R., Ranjan, S. K. and Nair, C. K. (2003) Effect of vinblastine sulfate on gamma-radiation-induced DNA single-strand breaks in murine tissues. Mutat. Res. **536**:15-25.

[56] Lin, X., Zhang, F., Bradbury, C. M., Kaushal, A., Li, L., Spitz, D. R., Aft, R. L. and Gius, D. (2003) 2-Deoxy-D-glucose-induced cytotoxicity and radiosensitization in tumor cells is mediated via disruptions in thiol metabolism. Cancer Res. **63**: 3413-3417.

[57] Weiss, J. F. and Landauer, M. R. (2000) Radioprotection by antioxidants. Ann. N. Y. Acad. Sci. **899**: 44-60.

[58] Jonathan, E. C., Bernhard, E. J. and McKenna, W. G. (1999) How does radiation kill cells? Curr. Opin. Chem. Biol. **3**: 77-83.

[59] Kang, K. A., Lee, K. H., Chae, S., Koh, Y. S., Yoo, B. S., Kim, J. H., Ham, Y. M., Baik, J. S., Lee, N. H. and Hyun, J. W. (2005) Triphlorethol-A from *Ecklonia cava* protects V79-4 lung fibroblast against hydrogen peroxide induced cell damage. Free Radic. Res. **39**: 883-892.

7. 3. Part III

- [60] Tenhunen, R.; Marver, H. S.; Schmid, R. The enzymatic conversion of heme to bilirubin by microsomal heme oxygenase. *Proc. Natl. Acad. Sci. USA.* **61**:748-755; 1968.
- [61] Maines, M. D. Heme oxygenase: function, multiplicity, regulatory mechanisms, and clinical applications. *FASEB J.* **2**:2557-2568;1988.
- [62] Stocker, R.; Yamamoto, Y.; McDonagh, A. F.; Glazer, A. N. Bilirubin is an antioxidant of possible physiological importance. *Science* **235**:1043-1046;1987.
- [63] Applegate, L. A.; Luscher, P.; Tyrrell, R. M. Induction of heme oxygenase: a general response to oxidant stress in cultured mammalian cells. *Cancer Res.* **51**:974-978;1991.
- [64] Rizzardini, M.; Carelli, M.; Cabello Porras, M. R.; Cantoni, L. Mechanisms of endotoxin-induced haem oxygenase mRNA accumulation in mouse liver: synergism by glutathione depletion and protection by N-acetylcysteine. *Biochem. J.* **304**:477-483;1994.
- [65] Rossi, A.; Santoro, M. G. Induction by prostaglandin A1 of haem oxygenase in myoblastic cells: an effect independent of expression of the 70 kDa heat shock protein. *Biochem. J.* **308**:455-463;1995.
- [66] Choi, A. M.; Alam, J. Heme oxygenase-1: function, regulation, and implication of a novel stress-inducible protein in oxidant-induced lung injury. *Am. J. Respir. Cell. Mol. Biol.* **15**:9-19;1996.

- [67] Lee, P. J.; Alam, J.; Wiegand, G. W.; Choi, A. M. Overexpression of heme oxygenase-1 in human pulmonary epithelial cells results in cell growth arrest and increased resistance to hyperoxia. *Proc. Natl. Acad. Sci. USA.* **93**:10393-10398;1996.
- [68] Dennery, P. A.; Sridhar, K. J.; Lee, C. S.; Wong, H. E.; Shokoohi, V.; Rodgers, P. A.; Spitz, D. R. Heme oxygenase-mediated resistance to oxygen toxicity in hamster fibroblasts. *J. Biol. Chem.* **272**:14937-14942;1997.
- [69] Yamada, N.; Yamaya, M.; Okinaga, S.; Lie, R.; Suzuki, T.; Nakayama, K.; Takeda, A.; Yamaguchi, T.; Itoyama, Y.; Sekizawa, K.; Sasaki, H. Protective effects of heme oxygenase-1 against oxidant-induced injury in the cultured human tracheal epithelium. *Am. J. Respir. Cell. Mol. Biol.* **21**:428-435;1999.
- [70] Foresti, R.; Motterlini, R. The heme oxygenase pathway and its interaction with nitric oxide in the control of cellular homeostasis. *Free Radic. Res.* **31**:459-475 ;1999.
- [71] Minamino, T.; Christou, H.; Hsieh, C. M.; Liu, Y.; Dhawan, V.; Abraham, N. G.; Perrella, M. A.; Mitsialis, S. A. Kour Targeted expression of heme oxygenase-1 prevents the pulmonary inflammatory and vascular responses to hypoxia. *Proc. Natl. Acad. Sci. USA.* **98**:8798-8803;2001.
- [72] Tulis, D. A.; Durante, W.; Peyton, K. J.; Evans, A. J.; Schafer, A. I. Heme oxygenase-1 attenuates vascular remodeling following balloon injury in rat carotid arteries.

Atherosclerosis **155**:113-122;2001.

[73] Nguyen, T.; Sherratt, P. J.; Pickett, C. B. Regulatory mechanisms controlling gene expression mediated by the antioxidant response element. *Annu. Rev. Pharmacol. Toxicol.* **43**:233-260;2003.

[74] Rushmore, T. H.; Morton, M. R.; Pickett, C. B. The antioxidant responsive element. Activation by oxidative stress and identification of the DNA consensus sequence required for functional activity. *J. Biol. Chem.* **266**:11632-11639;1991.

[75] Alam, J.; Stewart, D.; Touchard, C.; Boinapally, S.; Choi, A.M; Cook, J. L. Nrf2, a Cap'n/Collar transcription factor, regulates induction of the heme oxygenase-1 gene. *J. Biol. Chem.* **274**:26071-26078;1999.

[76] Wild, A. C.; Moinova, H. R; Mulcahy, R. T. Regulation of gamma-glutamylcysteine synthetase subunit gene expression by the transcription factor Nrf2. *J. Biol. Chem.* **274**:33627-33636;1999.

[77] Hayes, J. D; McLellan, L. I. Glutathione and glutathione-dependent enzymes represent a co-ordinately regulated defence against oxidative stress. *Free Radic. Res.* **31**:273-300;1999.

[78] Yu, R.; Chen, C.; Mo, Y. Y.; Hebbar, V.; Owuor, E. D.; Tan, T. H; Kong, A. N.

Activation of mitogen-activated protein kinase pathways induces antioxidant response element-mediated gene expression via a Nrf2-dependent mechanism. *J. Biol. Chem.* **275**:39907-39913;2000.

[79] Zipper, L. M; Mulcahy, R. T. Inhibition of ERK and p38 MAP kinases inhibits binding of Nrf2 and induction of GCS genes. *Biochem. Biophys. Res. Commun.* **278**:484-492;2000.

[80] Clark, J. E.; Foresti, R.; Sarathchandra, P.; Kaur, H.; Green, C. J; Motterlini, R. Heme oxygenase-1-derived bilirubin ameliorates postischemic myocardial dysfunction. *Am. J. Physiol. Heart Circ. Physiol.* **278**:643-651;2000.

[81] Motterlini, R.; Gonzales, A.; Foresti, R.; Clark, J. E.; Green, C. J; Winslow, R. M. Heme oxygenase-1-derived carbon monoxide contributes to the suppression of acute hypertensive responses in vivo. *Circ. Res.* **83**:568-577;1998.

[82] Foresti, R.; Sarathchandra, P.; Clark, J. E.; Green, C. J; Motterlini, R. Peroxynitrite induces haem oxygenase-1 in vascular endothelial cells: a link to apoptosis. *Biochem. J.* **339**:729-736 ;1999.

[83] Otterbein, L. E.; Bach, F. H.; Alam, J.; Soares, M.; Tao Lu, H.; Wysk, M.; Davis, R. J.; Flavell, R. A; Choi, A. M. Carbon monoxide has anti-inflammatory effects involving the mitogen-activated protein kinase pathway. *Nature* **6**:422-428;2000.

- [84] Scapagnini, G.; Foresti, R.; Calabrese, V.; Giuffrida Stella, A. M.; Green, C. J.; Motterlini, R. Caffeic acid phenethyl ester and curcumin: a novel class of heme oxygenase-1 inducers. *Mol. Pharmacol.* **61**:554-561;2002.
- [85] Balogun, E.; Hoque, M.; Gong, P.; Killeen, E.; Green, C. J.; Foresti, R.; Alam, J.; Motterlini, R. Curcumin activates the heme oxygenase-1 gene via regulation of Nrf2 and the antioxidant-responsive element. *Biochem. J.* **371**:887-896;2003.
- [86] Foresti, R.; Hoque, M.; Monti, D.; Green, C. J.; Motterlini, R. Differential activation of heme oxygenase-1 by chalcones and rosolic acid in endothelial cells, *J. Pharmacol. Exp. Ther.* **312**:686-693;2004.
- [87] Motterlini, R.; Foresti, R.; Bassi, R.; Green, C. J. Curcumin, an antioxidant and anti-inflammatory agent, induces heme oxygenase-1 and protects endothelial cells against oxidative stress. *Free Radic. Biol. Med.* **28**:1303-1312;2000.
- [88] Oh, G. S.; Pae, H. O.; Moon, M. K.; Choi, B. M.; Yun, Y. G.; Rim, J. S.; Chung, H. T. Pentoxifylline protects L929 fibroblasts from TNF-alpha toxicity via the induction of heme oxygenase-1. *Biochem. Biophys. Res. Commun.* **302**:109-113;2003.
- [89] Chen, C. Y.; Jang, J. H.; Li, M. H.; Surh, Y. J. Resveratrol upregulates heme oxygenase-1 expression via activation of NF-E2-related factor 2 in PC12 cells. *Biochem.*

Biophys. Res. Commun. **331**:993-1000;2005.

[90] Kang, H. S.; Chung, H. Y.; Kim, J. Y.; Son, B. W.; Jung, H. A.; Choi, J. S. Inhibitory phlorotannins from the edible brown alga *Ecklonia stolonifera* on total reactive oxygen species (ROS) generation. *Arch. Pharm. Res.* **27**:194-198;2004.

[91] Kang, K.; Park, Y.; Hwang, H. J.; Kim, S. H.; Lee, J. G.; Shin, H. C. Antioxidative properties of brown algae polyphenolics and their perspectives as chemopreventive agents against vascular risk factors. *Arch. Pharm. Res.* **26**:286-293;2003.

[92] Lee, J. H.; Oh, H. Y.; Choi, J. S. Preventive effect of *Ecklonia stolonifera* on the frequency of benzo(a)pyrene-induced chromosomal aberrations. *J. Food Sci. Nutr.* **1**:64-68;1996.

[93] Lee, J. H.; Kim, N. D.; Choi, J. S.; Kim, Y. J.; Moon, Y. H.; Lim, S. Y.; Park, K. Y. Inhibitory effects of the methanolic extract of an edible brown alga, *Ecklonia stolonifera* and its component, phloroglucinol on aflatoxin B1 mutagenicity in vitro (Ames test) and on benzo(a)pyrene or N-methyl N-nitrosourea clastogenicity in vivo (mouse micronucleus test). *Nat. Prod. Sci.* **4**:105-114;1998.

[94] Han, E. S.; Kim, J. W.; Eom, M. O.; Kang, I. H.; Kang, H. J.; Choi, J. S.; Ha, K. W.; Oh, H. Y. Inhibitory effect of *Ecklonia stolonifera* on gene mutation on mouse lymphoma

tk^{+/+} locus in L5178Y-3.7.2.C cell and bone marrow micronuclei formation in ddY mice.

Environ. Mutagen. Carcinogen. **20**:104-111;2000.

- [95] Nagayama, K.; Iwamura, Y.; Shibata, T.; Hirayama, I; Nakamura, T. Bactericidal activity of phlorotannins from the brown alga *Ecklonia kurome*. *J. Antimicrob. Chemother.* **50**:889-893;2002.
- [96] Kang, K. A.; Lee, K. H.; Chae, S.; Koh, Y. S.; Yoo, B. S.; Kim, J. H.; Ham, Y. M.; Baik, J. S.; Lee, N.; H; Hyun, J. W. Triphlorethol-A from *Ecklonia cava* protects V79-4 lung fibroblast against hydrogen peroxide induced cell damage. *Free Radic. Res.* **39**:883-892;2005.
- [97] Kang, K. A.; Zhang, R.; Lee, K. H.; Chae, S.; Kim, B. J.; Kwak, Y. S; Park, J. W.; Lee, N. H; Hyun, J. W. Protective Effect of Triphlorethol-A from *Ecklonia cava* against Ionizing Radiation *in vitro*. *J. Rad. Res.* **47**:61-68;2006.
- [98] Kang, K. A.; Chae, S.; Lee, K. H.; Zhang, R.; Jung, M. S.; Kim, S. Y.; Kim, H. S.; Joo, H. G.; Park, J. W.; Ham, Y. M.; Baik, J. S.; Lee, N. H; Hyun, J. W. Eckol isolated from *Ecklonia cava* attenuates oxidative stress induced cell damage in lung fibroblast cells. *FEBS Letters* **579**:6295-6304.
- [99] Kang, K. A.; Lee, K. H.; Chae, S.; Zhang, R.; Jung, M. S.; Ham, Y. M.; Baik, J. S.; Lee, N. H; Hyun, J. W. Cytoprotective effect of phloroglucinol on oxidative stress induced cell damage via catalase activation. *J. Cell. Biochem.* **97**:609-620;2006.
- [100] Kietzmann, T.; Samoylenko, A; Immenschuh, S. Transcriptional regulation of heme

oxygenase-1 gene expression by MAP kinases of the JNK and p38 pathways in primary cultures of rat hepatocytes. *J. Biol. Chem.* **278**:17927-17936;2003.

[101] Oguro, T.; Hayashi, M.; Nakajo, S.; Numazawa, S; Yoshida, T. The expression of heme oxygenase-1 gene responded to oxidative stress produced by phorone, a glutathione depletor, in the rat liver; the relevance to activation of c-jun n-terminal kinase. *J. Pharmacol. Exp. Ther.* **287**:773-778;1998.

[102] Itoh, K.; Chiba, T.; Takahashi, S.; Ishii, T.; Igarashi, K.; Katoh, Y.; Oyake, T.; Hayashi, N.; Satoh, K.; Hatayama, I.; Yamamoto, M; Nabeshima, Y. An Nrf2/small Maf heterodimer mediates the induction of phase II detoxifying enzyme genes through antioxidant response elements. *Biochem. Biophys. Res. Commun.* **236**:313-322;1997.

[103] Hayes, J. D.; Chanas, S. A.; Henderson, C. J.; McMahon, M.; Sun, C.; Moffat, G. J.; Wolf, C. R; Yamamoto, M. The Nrf2 transcription factor contributes both to the basal expression of glutathione S-transferases in mouse liver and to their induction by the chemopreventive synthetic antioxidants, butylated hydroxyanisole and ethoxyquin. *Biochem. Soc. Trans.* **28**:33-41;2000.

[104] Chan, K.; Kan, Y. W. Nrf2 is essential for protection against acute pulmonary injury in mice. *Proc. Natl. Acad. Sci. USA.* **96**:12731-12736;1999.

[105] Chan, K.; Han, X. D; Kan, Y. W. An important function of Nrf2 in combating

- oxidative stress: detoxification of acetaminophen. *Proc. Natl. Acad. Sci. USA.* **98**:4611-4616;2001.
- [106] Kim, Y. C.; Masutani, H.; Yamaguchi, Y.; Itoh, K.; Yamamoto, M; Yodoi, J. Hemin-induced activation of the thioredoxin gene by Nrf2. A differential regulation of the antioxidant responsive element by a switch of its binding factors. *J. Biol. Chem.* **276**:18399-18406;2001.
- [107] Kwak, M. K.; Itoh, K.; Yamamoto, M; Kensler, T. W. Enhanced expression of the transcription factor Nrf2 by cancer chemopreventive agents: role of antioxidant response element-like sequences in the nrf2 promoter. *Mol. Cell. Biol.* **22**:2883-2892;2002.
- [108] Kobayashi, M; Yamamoto, M. Molecular mechanisms activating the Nrf2-Keap1 pathway of antioxidant gene regulation. *Antioxid. Redox. Signal.* **7**:385-394;2005.
- [109] Itoh, K.; Wakabayashi, N.; Katoh, Y.; Ishii, T.; Igarashi, K.; Engel, J. D; Yamamoto, M. Keap1 represses nuclear activation of antioxidant responsive elements by Nrf2 through binding to the amino-terminal Neh2 domain. *Genes Dev.* **13**:76-86;1999.
- [110] Owuor, E. D; Kong, A. N. Antioxidants and oxidants regulated signal transduction pathways. *Biochem. Pharmacol.* **64**:765-770;2002.
- [111] Zipper, L. M; Mulcahy, R. T. Erk activation is required for Nrf2 nuclear localization

during pyrrolidine dithiocarbamate induction of glutamate cysteine ligase modulatory gene expression in HepG2 cells. *Toxicol. Sci.* **73**:124-134;2003.

[112] Yu, R.; Chen, C.; Mo, Y. Y.; Hebbar, V.; Owuor, E. D.; Tan, T. H.; Kong, A. N.

Activation of mitogen-activated protein kinase pathways induces antioxidant response element-mediated gene expression via a Nrf2-dependent mechanism. *J. Biol. Chem.* **275**:39907-39913;2000.

[113] Kutty, R. K; Maines, M. O. Oxidation of heme c derivatives by purified heme oxygenase in the rat liver. *J. Biol. Chem.* **257**:9944-9952;1982.

[114] Chen, J. C.; Huang, K. C.; Lin, W. W. HMG-CoA reductase inhibitors upregulate heme oxygenase-1 expression in murine RAW264.7 macrophages via ERK, p38 MAPK and protein kinase G pathways. *Cell Signal.* **18**:32-39;2006.

7. 4. Part IV

- [115] Kawaguchi, Y., Tanaka, H., Okada, T., Konishi, H., Takahashi, M., Ito, M., and Asai, J. 1996. The effects of ultraviolet A and reactive oxygen species on the mRNA expression of 72-kDa type IV collagenase and its tissue inhibitor in cultured human dermal fibroblasts. *Arch. Dermatol. Res.* 288:39-44.
- [116] Scharffetter-Kochanek, K., Wlaschek, M., Briviba, K., and Sies, H. 1993. Singlet oxygen induces collagenase expression in human skin fibroblasts. *FEBS Lett.* 331:304-306.
- [117] Tanaka, H., Okada, T., Konishi, H., and Tsuji, T. 1993. The effect of reactive oxygen species on the biosynthesis of collagen and glycosaminoglycans in cultured human dermal fibroblasts. *Arch. Dermatol. Res.* 285:352-355.
- [118] Brenneisen, P., Briviba, K., Wlaschek, M., Wenk, J., and Scharffetter-Kochanek, K. 1997. Hydrogen peroxide (H₂O₂) increases the steady-state mRNA levels of collagenase/MMP-1 in human dermal fibroblasts. *Free Radic. Biol. Med.* 22:515-524.
- [119] Varani, J., Perone, P., Fligiel, S. E., Fisher, G. J., and Voorhees, J. J. 2002. Inhibition of type I procollagen production in photodamage: correlation between presence of high molecular weight collagen fragments and reduced procollagen synthesis. *J. Invest. Dermatol.* 119:122-129.
- [120] Ho, J. N., Lee, Y. H., Lee, Y. D., Jun, W. J., Kim, H. K., Hong, B. S., Shin, D. H., and

- Cho, H. Y. 2005. Inhibitory effect of Aucubin isolated from *Eucommia ulmoides* against UVB-induced matrix metalloproteinase-1 production in human skin fibroblasts. *Biosci. Biotechnol. Biochem.* 69:2227-2231.
- [121] Frost, J. A., Geppert, T. D., Cobb, M. H., and Feramisco, J. R. 1994. A requirement for extracellular signal-regulated kinase (ERK) function in the activation of AP-1 by Ha-Ras, phorbol 12-myristate 13-acetate, and serum. *Proc. Natl. Acad. Sci. USA.* 91:3844-3848.
- [122] Westermarck, J., and Karari, V. M. 1999. Regulation of matrix metalloproteinase expression in tumor invasion. *FASEB J.* 13:781-792.
- [123] Rajagopalan, S., Meng, X. P., Ramasamy, S., Harrison, D. G., and Galis, Z. S. 1996. Reactive oxygen species produced by macrophage-derived foam cells regulate the activity of vascular matrix metalloproteinases in vitro. Implications for atherosclerotic plaque stability. *J. Clin. Invest.* 98:2572-2579.
- [124] Nelson, K. K., and Melendez, J. A. 2004. Mitochondrial redox control of matrix metalloproteinases. *Free Radic. Biol. Med.* 37:768-784.
- [125] Kheradmand, F., Werner, E., Tremble, P., Symons, M., and Werb, Z. 1998. Role of Rac1 and oxygen radicals in collagenase-1 expression induced by cell shape change. *Science* 280:898-902.
- [126] Zaw, K. K., Yokoyama, Y., Abe, M., and Ishikawa, O. 2006. Catalase restores the

- altered mRNA expression of collagen and matrix metalloproteinases by dermal fibroblasts exposed to reactive oxygen species. *Eur. J. Dermatol.* 16:375-379.
- [127] Cho, Y. H., Kim, J. H., Sim, G. S., Lee, B. C., Pyo, H. B., and Park, H. D. 2006. Inhibitory effects of antioxidant constituents from *Melothria heterophylla* on matrix metalloproteinase-1 expression in UVA-irradiated human dermal fibroblasts. *J. Cosmet. Sci.* 57:279-289.
- [128] Kang, K. A., Zhang, R., Lee, K. H., Chae, S., Kim, B. J., Kwak, Y. S., Park, J. W., Lee, N. H. and Hyun, J.W. 2006. Protective Effect of Triphlorethol-A from *Ecklonia cava* against Ionizing Radiation *in vitro*. *J. Rad. Res.* 47:61-68.
- [129] Kang, K. A., Lee, K. H., Park, J. W., Lee, N. H., Na, H. K., Surh, Y. J., You, H. J., Chung, M. H., and Hyun, J. W. 2007. Triphlorethol-A induces heme oxygenase-1 via activation of ERK and NF-E2 related factor 2 transcription factor. *FEBS Lett.* 581:2000-2008.
- [130] Tsareva, S. A., Moriggl, R., Corvinus, F. M., Wiederanders, B., Schütz, A., Kovacic, B., and Friedrich, K. 2007. Signal Transducer and Activator of Transcription 3 Activation Promotes Invasive Growth of Colon Carcinomas through Matrix Metalloproteinase Induction. *Neoplasia* 9: 279–291.
- [131] del Rio, L. A., Sandalio, L. M., Palma, J. M., Bueno, P., and Corpas, F. J. 1992.

- Metabolism of oxygen radicals in peroxisomes and cellular implications. *Free Rad. Biol. Med.* 13:557-580.
- [132] Rogakou, E. P., Pilch, D. R., Orr, A. H., Ivanova, V. S., and Bonner, W. M. 1988. DNA double-stranded breaks induce histone H2AX phosphorylation on serine 139. *J. Biol. Chem.* 273:5858-5868.
- [133] Crawford, H. C., and Matrisian, L. M. 1996. Mechanisms controlling the transcription of matrix metalloproteinase genes in normal and neoplastic cells. *Enzyme Protein* 49:20-37.
- [134] Whitmarsh, A. J., and Davis, R. J. 1996. Transcription factor AP-1 regulation by mitogen-activated protein kinase signal transduction pathways. *J. Mol. Med.* 74:589-607.
- [135] Fisher, G. J., Kang, S., Varani, J., Bata-Csorgo, Z., Wan, Y., Datta, S., and Voorhees, J. J. 2002. Mechanisms of photoaging and chronological skin aging. *Arch. Dermatol.* 138:1462-1470.
- [136] Fisher, G. J., Datta, S. C., Talwar, H. S., Wang, Z. Q., Varani, J., Kang, S., and Voorhees, J. J. 1996. Molecular basis of sun-induced premature skin ageing and retinoid antagonism. *Nature* 379:335-339.
- [137] Kang, S., Chung, J. H., Lee, J. H., Fisher, G. J., Wan, Y. S., Duell, E. A., and Voorhees, J. J. 2003. Topical N-acetyl cysteine and genistein prevent ultraviolet-light-induced

signaling that leads to photoaging in human skin in vivo. *J. Invest. Dermatol.* 120:835-

841.



8. Abstract in Korean

활성산소는 염증, 노화, 암, 동맥경화, 고혈압과 당뇨병에 기여하는 인자로 조직 손상에도 관련이 있는 것으로 알려졌다. 이러한 활성산소를 제거하는 항산화 물질들은 앞서 나열한 다양한 질환으로부터 예방 또는 치료 효과를 보이는 등의 연구 결과들이 진행 중이다.

이중 H₂O₂ 라는 주요한 활성산소는 hydroxyl radical 를 형성하게 되는데, 이 hydroxyl radical 이 고도로 반응하여 세포 DNA 손상을 일으키고, 결국은 세포사멸이르게 만든다. 어떤 항산화물질들은 이러한 활성산소에 의한 DNA 손상으로부터 세포를 보호 한다는 연구가 있었고, 따라서 천연항산화물질 또는 합성 항산화물질에 대한 심층적인 연구가 필요하다. 그 중에서도 특히, 합성 항산화물질 보다 부작용이 적은 천연물에서 보다 안정하고 강력한 항산화제를 확보하기 위해 노력하는 추세이고, 비교적 항산화 활성 의 다양한 연구로 많이 알려져 있는 육상식물이 아닌 해양생물의 생리활성물질에 초점을 맞추었다.

감태(*Ecklonia cava*)는 비식용 해조류로 갈조 식물 다시마목(Laminariales) 미역과(*Alariaceae*)의 식물로 우리나라 남해안과 제주연안, 일본에 서식하고 있다.

감태의 생리활성 물질은 Phlorotannin 이며 이들에 대한 생리활성은 HIV-1 역전사효소 저해활성, xanthin oxidase 저해활성, tyrosine 활성 억제 효과 등이 보고된바 있다.

이러한 phlorotannin 으로 eckol, phloroglucinol, dieckol, triphlorethol-A 등이 밝혀졌고, 이중에서도 triphlorethol-A 의 항산화활성이 가장 뛰어난 것을 관찰하였다.

triphlorethol-A 는 phloroglucinol 의 open-chain trimer 구조를 가지고 있다.

따라서 우리는 triphlorethol-A 를 가지고 다양한 산화적인 스트레스에서 세포 보호효과를 내고 이 보호 작용이 어떠한 기전으로 일어나는지를 연구해보았다.

우리는 햄스터 폐 섬유아세포에서 H₂O₂ 와 radiation 으로 유도된 산화적인 스트레스로부터 ROS 를 제거하여 triphlorethol-A 가 세포보호 작용을 일으키는 것을 관찰할 수 있었고, 또한, 이러한 triphlorethol-A 가 항산화 효소들의 활성을 유도 하였는데 그 중에서도 Hem oxygenase-1(HO-1)이라는 항산화효소는 Nrf2 라는 전사인자의 활성화를 통하여 유도 된다는 것을 관찰할 수 있었다.

마지막으로 ROS 의 생성으로 산화적인 스트레스가 야기될때, matrix metalloproteinases (MMPs)의 합성과 노화가 유도된다.

그래서 우리는, triphlorethol-A 의 산화적인 스트레스로부터 세포보호작용이 사람 피부세포에서도 작용을 하는지 실험해보았다.

H₂O₂ 로 사람 피부세포에 산화적인 스트레스를 주어 collagen 을 분해하는 MMP-1 의 발현이 증가하는 것을 확인하였고, triphlorethol-A 가 이 MMP-1 을 감소시키는 것을 관찰할 수 있었다.

결과를 종합해 보면 triphlorethol-A 는 H₂O₂ 나 radiation 로 유도되는 산화적인 스트레스로부터 햄스터 폐 섬유아세포를 보호하였는데, 이는 활성산소를 제거하고, 항산화 효소 HO-1 활성을 유도하여 세포보호 작용을 일으키는 것을 알 수 있었고, 산화적인 스트레스에 의한 노화를 억제 시키는 데에도 큰 효과를 가지고 있는 것을 알 수 있었다. 따라서 triphlorethol-a 가 radiation 으로부터 세포를 보호할 수 있는 radioprotector 나 노화를 억제하는 anti-aging 개발에 기초를 제공할 것으로 사료 된다.

주요어: 활성산소, 항산화 효소, Heme oxygenase -1, Matrix metalloproteinases (MMPs)-1, Radioprotector, Anti-Aging

감사의 글

지난 4년 동안 제가 박사라는 타이틀을 얻기 위해 나름 노력을 해왔다고 스스로 위로해봅니다. 아직 부족한 부분이 너무나 많은 것을 지금 이순간에도 느끼고 있기 때문인데, 앞으로 이부분을 알차게 채워야하는 과정을 거치면서 완전한 박사 타이틀에 걸맞는 제가 되지 않을까 합니다. 본 논문이 완성되기까지 항상 사랑으로 옆에서 지켜 봐 주신 많은 분들께 이 지면을 빌어 감사의 말씀을 드립니다.

먼저 본 논문에 대한 연구의 수행과 논문의 완성이 있기까지 항상 격려와 애정을 아끼지 않으시고 지도해주신 현진원 교수님께 진심으로 감사드립니다. 그리고 바쁘신 가운데에도 격려와 지도로 부족함이 많은 논문을 세심하게 심사하여 주신 박덕배 교수님, 조문제 교수님, 은수용 교수님, 강희경 교수님께도 감사 드립니다. 또한 대학원 과정 동안 늘 관심과 조언으로 이끌어 주신 고영상 교수님, 유은숙 교수님, 강현욱 교수님, 이영기 교수님, 정영배 교수님, 이근화 교수님, 김수영 교수님, 홍성철 교수님, 배종면 교수님께도 깊은 감사를 드립니다.

아울러 같은 실험실에서 아무것도 몰랐던 저에게 실험의 기본부터 가르쳐주시고 늘 많은 도움을 주시는 의과대학 생화학교실의 임희경 언니, 영미언니 늘 좋은 일들만 있으시길 빌게요.

그리고 저에게 늘 힘이 되어주셨던 헤자언니 행복하세요! 석사 동기 이자나 때문에 늘 고생하는 내친구 현재희 언제나 고맙다 ㅠ.ㅠ

그리고 실험실 막내둥이에서 이제는 어느새 박사 2년차를 넘어서는 친구 같은 진영이(그래도 언제나 막내둥이 같은 이미지야^^;)

결혼한 정은언니 행복하죠.? ^^ 파이팅!

지은언니..얼굴은 자주 볼수 없지만 그래도 언니한테 참 고마워요 알죠.? 나랑 은근히 맞는 구석이 있는 의대 막내둥이 부혜진. 언제나 파이팅! 열심히 하길~!

우리 생화학교실 미경언니, 장예 고마워요 나 많이 도와줘서.. 앞으로도 잘 부탁드립니다 기천, 동욱, 지홍이 열심히 하거라,

약리학 교실 경진, 정일, 선순, 민경, 은진, 변윤영 선생님, 조직학 보연, 최수길 선생님 모두모두 열심히 하시고 잘되길 빌게요.

그리고 이들은 비롯한 여러 실험실 선생님들께도 고마운 마음을 전합니다.

나의 푸념을 모두 받아주는 친구들 경은, 은정, 지성, 희정, 미정, 현정, 순제, 승혜, 은진, 고등학교 선후배님들 저 해냈어요. 늘 고마워요.

끝으로 부족한 큰 딸 옆에서 늘 지켜주시는 엄마, 아빠, 할아버지(아프지 마세요), 동생 경훈에게 고마움과 사랑의 마음을 전하며, 아 논문을 바칩니다. 열심히 할게요. 모두모두 감사합니다.